In Vitro Study of Wear, Fatigue, and Colour Behaviour of Novel CAD/CAM Monolithic All-Ceramic Materials

Doctoral thesis

to obtain a doctorate

from the Faculty of Medicine

of the University of Bonn

Ahmed Mahmoud Sherif Mohamed Elsayyed Fouda

From Ismailia / Egypt

2023

Written with authorization of
the Faculty of Medicine of the University of Bonn

First reviewer: Prof. Dr. rer. nat. Christoph Bourauel
Second reviewer: PD Dr. Nils Heim

Day of oral examination: 14.03.2023

From the Poliklinik für Zahnärztliche Prothetik, Propädeutik und Werkstoffwissenschaften der Universität Bonn

Director: Prof. Dr. med. dent. Helmut Stark

- Stiftungsprofessur für Oralmedizinische Technologie –

Prof. Dr. rer. nat. Christoph Bourauel

Dedicated to my beloved parents

Table of contents

	List of Abbreviations	**7**
1.	**Introduction**	**9**
1.1	Review of Literature	11
1.1.1	Dental ceramics	11
1.1.2	Monolithic versus bilayered restorations	12
1.1.3	Manufacturing techniques of dental ceramic restorations	13
1.1.4	Computer-Aided Design/Computer-Assisted Manufacturing (CAD/CAM)	14
1.1.5	Glass-based ceramics	15
1.1.6	Zirconia	18
1.1.7	Wear	23
1.1.8	Strength of dental ceramics	28
1.1.9	Aesthetics	29
1.1.10	Microstructure analysis methods	34
1.1.11	Previous studies in literature	36
2.	**Aim of Study**	**40**
3.	**Materials and Methods**	**41**
3.1	Materials	41
3.2	Wear and surface roughness	41
3.2.1	Ceramic specimens' preparation	41
3.2.2	Enamel antagonists	45
3.2.3	Wear simulation	47
3.2.4	Wear quantification	49
3.2.5	Surface roughness	54
3.2.6	Scanning electron microscope (SEM)	55
3.2.7	Energy Dispersive X-ray Spectroscopy (EDS)	57
3.3	Fracture load testing	57
3.3.1	Specimen preparation	57
3.3.2	Designing and milling of CAD/CAM crowns	58

3.3.3	Finishing and cementation of crowns	62
3.3.4	Thermomechanical ageing and static loading	64
3.4	Effect of ageing on CIE L*a*b* parameters and change of colour (∆E)	66
3.5	Colour testing	67
3.5.1	Translucency parameter (TP)	67
3.5.2	Colour match to the selected shade	67
3.6	Statistical analysis	69
4.	**Results**	**70**
4.1	Enamel wear	70
4.2	Ceramic wear	71
4.3	Surface roughness	72
4.4	Microstructural analysis	72
4.5	Load to fracture	79
4.6	Change of Colour (∆E) after thermomechanical ageing	79
4.7	Translucency parameter (TP)	82
4.8	Change of colour (∆E) from selected shade (A3)	82
4.9	X-ray diffraction pattern analysis (XRD)	84
5.	**Discussion**	**87**
5.1	Discussion of materials selection and methodology	87
5.2	Discussion of Results	88
5.2.1	Discussion of wear results	88
5.2.2	Discussion of fracture strength results	92
5.2.3	Discussion of colour and translucency results	96
5.3	Conclusions	98
6.	**Summary**	**99**
7.	**Figures**	**101**
8.	**Tables**	**105**
9.	**References**	**106**
10.	**Acknowledgments**	**131**

List of Abbreviations

ANOVA	Analysis of Variance
CAD/CAM	Computer Aided Design/Computer Assisted Manufacturing
CIE	Commission International de l'Eclairage
CLSM	Confocal Laser Scanning Microscope
CR	Contrast Ratio
CTE	Coefficient of Thermal Expansion
DICOM	Digital Imaging and Communications
EDX	Energy Dispersive X-ray Spectroscopy
FLD	Fully Stabilised Lithium Disilicate
FPD	Fixed Partial Denture
FSZ	Fully Stabilised Zirconia
IOS	Intra Oral Scanner
LD	Lithium Disilicate
LTD	Low Temperature Degradation
MPa	Mega Pascal
PFM	Porcelain-Fused-to-Metal
PLD	Partially Stabilised Lithium Disilicate
PSZ	Partially Stabilised Zirconia
SEM	Scanning Electron Microscopy
SMZ	Super-translucent Monolithic Zirconia
STL	Stereolithography
temp.	Temperature
TMJ	Temporomandibular Joint
TP	Translucency Parameter
T_t%	Light Transmittance Percentage
UMZ	Ultra-Translucent Monolithic Zirconia
wt.%	Weight Percent
XRD	X-ray Diffraction

Y-TZP	Yttria-Stabilised Tetragonal Zirconia Polycrystals
ZLS	Zirconia-Reinforced Lithium Silicate
∆E	Colour Difference
µCT	Micro Computed Tomography
3Y-TZP	3mol % Yttria-Stabilised Tetragonal Zirconia Polycrystals
4Y-TZP	4mol % Yttria-Stabilised Tetragonal Zirconia Polycrystals
5Y-PSZ	5mol % Partially-Stabilised Zirconia

1. Introduction

In recent years, the trend toward non-metal aesthetic restorations is gaining momentum due to the rapid development in dental ceramic materials and the increased aspirations of patients for a perfect aesthetic outcome. The dental market has seen a recent influx of novel aesthetic restorative products whose compositions, properties, and indications vary widely. Therefore, selecting the best material for a given case requires a thorough understanding of the material's properties to ensure the success of the treatment plan (Conrad et al., 2007). Ceramic restorations, in general, offer excellent aesthetics, biocompatibility, and the ability to replicate a natural appearance (Sailer et al., 2015). During mastication, dental restorations are subject to destructive stresses of different types and magnitudes (Aboushelib et al., 2016; Kelly, 1997), and the brittle nature of ceramics makes them vulnerable to failure (Zhang et al., 2013). In order to achieve a balance between strength and aesthetics, ceramic restorations were composed of a robust core and an aesthetic layer of feldspathic porcelain (Della Bona and Kelly, 2008). However, the weak veneer layers of bilayered ceramic restorations are prone to chipping or delamination due to mismatches in thermal expansion coefficients between the veneer and ceramic core (Jian et al., 2016).

Advances in computer-aided design/computer-assisted manufacturing (CAD/CAM) technologies have enabled the development of monolithic ceramic restorations that can be milled in full-contour from prefabricated CAD/CAM blocks (Blatz and Conejo, 2019). Monolithic ceramic restorations have solved the problem of veneer chipping and delamination; however, they still need to be investigated for their mechanical and aesthetic properties (Silva et al., 2017). The materials available for monolithic application could be classified into glass ceramics, high strength ceramics, and resin-based ceramics (Gracis et al., 2015). Glass-ceramics are characterised by their high translucency and ability to mimic the appearance of natural teeth. Moreover, they can be adhesively bonded to the tooth structure due to their etchability (Blatz et al., 2003; Zhang and Lawn, 2018). However, due to the low strength of the early generations, their use was limited to single units in the anterior region (Pjetursson et al., 2007). Recently, modified glass-ceramics with increased strength and extended indications became available (Dupree et al., 1990).

Alternatively, high-strength polycrystalline ceramics, such as zirconia, have a high strength of up to 1200 MPa and can be used for single and multi-unit restorations in the

anterior and posterior regions of the jaw (Conejo et al., 2017). However, monolithic zirconia restorations were subject to the disadvantages of high opacity, poor aesthetics, and significant abrasiveness to opposing teeth. The continuous modification of zirconia has led to the development of new generations of monolithic zirconia with enhanced translucency (Zhang et al., 2016a). However, the increase in translucency came at the expense of the material's strength (Zhang, 2014).

The success of a restoration is determined by its ability to restore function and aesthetics, as well as to withstand the harsh oral environment for many years without fracture or change in colour and without causing excessive wear to the opposing teeth. Several factors influence enamel wear including material microstructure and surface conditions as well as tribological and clinical factors (Borrero-Lopez et al., 2014; Preis et al., 2012; Sripetchdanond and Leevailoj, 2014). A dental crown material should ideally exhibit wear characteristics similar to natural enamel (Ghazal and Kern, 2009). Some restorative ceramic materials, such as zirconia, may cause aggressive wear to the opposing enamel due to their high hardness and flexural strength (Wiedenmann et al., 2020).

The ability of restorative materials to resist fatigue is another critical aspect that affects long-term success and should be investigated. Repeated subcritical masticatory loads may result in "subcritical crack growth" that starts at voids and defects occurring during the manufacturing process and continues to grow over time (Zhang et al., 2013). Eventually, this can result in the fracture of the restoration under low masticatory loads. Examining the long-term durability of ceramic restorations should also include the stability of colour over time. Previous studies have reported changes in colour after simulated ageing conditions (Dikicier et al., 2014; Heydecke et al., 2001; Kurt and Turhan Bal, 2019; Liebermann et al., 2021). As of today, there is insufficient data in the literature reporting on the effect of fatigue on the colour stability of ceramics, even though aesthetics is one of the main reasons for using them.

1.1 Review of Literature

1.1.1 Dental ceramics

"*Ceramics*" are defined as non-metallic, inorganic materials that are produced by the fusion of raw minerals at high temperatures (Rosenblum and Schulman, 1997). Ceramics are generally inert, biocompatible, wear-resistant, and hard, but have relatively low fracture toughness and are susceptible to tensile fracture (Abdul-Hamid et al., 2018). Dental ceramics are a group of ceramic materials that are used to restore missing or defective dental structures (Shenoy and Shenoy, 2010). For decades, served the porcelain-fused-to-metal (PFM) restorations as the gold standard for tooth replacements as they combine the high mechanical properties of metal frameworks and the high aesthetic properties of veneering porcelain (Zhang and Kelly, 2017). The development in the field of imaging and the subsequent improvement in image quality and clarity has been accompanied by a rise in patients' expectations for better aesthetics, and metal-ceramic restorations no longer meet these expectations. That was the motivation for researchers to shift to non-metallic alternatives. All-ceramic restorations were developed to overcome the drawbacks of metallic restorations such as biological incompatibility, allergy, opacity, and inability to achieve natural aesthetics (Bumgardner and Lucas, 1995; Poggio et al., 2017; Stejskal et al., 1999; Venclikova et al., 2007). The ability of ceramic materials to transmit light similarly to the tooth structures allows them to mimic the natural look of teeth (Poggio et al., 2017). According to previously published studies, the percentage of crowns and fixed prostheses that are made of PFM in the US has dropped from 80 % to 16.9 %, while the use of all-ceramic restorations has been raised up to 80.2 % (Christensen, 2014; Zhang and Kelly, 2017).

A disadvantage of dental ceramics is that they are brittle and have a low tensile strength which allows only 0.1 % to 0.2 % strain before they break (Shenoy and Shenoy, 2010). The manufacturing of dental ceramics has advanced rapidly over the last decade, introducing several novel all-ceramic materials with enhanced physical properties and strength, and can be used to restore single and multiple teeth anteriorly and posteriorly (da Silva et al., 2012). Several methods were employed to enhance the strength of dental ceramics including chemical and ion exchange strengthening, dispersion strengthening, fine microstructure strengthening, and nano-composite strengthening (Abdul-Hamid et al.,

2018). All these techniques are aimed at enhancing the strength of dental ceramics by creating residual compressive stresses within the surface of the restoration that deflect and stop the propagation of the initiated cracks.

Different classification systems are used to classify the dental ceramic restorations. They can be classified by the number of layers into monolithic (full contour) and bilayered, or by the microstructure of the material into glass-based ceramics, high-strength polycrystalline ceramics, and resin-based ceramics.

1.1.2 Monolithic versus bilayered restorations

All-ceramic restorations can be used in one of two forms: bilayered or monolithic. The bilayered restoration consists of a high-strength core or framework that is veneered with an aesthetic porcelain layer. The core provides adequate strength to resist the biting forces and supports the weaker veneer layer, whereas the porcelain veneer is responsible for superior aesthetics. The PFM restorations are considered the gold standard for the bilayered fixed partial dentures (FPDs) owing to their excellent clinical performance and high survival rate (Silva et al., 2017). However, PFM restorations have limitations such as low biocompatibility, the rise in the cost of precious metals, opacity as well as the dark metal colour of the core which is responsible for the unnatural look of the final restoration (Zarone et al., 2011). All these factors are responsible for the shift toward the use of ceramic cores in multi-layered restorations.

The development of high crystalline content ceramic materials enabled the fabrication of ceramic infrastructures with sufficient strength to withstand the chewing forces (Silva et al., 2017). Owing to their adequate strength and outstanding aesthetics, all-ceramic bilayered restorations are indicated for single and multi-unit FPDs in the anterior and posterior regions of the mouth whenever aesthetics is of high importance (Conrad et al., 2007). Nevertheless, the bilayered restorations have few limitations. One frequent problem was the fracture of the weak veneer layer under load (Bindl and Mormann, 2002; Esquivel-Upshaw et al., 2004; Wolfart et al., 2009). Another problem was the chipping or delamination of the veneer layer due to the mismatching of the thermal expansion coefficients between the core and the veneer, which causes tensile stress at the core/veneer interface (Conrad et al., 2007; Rekow et al., 2011; Wolfart et al., 2009).

Monolithic restorations were developed to overcome the veneer fracture, chipping, and delamination that occurs in the bilayered restorations (Christensen, 2014; Zhang et al., 2016b). They are more durable since they consist of only one material (Schultheis et al., 2013). The strength of monolithic ceramics ranges from 450 to 1200 MPa according to the ceramic type (Bajraktarova-Valjakova et al., 2018), which is higher than that of the veneering porcelain that does not exceed 150 MPa, therefore the problem of veneer fracture was solved (Zhang and Kelly, 2017). Moreover, the absence of veneering ceramic in monolithic restoration eliminates the risk of veneer wear over time and helps in keeping the occlusion stable during service, particularly in the presence of occlusal discrepancies that could lead to TMJ disorders (Ciancaglini et al., 2002; Zarone et al., 2019). Monolithic ceramics are characterised by high crystalline content to provide adequate strength, which make them less translucent than veneering feldspathic porcelain and have less aesthetic quality. The use of monolithic restorations was increased after the development of CAD/CAM technology as it reduced the production time and improved the cost effectiveness (Johansson et al., 2014). The CAD/CAM ceramics are commercially available in the form of white non-coloured blocks that require staining and characterisation after milling, or in a pre-shaded monochromatic or multi-coloured form.

1.1.3 Manufacturing techniques of dental ceramic restorations

Several techniques are used to fabricate dental ceramic restorations (Raju et al., 2015). An older technique was powder slurry, which was used to fabricate porcelain jacket crowns. The ceramic crown produced by this technique had superior translucency, however, its low mechanical strength and poor marginal integrity rendered it obsolete (Griggs, 2007). The powder slurry technique is still used for the build-up of porcelain veneers over the metal frameworks in metal-ceramic restorations. Another technique is the slip casting which was used to fabricate infiltrated ceramics. It involves the application of aqueous porcelain slip on a refractory die and then fired at a high temperature. The porous alumina-based ceramic core is subsequently infiltrated with low viscosity molten glass that fills the pours and increases the strength and toughness of the core. The opaque infiltrated core must be veneered with porcelain to achieve good aesthetics (Holand et al., 2000). Lost-wax heat pressing technique evolved with the rise of pressable ceramics and is still used until now. The pressable ceramics are provided in the form of prefabricated ceramic

ingots. The ingots are molten at high temperatures and then slowly pressed into a mould made by the lost wax technique (Griggs, 2007). They share the advantages of good internal fit and marginal adaptation with metal alloys since they are processed by the same technique (Sulaiman et al., 1997; Yeo et al., 2003). Recently, the CAD/CAM technique has been developed and produced an evolution in the all-ceramic restorations. Some materials can be produced by more than one technique, e.g., glass-ceramics. Other materials are only fabricated using the CAD/CAM e.g., zirconia.

1.1.4 Computer-Aided Design/Computer-Assisted Manufacturing (CAD/CAM)

Rapid developments in CAD/CAM technologies, combined with advances in biomaterials have significantly altered the shape, quality, and efficiency of the provided dental services in all disciplines of dentistry, especially in the field of prosthetic dentistry (Alghazzawi, 2016). The first CAD/CAM system was introduced in the 80s of the last century and was used only in a limited number of procedures including inlays and onlays (Mormann, 2006). Then manufacturers continued to improve the system and were able to fabricate crowns and veneers. More recently, developed software and improved milling units are able to produce FPDs, removable dentures, implants, abutments, and even orthodontic appliances (Davidowitz and Kotick, 2011).

The CAD/CAM system has reduced the multiple error-introducing steps of the conventional fabrication methods and automated the production procedures thereby increasing the precision of the prosthesis and reducing the overall fabrication time and cost (Abduo et al., 2014). The digital workflow consists of three steps: data acquisition, computer-assisted virtual designing of the restoration, and computer-guided milling of the designed restoration (Alghazzawi, 2016). The newly developed intra-oral scanners (IOS) used for data acquisition were reported to provide data with equal or higher accuracy and precision than conventional impressions (Nedelcu et al., 2018). Moreover, the digital impression has an advantage over conventional impression in terms of patient comfort, timesaving, ease of manipulation, real-time visualisation, fast recapturing, elimination of the risk of distortion, and long-term data preservation (Chiu et al., 2020; Yuzbasioglu et al., 2014). Additionally, the advanced 5-axis milling machines allow the fabrication of single and multi-unit restorations with excellent marginal adaptation and excellent fit (Dahl et al., 2018; Dolev et al., 2019; Kirsch et al., 2017).

In parallel with the development of CAD/CAM systems, new materials have been developed for restorative treatments. Currently, the new systems can utilise a wide range of materials including resin, metals, and ceramics. Aesthetic ceramics have remarkably increased the potential use of CADCAM in prosthodontics, particularly after the development of high-strength ceramics, e.g., zirconia. The fabrication of zirconia restorations can only be made by computer-aided manufacturing (Sadan et al., 2005). The possibility of fabricating strong and tough CAD ceramic restorations has expanded the indications of metal-free restorations to include posterior single restorations and multi-unit FPDs (Abduo et al., 2014). Additionally, CAD/CAM has enabled the production of highly aesthetic glass-ceramic restorations from blocks manufactured under standardised production conditions with improved mechanical and physical properties, eliminating the human errors and variations that occur in conventional methods.

1.1.5 Glass-based ceramics

Glasses are amorphous solids that consist mainly of silicon dioxide (SiO_2) and have no crystalline phases. They are transparent, hard, brittle, and have low thermal conductivity. Ceramics are composed mainly of crystalline grains. Glass-ceramics are a group of materials that consist of one or more crystalline phases embedded in a glass matrix. The crystalline content varies between 30 % and 70 % (Fu et al., 2020). The combination of desirable physical and chemical properties of glass-ceramics makes them highly attractive for clinicians and patients. They exhibit excellent aesthetics, adequate strength, biocompatibility, and wear resistance (Montazerian and Zanotto, 2017; Ritzberger et al., 2010). This category includes Leucite-based glass ceramics, Lithium disilicate-based glass ceramics, and Zirconia-toughened silicate ceramics.

1.1.5.1 Leucite-based glass-ceramic

It is composed of potassium-aluminium-silicate ($KAlSi_2O_6$) homogeneously dispersed in a glass matrix. The addition of leucite crystals aimed to control the thermal expansion coefficient and increase the strength of glass-ceramic (Byeon and Song, 2018). The crystal size is 1-5 µm and constitutes 35-45 vol.% of the final product (Ritzberger et al., 2010). It is characterised by excellent aesthetics and biocompatibility. Owing to the high silica content (60 - 65 wt.%) the material is highly translucent. Due to relatively low fracture strength

(120 – 160 MPa), it is mainly indicated for inlays, onlays, and anterior crowns (Montazerian and Zanotto, 2017).

1.1.5.2 Lithium disilicate

Lithium disilicate was first introduced in 1998 in the pressable form as a strength enhanced upgrade of its predecessor pressable leucite-reinforced ceramic (Holand et al., 2000). It exhibited flexural strength of approximately 350 MPa and fracture toughness of 2.9 MPa$\sqrt{m}$ (Fu et al., 2020) and was indicated for veneers, crowns, and 3-unit FDPs up to the second premolar (Ritzberger et al., 2010). Due to their relatively high opacity, early generations were mostly used as a core for bilayered restorations which had to be subsequently veneered with a fluoroapatite glass-ceramic to replicate the optical properties of natural teeth. The pressable bilayered lithium disilicate reported high clinical survival rates for single crowns and 3-unit FPDs after 5 to 8 years (Marquardt and Strub, 2006; Wolfart et al., 2009). Most of the failures were reported for veneer fractures or connector failure.

The first CAD/CAM lithium disilicate was released in 2006 under the name IPS e.max CAD (Ivoclar Vivadent, Schaan, Lichtenstein). The early CAD/CAM version had lower biaxial strength and toughness than the pressable form, therefore it was only indicated for veneers, inlays, onlays, and single anterior crowns (Wiedhahn, 2007; Tysowsky, 2009). Over the years, the material went through several enhancements in strength and translucency and its indications were expanded to include full-contour single and multi-unit FDPs (Giordano, 2006). Currently, lithium disilicate is considered by most dentists the material of choice for anterior aesthetic crowns (Makhija et al., 2016) as it combines high biaxial flexural strength and superior aesthetic properties (Albakry et al., 2003; Conejo et al., 2017). A 100 % survival rate was reported clinically for single crowns made of lithium disilicate after 2 years (Li et al., 2014).

Monolithic lithium disilicate CAD/CAM blocks are available in the market in different sizes, shades, and translucencies (Reich et al., 2014). The blocks are supplied in a soft partially crystallised form characterised by their bluish colour and consist of 40 % lithium metasilicate (Li_2SiO_3) crystals and lithium disilicate ($Li_2Si_2O_5$) nuclei. The material in the “blue phase” has a flexural strength of 140 MPa which is easier to mill without causing excessive wear to the milling burs (Chen et al., 2008; Marchesi et al., 2021). After milling, the restoration is subjected to a firing cycle in a special furnace for a temperature of 840 °C in a

process called “Crystallisation”. During firing, the lithium metasilicate crystals transform into lithium disilicate crystals, which is accompanied by an increase in strength (Belli et al., 2017). After crystallisation, the restoration reaches its ultimate strength (450 MPa) and final shade and consists of 70% interlocking needle-shaped lithium disilicate crystals with lengths ranging between 0.5 and 4 µm (Holand et al., 2000; Ramos et al., 2016).

In a trial to save time and laboratory costs, GC (GC Corporation, Tokyo, Japan) introduced a new fully crystallised lithium disilicate CAD/CAM block (LiSi CAD). The blocks are available in different shades and translucencies and do not require firing after milling. The restoration can be polished chairside using a ceramic polishing kit and then becomes ready for delivery. According to the manufacturer, glazing is possible however is not mandatory. There is a lack of sufficient data about fully crystallised lithium disilicate blocks; therefore, more in-vitro and in-vivo studies are recommended.

1.1.5.3 Zirconia-reinforced lithium silicate

One of the methods employed to strengthen glass-ceramics is the addition of ZrO_2 to the glass matrix (Clarke and Schwartz, 2011). Zirconia-reinforced lithium silicate (ZLS) ceramics were developed as a modification to improve the mechanical and aesthetic performance of silicate-based ceramics (Zarone et al., 2021). They are composed of lithium metasilicate, and lithium orthophosphate crystalline phases in addition to 10 % tetragonal zirconia fillers, all embedded in a homogeneous glassy matrix.

The addition of zirconia fillers was aimed at increasing strength values through crack deflection (Elsaka and Elnaghy, 2016). According to Huang et al. (2014), the flexural strength and fracture toughness of lithium disilicate ceramics increased significantly when the percentage of the added ZrO_2 was between 15 and 30 wt.% while adding less than 10 % ZrO_2 has changed the morphology of the $Li_2Si_2O_5$ crystals from rod-shaped to spherical with an accompanying decrease in strength due to the loss of the tight interlocking effect of the rod-shaped crystals. The reinforcing mechanism depends on the difference in the coefficient of thermal expansion (CTE) between the glass phase and the crystalline phases. This resulted in the development of residual compressive stress in the glass matrix and tensile stress in the zirconia and lithium disilicate crystalline phases during cooling after sintering. This mismatch in the CTE has also played a role in the increase of fracture toughness through the “bridging toughening mechanism” in which the tensioned crystals

act as a bridge in the middle of the fracture line and the crack propagation is resisted. In addition, the transformation toughening mechanism of zirconia crystals is accompanied by volume expansion that reduces the stress concentration and prevents the further propagation of the crack (Huang et al., 2014).

The ZLS has 15 – 20 wt.% lithium silicate, 8 – 12 wt.% Zirconia and 55 – 65 wt.% silica (Bajraktarova-Valjakova et al., 2018). The crystalline phases in ZLS are more rounded and smaller in size than in lithium disilicate (Belli et al., 2017). The flexural strength after glazing is 370–420 MPa (Bajraktarova-Valjakova et al., 2018). One disadvantage reported for ZLS is their poor machinability compared to other glass-ceramics (Chen et al., 2020). The material is available commercially under two brand names: Celtra Duo (Dentsply Sirona, DeguDent, Hanau, Germany) and Suprinity (Vita Zahnfabrik, Bad Säckingen, Germany). They are provided in the form of CAD/CAM blocks of assorted sizes, shades, and translucencies. Vita Suprinity blocks are provided in a pre-crystalline state that requires firing after milling to reach their final strength, whereas Celtra Duo is provided in a fully crystallised block form. Even though firing of Celtra Duo restorations may not be obligatory, it has been reported to increase the material's strength (Attaallah et al., 2019; Schweitzer et al., 2020).

1.1.6 Zirconia

The name “zirconium” represents a chemical element (Zr) with the atomic number 40 and is taken from the Persian word “Zargun” which means “gold in colour” (Abd El-Ghany and Sherief, 2016). The oxide of zirconium metal (ZrO_2) is known as “zirconia” and was discovered by Martin Heinrich Klaproth, a German chemist, in 1789 (Piconi and Maccauro, 1999). In 1969, zirconia was used for the first time in the medical field as a hip head replacement prothesis (Cales, 2000). Since then, attention has turned to zirconia as a biomedical material that can be used in several medical disciplines due to its unique properties such as inertness and hardness. Over 20 years ago, zirconia was introduced as a prosthetic material for dental use following the advent of CAD/CAM technology in dentistry.

Zirconia can exist in three crystallographic phases: monoclinic, tetragonal, and cubic (Fig. 1). The monoclinic phase is stable at room temperature, but it has poor mechanical properties. The cubic phase is stable at elevated temperatures (above 2370 °C) and provides

moderate mechanical properties to the material. The tetragonal phase exhibits the best mechanical properties, and it is only stable between 1170 °C and 2370 °C (Hannink et al., 2000; Ruiz and Readey, 1996). The heating of zirconia is accompanied by volume reduction due to phase transformation and accompanying shifts in lattice positions. During cooling, the phase transformation from cubic to tetragonal is accompanied by an approximately 2.3 % increase in volume, and an additional 4-5 % during the transformation from tetragonal to monoclinic. This sudden increase in volume during cooling produces excessive intolerant tension that leads eventually to the development of catastrophic cracks and breakdown of the ceramic structure. To be able to use zirconia as restorative ceramic, stabilising oxides were added to prevent phase transformation and to enable the stabilisation of tetragonal or cubic phases at room temperature (Abd El-Ghany and Sherief, 2016; Stawarczyk et al., 2017).

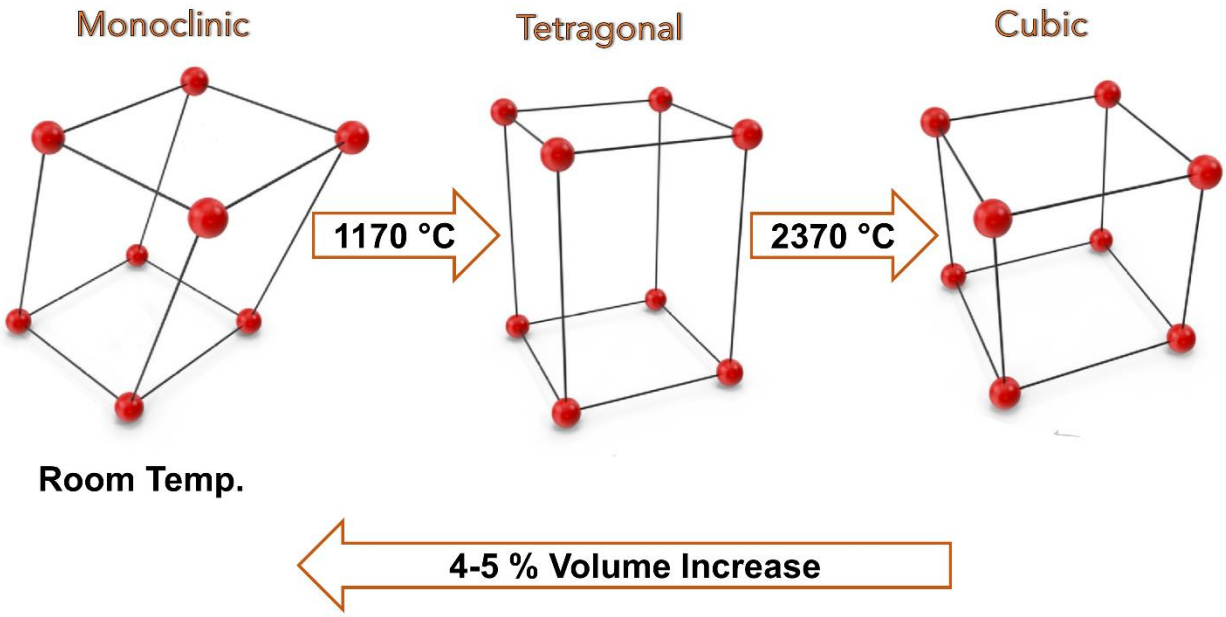

Fig. 1: Shows the three crystallographic forms of zirconia: monoclinic, tetragonal, and cubic. Transformation between phases is accompanied by volume change.

1.1.6.1 Transformation toughening

The transformation toughening phenomenon of ZrO_2 was first discovered in 1975 (Garvie et al., 1975). It is a characteristic process that takes place in the Y-TZP under stress. The brittle nature of ceramics does not allow the material to accommodate increased strain conditions, therefore high stresses induce cracks (Zmak et al., 2019). The concentrated energy at the crack tip induces localised phase transformation from tetragonal to monoclinic associated with an approximate 3 % volume expansion. Consequently, compressive stresses are formed around the tip of the crack preventing further propagation (Fig. 2). Transformation toughening is responsible for the high fracture toughness of zirconia.

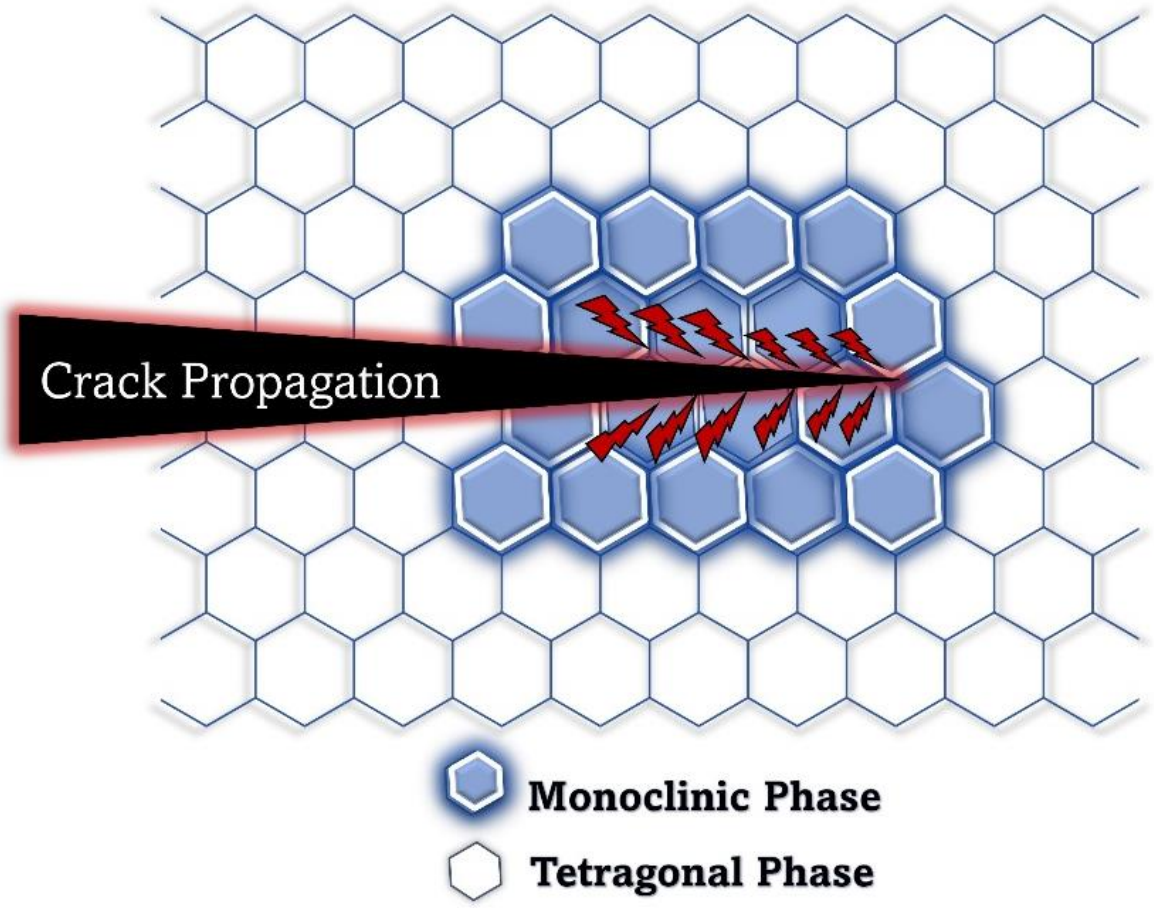

Fig. 2: Shows the mechanism of the "transformation toughening phenomenon". The volume increase accompanied with *t-m* phase transformation at the propagating crack's tip creates compressive stresses that limits further crack propagation. (Modified from Zmak et al., 2019).

1.1.6.2 Hydrothermal ageing of zirconia

One of the drawbacks of Y-TZP is the susceptibility to progressive hydrothermal ageing in moist environments at room temperature. The so-called low-temperature degradation (LTD) involves water penetration into the surface microcracks of the restoration, leading to destabilisation and transformation of the metastable tetragonal zirconia phase to the more stable monoclinic phase without any external mechanical stress. Local volume expansions due to phase transformation result in compressive stresses, leading to the collapse of grain boundaries. This is followed by the further penetration of fluids and microcracks, which transfer internal stresses deeper into the bulk of the material, ultimately leading to a degradation in strength. Incorporating a small amount of oxide additives such as alumina, retaining a smaller grain size, and increasing cubic phase content can help prevent or reduce LTD (Harada et al., 2016; Zhang and Lawn, 2018).

1.1.6.3 Generations of zirconia

Stawarczyk et al. (2017) classified the zirconia into 3 generations that are different in composition, properties, and indications. The first generation of zirconia is the 3 mol% yttrium partially stabilised tetragonal zirconia polycrystals (3Y-TZP), which is mostly referred to as “conventional zirconia”. It is hard white opaque zirconia consisting of tetragonal crystals and has a high light refractive index. The characteristic opacity of this generation is attributed to the small grain sizes (in the range ~0.5 to 1 μm) which encompass the visible light wavelength spectrum, in addition to the birefringence property of the tetragonal phase (Zhang and Lawn, 2018). It has high flexural strength (900 – 1400 MPa) and high fracture toughness (9 – 12 MPa $\sqrt{m}$). The higher toughness is due to the transformation toughening phenomenon. Due to its high opacity and hardness, it is used as a framework that must be covered by porcelain veneer to give the desired aesthetics and prevent excessive wear of opposing dentition (Miyazaki et al., 2013). The high strength and toughness of the material allowed it to be used for the fabrication of a framework for a long-span fixed dental prosthesis (FDP) in load-bearing areas (Piconi and Maccauro, 1999; Zhang et al., 2019).

The second generation was introduced in 2012 as a modification of the first generation by reducing the number and grain size of the aluminium oxide (Al_2O_3) grains and relocating them relative to the zirconia grains. This modification allowed more light transmission and relatively increased translucency. In this generation, zirconia was allowed to be used as

a monolithic restoration for the first time. However, since the aesthetic quality was still inferior to that of glass ceramics, products from this generation were only used as full-contour restorations in less aesthetic areas (e.g., posterior).

The third generation is referred to as partially stabilised zirconia (PSZ) with more than 50 % stabilised cubic phases. Other authors refer to it as fully stabilised zirconia (FSZ). The stabilisation of the cubic phase is achieved through the increase of yttrium percentage to more than 3 mol%. The first introduced example in this generation was the 5Y-PSZ in which about 5 mol% yttrium oxide (approximately 9.5 wt.%) was added, which resulted in more than 53 % cubic phase in the sintered material. The translucency of the third generation was remarkably increased due to the isotropic nature of the cubic crystals that allow more even light transmittance in all spatial directions. Furthermore, the larger grain size (~1.5 µm) and higher volume of the cubic crystals allow more light transmittance at the grain boundaries. However, the substitution of tetragonal phases with cubic phases was accompanied by a noticeable drop in the mechanical properties (Pereira et al., 2018). The decrease in strength and toughness is due to the absence of stress-induced transformation in the cubic zirconia (Zhang et al., 2016a). Furthermore, a recent investigation attributed the reduced mechanical properties to the wider dimensions of cubic grains than tetragonal ones which segregate more stabilising oxides; therefore, the tetragonal phase becomes more susceptible to ageing (Camposilvan et al., 2018).

In several studies it was reported that the translucency of this generation is comparable to that of silicate ceramics, therefore it has almost the same indications as lithium disilicate (Zarone et al., 2019). Due to the low strength relative to conventional zirconia, it can be used for short-span FDPs of a maximum of 3 units. To achieve a balance between strength and translucency the added yttrium oxide content was reduced in the following products to around 4 mol%, which resulted in less amount of stabilised cubic phases in the final material. According to recent studies, the fourth generation is the most recent and refers to the multilayer zirconia that has a multichromatic structure with shade and translucency gradients as well as strength gradients similar to that found in the natural tooth (Kaizer et al., 2020; Kolakarnprasert et al., 2019; Vardhaman et al., 2020). In this system, the final restoration is composed of two types of zirconia (e.g., 5Y-PSZ/3Y-PSZ or 5Y-PSZ/4Y-PSZ) with an intermediate transition zone (Badr et al., 2022).

1.1.7 Wear

1.1.7.1 Tooth wear

Wear is defined as “a progressive loss of substance from the operating surface of a body occurring as a result of relative motion at the surface” (Yamaguchi, 1990). In dentistry, wear is a broad term that describes the irreversible surface loss of tooth hard tissues due to causes other than caries or trauma. Tooth wear is a multifactorial process and could be due to erosion, abfraction, abrasion, or attrition. Attrition is the loss of tooth structure at the biting surfaces during mastication due to tooth-to-tooth contact (Eccles, 1982). Attrition is sometimes referred to as physiological tooth wear and it can occur at the occlusal surfaces between opposing teeth or at the interproximal tooth surfaces between adjacent teeth (Davies et al., 2002). Physiological tooth wear can be beneficial for the adaptation of the teeth to changes in the dental arch and the achievement of balanced occlusion (Kaidonis, 2008). The normal rate of physiological wear due to mastication was reported to be approximately 20-38 µm vertical enamel loss per year (Lambrechts et al., 1989). Pathological tooth wear is the abnormal loss of surface tooth structure at a rate that exceeds the acceptable limits and affects the oral health-related quality of life (Warreth et al., 2020).

In mastication, the chewing cycle is divided into three phases (Ghuman, 2016): the first phase starts with the separation of maxillary and mandibular teeth as the jaws move away from each other and ends shortly before the jaws return to the closing position. There is no force applied to the teeth during this phase, and it is not involved in the wear process. The second phase starts when the teeth contact the food bolus and ends with intercuspation. In this phase, the food is crushed, and abrasion is responsible for the wear. In the third phase, the opposite teeth are in direct contact and slide against each other to tear the food bolus. During this phase attrition and abrasion are involved in the wear process. The third phase ends when the teeth separate again, and a new chewing cycle begins. A variety of oral-related factors influence the degree of tooth wear such as food type, oral habits, enamel quality, and neuromuscular behaviour (Johansson et al., 1993; Mair et al., 1996).

Apart from the oral-related factors, dental restorations may cause progressive enamel wear in opposite teeth to varying degrees depending on the physical, chemical,

microstructural, and surface properties of the restorative material used. Therefore, there is considerable concern among clinicians regarding the wear process between ceramic restorations and tooth substrates. Ceramic materials designed for crowns and FDPs should have microstructural and bio-tribological properties similar to those of natural teeth to prevent excessive wear on the enamel of the antagonist (Mitov et al., 2012). If the abrasiveness of a dental ceramic exceeds a certain limit it becomes unsuitable for clinical use (Nakashima et al., 2016). The higher abrasiveness of restorative material will lead over time to adverse consequences such as loss of anatomy, exposure of sensitive tissues, deterioration of occlusion, and the development of TMJ problems (Jacobi et al., 1991).

Dental ceramic materials were reported to induce higher enamel wear than other restorative materials according to some researchers (Sripetchdanond and Leevailoj, 2014; Zandparsa et al., 2016). It has been demonstrated that the veneering porcelain in bilayered restorations produces excessive wear on the opposing dentition (Zurek et al., 2019). Despite the absence of the abrasive veneer layer in monolithic restorations, the continuous development of the physical properties of monolithic ceramic materials raises concerns about their wear performance after prolonged friction against natural teeth during mastication. Monolithic zirconia was reported to produce less wear in antagonist enamel than feldspathic porcelain, leucite reinforced glass, and enamel (Nakashima et al., 2016). Contrarily, lithium disilicate produced significantly greater enamel loss in antagonist teeth, however, the enamel loss was similar to that produced by natural teeth (Nakashima et al., 2016; Sripetchdanond and Leevailoj, 2014). In other studies, no significant difference in antagonist enamel wear between zirconia and glass-based ceramics were reported (Ludovichetti et al., 2018).

Several factors have been investigated for their role in the wear potential of ceramic materials such as hardness, surface roughness, elastic modulus, and coefficient of friction (Freddo et al., 2016; Lawson et al., 2016; Mormann et al., 2013). The role of hardness in the wear of the antagonist is still controversial. Some authors reported that enamel wear increases when the hardness of the opposing material increases (Ludovichetti et al., 2018; Mormann et al., 2013), while others reported no correlation between hardness and wear potential (Freddo et al., 2016; Heintze et al., 2008; Oh et al., 2002; Seghi et al., 1991).

Several studies have demonstrated that enamel wear caused by dental ceramics is closely related to fracture toughness and surface roughness rather than hardness (Fischer et al., 1989; Metzler et al., 1999). There has been evidence that antagonist wear occurs more pronounced when the fracture toughness of the enamel is significantly lower than that of the ceramic material (Heintze et al., 2008). Similarly, Ghazal and Kern (2009) reported a significant correlation between the volumetric enamel loss and the surface roughness of the antagonistic ceramic (r=0.667). The intrinsic and machining-induced surface flaws were reported to reduce the strength and increase the abrasiveness of dental ceramics (Oh et al., 2002). Therefore, meticulous finishing of the restoration before cementation is critical. Ceramic restorations in general can be polished or glazed. Surface glazing increases the strength of the restorations and produces a glossy surface. It was once believed that glazed surfaces cause less wear to opposing dentition, however, this was reported to be only limited to a short period after cementation. According to Jagger and Harrison, the glaze layer is removed after approximately 2 days of intraoral wear leaving a rougher surface behind (Jagger and Harrison, 1994). Chairside occlusal adjustments remove the glaze layer and increase the abrasiveness of the restoration. Few studies reported that polishing can produce similar or even smoother surfaces and less enamel wear than glazing (Jacobi et al., 1991; Jagger and Harrison, 1994; Raimondo et al., 1990). Magne et al. (1999) reported no difference in wear characteristics of feldspathic and aluminous porcelain between chairside polished and laboratory glazed specimens.

1.1.7.2 Ceramic Wear

Similar to teeth, restorations are also prone to wear during mastication. While the type of ceramic might strongly affect wear behaviour, many other factors should be contributing to the complexity of the wear process. Surface friction during chewing and parafunctional habits like bruxism and clenching cause wear to the ceramic surface, especially in the presence of moisture (Preis et al., 2012). Also, the nature of the antagonist, abrasiveness of food, and patient's habits are among the wear contributing factors (Johansson et al., 1993; Kim et al., 2001). The choice of the ceramic material and the appropriate surface treatment plays an important role in minimising the wear of both restoration and antagonist (Preis et al., 2012). Ceramic materials should have sufficient hardness to withstand the forces of mastication and preserve their surface integrity while remaining non-abrasive to

the opposing dentition. Ideally, dental restorative ceramic materials should undergo wear rates that are similar to physiological enamel wear rates.

1.1.7.3 Wear simulation in literature

The in-vivo evaluation of dental materials is essential for the accurate assessment of their performance. However, the complexity of the oral environment, high variability among patients, intraoral measurements, and high costs are typical barriers to clinical studies. Only in few studies in literature was the wear investigated in-vivo, but they were reported to be extremely complicated and time-consuming (Esquivel-Upshaw et al., 2006; Stober et al., 2014). So, it is usual to assess wear in-vitro under controlled conditions using wear simulators (Heintze, 2006).

The in-vitro studies in the literature that tested the wear of restorative materials and antagonists are generally divided into two types: two-body wear or three-body wear. In the two-body wear mechanism, there is direct contact between the restoration and the antagonist. This condition occurs usually in the oral cavity during non-masticatory tooth movement and at the end of the masticatory cycle. The three-body wear involves the addition of an intervening medium between the occluding surfaces. It represents the wear that occurs during food mastication. The abrasive potential of the diet may influence wear behaviour during three-body movement. Several media have been used to simulate food bolus in laboratory studies including cornmeal, poppy seeds, flour, rice, or polymethyl methacrylate beads (Amer et al., 2014; Koottathape et al., 2012; Wang et al., 2019). The three-body wear is lower than two-body wear since the occluding surfaces are in contact with softer food which has a lower friction coefficient (Ghazal and Kern, 2009; Wang et al., 2019). Most laboratory studies investigating the wear of dental ceramics and natural teeth are conducted in two-body wear in order to eliminate the intermediate medium variable and to focus on the more destructive attrition wear caused by tooth-restoration contact (Wang et al., 2019).

In literature, there is no standard protocol for testing wear in-vitro. Researchers use various wear devices/methods, parameters, antagonists, and wear quantification methods. Different chewing simulators and wear testing devices are being used such as ACTA, Alabama, Zurich, Willytech, Pin-on-disc, and others (Heintze et al., 2012; Lewis and Dwyer-Joyce, 2005). Other research centres have developed specially designed

machines to simulate the clinical wear process under controlled conditions (Koottathape et al., 2012). Different motions are used by different devices, including rotation/sliding, sliding, and vertical/sliding (Borrero-Lopez et al., 2019; Janyavula et al., 2013; Lawson et al., 2016). The sliding distance ranges from 0.6 to 8 mm (Heintze et al., 2008). The lateral movement during mastication was reported to be approximately 1.5 mm therefore in many studies the horizontal sliding distance was adjusted to 2 mm (Janyavula et al., 2013; Lawson et al., 2016). There is a wide range of cycles, from 10,000 to 1,200,000, though most studies use a cycle range between 120,000 and 400,000 with a frequency range of 1 to 1.6 Hz (Delong et al., 1992; Janyavula et al., 2013; Lawson et al., 2016; Mitov et al., 2012).

The applied force varies between 10 and 50 N. Some researchers applied much higher loads up to 200 N (Kaizer et al., 2019). The sample shape varied between anatomical and flat specimens. Different antagonists were reported, in some studies human teeth, bovine teeth, cusps of premolars, cusps of molars, zirconia sphere, metal, or ceramic steatite were utilised. In the studies that used natural teeth as an antagonist, some used standardised, and others used non-standardised teeth. The lubricant mediums used were artificial saliva, glycerine, distilled water, or demineralised water. Some devices provide additional thermocycling between 5 °C and 55 °C to the samples during the test. Because of the differences in wear testing protocols among different wear simulators, comparing the results of one study with those of another is difficult.

1.1.7.4 Wear quantification

Several methods have been used to quantify the amount of wear taking place on the occluding surfaces. Borrero-Lopez et al. (2019) used an optical microscope and SEM to measure the radius of the formed scar. Mitov et al. (2012) measured the vertical substance loss in enamel and ceramic using a laser microscope. Other studies used profilometry to measure the degree of developed roughness and/or generate 3D scans that are superimposed to determine the volumetric loss (DeLong et al., 1989; Janyavula et al., 2013; Ludovichetti et al., 2018; Magne et al., 1999). Zierden et al. (2018) quantified the ceramic wear by measuring the weight loss using a sensitive scale. As a part of their study, a micro-CT scanner was used to produce 3D images of teeth in intact and worn phases, and then the images were superimposed to quantify volumetric enamel loss.

1.1.8 Strength of dental ceramics

The strength of dental prostheses is one of the most decisive factors for the success of restorative treatment. The restorations are subjected to a wide range of chewing forces during mastication, ranging from 40 to 440 N in a normal situation, and may reach up to ~800 N for short periods in certain cases (Kelly, 1997). The distribution of masticatory stresses depends on the geometry of the prosthesis (Zhang et al., 2013). Stresses falling on tooth-shaped restorations divide into compressive and tensile components (Fu et al., 2020). Dental ceramics, being brittle in nature, are prone to crack propagation when subjected to tensile forces (Zhang et al., 2013). Although the failure of dental ceramic could happen abruptly under intense overload, it is more likely to fail as a result of cumulative subcritical stresses over an extended period which is referred to as “fatigue failure” (Zhang et al., 2013).

The reliability of ceramic restorations was once believed to be less than traditional PFM prostheses (Kelly, 2004), however, the poor aesthetics and absence of biocompatibility have pushed toward the rapid shift toward more aesthetic yet less tough alternatives. Recently, the trend toward monolithic restorations has added a challenge to dental ceramics due to the elimination of the high-strength core support. In recent years, the use of monolithic all-ceramic crowns has gained popularity over traditional multi-layered prostheses due to the elimination of veneer-related complications and the allowance for more conservative teeth preparations. In Germany, a practice-based research study conducted in 2020 found that 82 % of surveyed dentists preferred ceramic restorations for single-unit crowns, while only 14 % chose PFM (Rauch et al., 2021). Similarly, a survey in 2016 among dentists in the US found that only 9 % chose PFM, 17 % chose layered zirconia, and approximately 72 % chose monolithic ceramics. (Makhija et al., 2016).

The development of monolithic dental ceramics has witnessed a great challenge regarding the compromise between strength and aesthetics. Highly aesthetic porcelain ceramics have low fracture resistance. Conversely, high-strength ceramics such as alumina and zirconia have a lower aesthetic quality. Glass-ceramics were believed to be midway between both categories. Yttria-stabilised tetragonal zirconia polycrystal (Y-TZP) is the strongest among all restorative ceramics. Zirconia doped with 3 mol% yttria (3Y-TZP) has 1000 – 1200 MPa flexural strength, ~14 GPa hardness, and 4 – 8 MPa$\sqrt{m}$ fracture

toughness (Borrero-Lopez et al., 2019; Turon-Vinas and Anglada, 2018). Transformation toughening is responsible for the high fracture toughness and the crack resistance of conventional zirconia. Different factors influence fracture toughness such as sintering temperature, crystal morphology, grain size, and yttria content (Turon-Vinas and Anglada, 2018).

The 3Y-TZP was however not suitable for monolithic tooth restorations due to high opacity (Pecho et al., 2012). Researchers' relentless efforts to enhance the translucency of zirconia have led to the introduction of new zirconia generations that are reported to compete with glass-ceramics in terms of aesthetics (Harada et al., 2016). However, the improvement of translucency has come at the expense of strength (Zhang et al., 2016a). In the new translucent zirconia, strength has dropped to 500 - 800 MPa and fracture toughness to 2.2 - 3.5 MPa√m (Zhang and Lawn, 2018). Still, the strength of these new generations is equal to or higher than glass-ceramics. A mechanical advantage of the new translucent zirconia generations is the absence of low-temperature degradation (LTD) (Stawarczyk et al., 2017; Zhang et al., 2019), which was the main concern and potential risk in the old generations of zirconia (Zhang et al., 2016a). However, the mechanical and optical properties of the newest zirconia generations are not fully defined (Zhang et al., 2019).

Some studies measured the fracture strength of ceramic materials under static load-bearing tests which gives an idea about the initial material strength. However, only a few studies focused on the fatigue behaviour under cyclic loads (slow crack growth fatigue) (Baladhandayutham et al., 2015; Özcan and Jonasch, 2018). Exposing the material to a large number of load cycles in a humid environment simulates the clinical situation and allows a better understanding of the long-term mechanical stability of the ceramic prosthesis during function, especially for posterior mouth segments where high chewing loads are inevitable (Özcan and Jonasch, 2018).

1.1.9 Aesthetics

The eyes and mouth are the most common features associated with facial attraction (Baldwin, 1980). In dentistry, the main objective of aesthetics is to create a pleasant smile which is one of the important skills for interactive communication (Joiner, 2004). Furthermore, aesthetic dental treatment has been said to affect psychological health and increase the patients' self-esteem (Davis et al., 1998). Aesthetic restorations are used to restore

damaged or missing teeth, correct misalignment, treat discolouration or adjust the proportions of teeth to be in harmony with the face of the patient (Joiner, 2004). The colour of the natural tooth depends on the interaction of the tooth hard tissues with the incident light before it reaches the observer's eye (Vanderburgt et al., 1990). Two optical properties have been shown to characterise the aesthetics of dental ceramics, namely: colour and translucency (Fu et al., 2020). An excellent aesthetic restoration is usually the result of a good colour match and adequate translucency (Pecho et al., 2012; Perez et al., 2010; Raptis et al., 2006).

1.1.9.1 Colour

The colour of dental ceramics is based on the commonly used CIELAB colour system which was introduced by the "Commission International de l'Eclairage" (CIE) and allowed the numeric description of the colour (Della Bona et al., 2014). In this system, three coordinate values (L*, a*, b*) are used to locate the object's colour within the CIELAB colour space (Fig. 3). The L* coordinate represents the degree of lightness in the range from 0 to 100. The a* coordinate represents the degree of redness or greenness. The b* coordinate represents the degree of yellowness or blueness. The colour difference between two objects is represented by (ΔE) and it can be used to evaluate the change in colour for the same object after a certain treatment. ΔE can be calculated based on differences between colour coordinates of two objects according to the following formula:

$$\Delta E = [(\Delta L)^2 + (\Delta a)^2 + (\Delta b)^2]^{1/2} ,$$

It was reported that an $\Delta E > 1.2$ can be detected by the human eye (Paravina et al., 2015). Moreover, $\Delta E > 3.5$ was reported to be the clinical perception threshold of colour mismatch in the dental practice (Bagis and Turgut, 2013; Turgut and Bagis, 2011; Yilmaz and Karaagaclioglu, 2011).

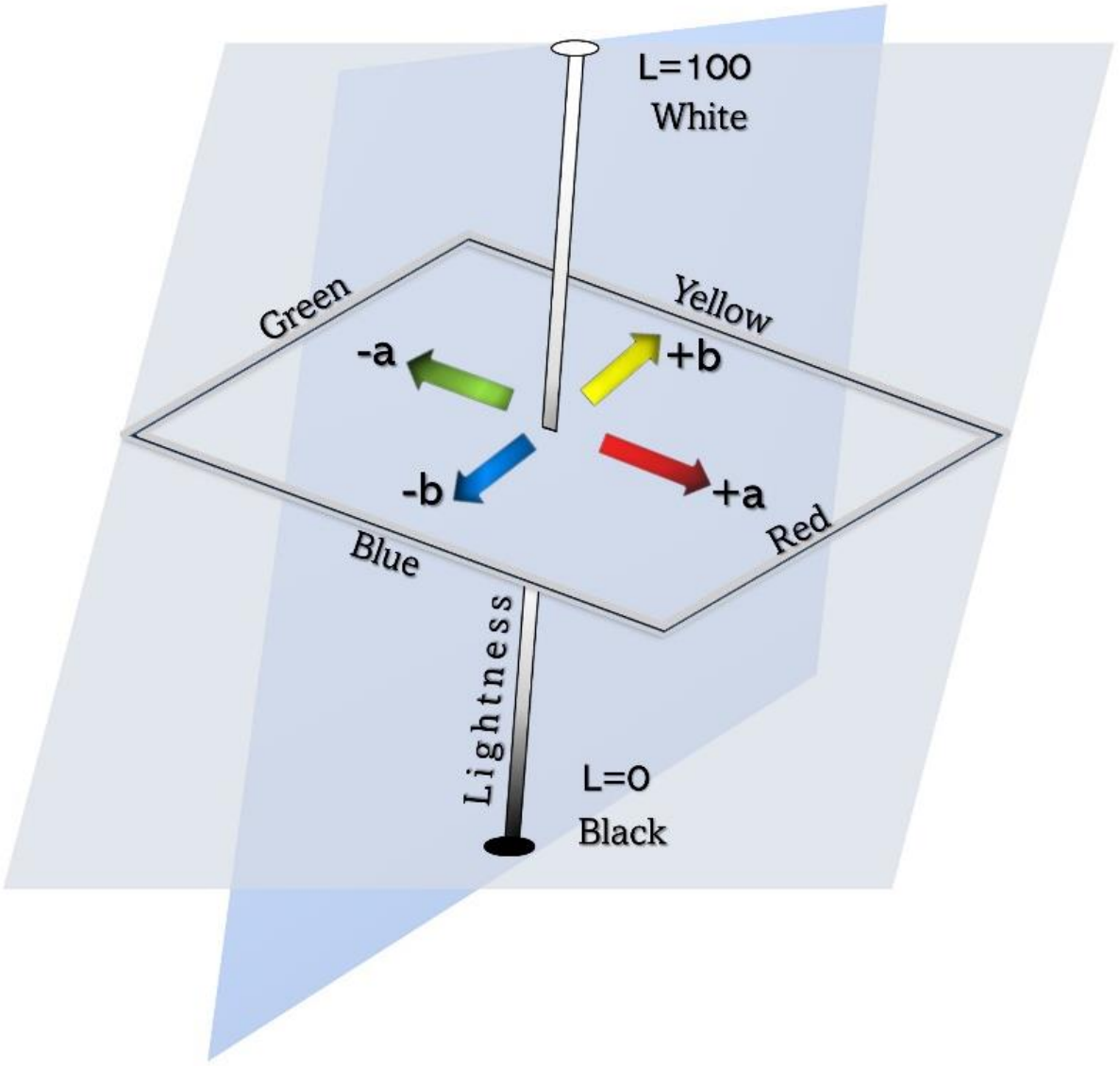

Fig. 3: The CIELAB colour space defined by the International Commission on Illumination. It consists of three axes that represent the colour: L axis indicates the lightness and ranges from 0 (black) to 100 (white), a* axis indicates the green-red colour range, and b* axis indicates the blue-yellow colour range.

Restoring the natural appearance of teeth during restorative treatment is challenging for both clinicians and laboratory technicians (Tabatabaian et al., 2021; Wee et al., 2002). Matching the natural human tooth is influenced by several factors involving colour, translucency, surface texture, fluorescence, and lighting conditions (Ozturk et al., 2008; Vichi et al., 2011). Moreover, tooth colour is a combination of the optical properties of two different hard dental tissues (enamel and dentin). Dentin is relatively thick, opaque, and chromatic while enamel is relatively thin, more translucent, and achromatic. If a dental ceramic material is to mimic the natural look of teeth, it must have a layering gradient similar to natural teeth (Corciolani et al., 2011).

Selecting the correct tooth shade is the first step in the achievement of good matching. Shade guides are used for shade selection in which the natural tooth tissues are compared with the tooth-shaped shade tabs. Various commercial shade guides are available, however, the most commonly used are “VITAPAN classical” and “VITA 3D Master” from VITA Zahnfabrik (Lehmann et al., 2017). The “Vitapan classical” consists of 4 groups based on hue, each is composed of 4 tabs that are arranged according to value and chroma. However, shade selection following this sequence was reported to be difficult (Lehmann et al., 2017). Therefore, the “Vita 3D master” shade guide was later introduced to simplify the shade selection process (Corciolani et al., 2011). In this system, shade is selected according to colour parameters in the following order (value - chroma - hue) and better matching to natural teeth is achieved (Corciolani et al., 2009). Ivoclar Vivadent has also introduced an A – D universal shade guide that corresponds to the shade standards for their products.

Shade selection using manual shade guides is highly subjective, and it depends on the observer’s colour perception at the moment of shade selection. The individual perception of colour is affected by several factors such as the operator’s experience, lightning condition, surface texture, eye fatigue, metamerism, and colour of adjacent structures such as gingiva, lips, and skin (Curd et al., 2006; Joiner, 2004; Najafi-Abrandabadi et al., 2018). To automate the shade capture process and eradicate human error, intraoral colourimeters and spectrophotometers have been developed (Posavec et al., 2016). The reliability and accuracy of these devices have been widely investigated in previous studies (Curd et al., 2006; Kim-Pusateri et al., 2009; Lagouvardos et al., 2009; Llena et al., 2011;

Weyhrauch et al., 2015). Some devices measure the CIELab and/or CIEch values and determine the tooth shade based on an internal database of available shade guides such as Vita 3D master or Vita Classical then convert the reading to the corresponding shade tab (Tabatabaian et al., 2021).

Nowadays, most manufacturers provide the CAD/CAM ceramic blocks in a colour-coded pre-shaded form. Some have integrated the gradient transition in colour between different layers of the block to resemble the natural tooth. Most ceramic CAD/CAM systems use the Vita Classical colour coding. Shades taken by other shade guide systems can be converted using shade converters.

1.1.9.2 Translucency

Appearance is a complex phenomenon that depends on many defining visual elements such as gloss, colour, texture, and translucency (Gigilashvili et al., 2021). Translucency is defined as the property of light transmission or diffuse reflection from a material's surface through a turbid medium (Brodbelt et al., 1980). It can be viewed as a phenomenon that lies in a level between total transparency and total opacity. Translucency has been described as an important aesthetic parameter and one of the primary factors influencing the performance of dental restorations in terms of aesthetic aspects (Winter, 1993; Xiao et al., 2014). A life-like natural appearance can only be achieved when the restoration has a similar translucency to the natural tooth (Pecho et al., 2012). Furthermore, the influence of translucency in aesthetic restorative materials on the masking ability of the underlying structures has a significant impact on the final aesthetics (Vichi et al., 2000). Another clinical implication of translucency in restorative materials is its influence on the penetration depth of light and the curing quality of the underlying light-cured cement (Lee, 2015), which has an impact on the long-term durability and stability of the restoration.

The translucency of the restorations is affected by several factors including material composition, microstructure, thickness, and surface finish (Akar et al., 2014; Subasi et al., 2018). The increase in crystalline content in an attempt to increase strength usually results in greater opacity (Church et al., 2017; Della Bona et al., 2014). Feldspathic porcelain has the highest translucency and the most natural look; however, it is the weakest of all ceramic materials (Datla et al., 2015). On the other hand, polycrystalline-based ceramics such as alumina and zirconia are the toughest and the most opaque at the same time

(Tabatabaian, 2018). The size and distribution of the crystallites also influence translucency (Pecho et al., 2012). Smaller and homogenously distributed crystals allow less light scattering, and more light is transmitted through the material. Elimination of porosity in the manufacturing phase is another way to enhance translucency (Zhang and Lawn, 2018). Moreover, translucency is significantly influenced by the thickness of the material. Church et al. (2017), reported a dramatic decrease in the translucency parameter of zirconia specimens as the thickness increased.

Several methods were used in literature to evaluate translucency. In some studies, the percentage of direct light transmittance was examined (Della Bona et al., 2014; Spink et al., 2013), in others the contrast ratio (CR) or the translucency parameter (TP) were calculated (Bagis and Turgut, 2013; Church et al., 2017; Kurt and Turhan Bal, 2019; Shono and Al Nahedh, 2012; Vichi et al., 2016). The CR is the difference in reflectance from an object against black and white backgrounds. The TP is the difference in colour parameters of material of given thickness when measured over black and white backgrounds (Della Bona et al., 2014). The lower the TP value the opaquer the material and vice versa (Pecho et al., 2012). The correlations between these parameters were examined in few studies (Barizon et al., 2013; Della Bona et al., 2014; Spink et al., 2013; Yu et al., 2009). Barizon et al. (2013) observed a significant correlation between CR and TP when examining the translucency of different ceramic materials. Based on their results, both parameters can be used to assess the relative translucency of dental ceramics.

1.1.10 Microstructure analysis methods

1.1.10.1 Scanning Electron Microscopy (SEM)

The SEM can produce high-resolution images of the specimen's surface at high magnifications up to 1,000,000X which cannot be achieved by conventional optical microscopy. It can be used to get information about the surface topography and crystalline structure of examined materials. Furthermore, SEM can be used in combination with an element dispersive X-ray unit to analyse the chemical composition of the material under investigation. An additional advantage over the optical microscope is the larger depth of field in the SEM that allows most of the examined area to be in focus regardless of the surface levelling (Vernon-Parry, 2000).

The SEM utilised an incident electron beam in which electrons are activated to energies up to 30 KV using an electron gun. The beam is focused by electromagnetic condenser lenses into a fine probe that is directed to the area of interest in the specimen. The “depth of penetration” inside the specimen’s surface is determined by the energy and angulation of the beam and the atomic masses of the specimen elements. Detectors are used to collect the secondary electrons in a high vacuum to form an image that shows the topography of the sample. The samples examined using this technique must be conductive, therefore non-conductive substances such as teeth and dental ceramics are subjected to sputtering using Au or Au/Pt prior to examination. The application of an ultra-thin coating of electrically-conducting material on the sample prevents the accumulation of static electric charge on the specimen during scanning and improves the resolution because secondary electron emission near the surface is enhanced (Paradella and Bottino, 2012).

SEM is commonly used in the research field for all disciplines of dentistry. It can be used to evaluate bacterial leakage in the root canal, gaps between root canal filling and dentin wall, fracture patterns of intra-radicular cement, the topography of dentin surface, the topography of enamel surface after different treatments, morphologies of implant surfaces of different materials and treatments, and so on (Saghiri et al., 2012). Magnifications ranging from 500X to 10,000X were used for examining the topography and crystal structures of restorative materials.

1.1.10.2 Energy dispersive X-ray analysis

Energy dispersive X-ray spectroscopy (EDX) is a non-destructive process by which the chemical elements present in a material are identified and counted (Orasugh et al., 2020). In this technique, a high-energy electron beam is directed to the examined sample. When the electron beam hits the atoms, electron holes are created due to the ejection of some electrons from the inner shell atomic orbit. When the ionized atoms return to their ground state, the outer shell electrons with higher energy are transmitted to fill up the electron holes in the inner shell orbit and they release the extra energy in form of an X-ray. The emitted X-ray has an amount of energy equal to the difference between the energies of the two orbital levels which is characteristic of each element (Fernandez-Segura and Warley, 2008).

1.1.10.3 X-ray diffraction

X-ray diffraction (XRD) is a powerful technique that is commonly employed in research and industry to determine the shape and amount of crystalline phases in materials (Gonon, 2021). The XRD analysis is done with an X-ray source of Cu Kα radiation (λ = 1.5406 Å). When the X-ray is directed to a crystalline material, they are diffracted by certain angles and intensities from every set of lattice planes in a sample. The deflection angle defines the shape of the unit cell (crystal or grain), while the peak intensity describes the arrangement of atoms in the unit cell. Every material has a unique periodic atomic arrangement, therefore the XRD pattern is characteristic of the material. Comparing the experimental pattern to diffraction patterns in the online databases enables quick phase identification for unknown crystalline samples (Cheng, 2021).

1.1.11 Previous studies in literature

1.1.11.1 Studies on wear

Lawson et al. (2016) measured the volumetric wear in LD (e.max CAD) and ZLS (Celtra Duo) rectangular shaped specimens as well as in enamel of antagonist premolar cusps after 400,000 cycles at 20 N force. Enamel specimens were used as a control. Both ceramic materials showed similar wear values; however, they both showed more wear than enamel. The antagonist wear was greater for the LD than ZLS or enamel. Ludovichetti et al. (2018) investigated the wear resistance and abrasiveness of monolithic CAD/CAM materials against bovine enamel after 200,000 wear cycles at a force of 15 N. The study included LD (e.max CAD), ZLS (Vita Suprinity), and 3Y-TZP (Lava Plus). The 3 materials showed similar abrasive potential to the antagonist; however, zirconia was significantly more wear resistant. Sripetchdanond and Leevailoj (2014) evaluated the wear of enamel caused by monolithic ceramic materials. The tested materials included monolithic zirconia (Lava All Zirconia) and LD (e.max Press). The authors used enamel specimens prepared from human permanent molars as antagonists. In a pin-on-disk wear machine, the enamel specimens were abraded against the ceramic specimens for 4,800 cycles at 20 rpm and 25 N force. The LD showed significantly higher average wear depth in the enamel (7.32 ± 2.06 µm) compared to monolithic zirconia (1.83 ± 0.75 µm).

1.1.11.2 Studies on strength and fatigue of dental ceramics

In an experiment by Zhang et al. (2016b), the fracture resistance of various monolithic ceramic crowns (Lava plus and IPS e.max CAD) was investigated. All crowns were able to sustain high biting forces, however, zirconia was more split resistant than lithium disilicate. Similarly, Church et al. (2017) reported significantly higher flexural strength of high translucent monolithic zirconia compared to lithium disilicate at different thicknesses. Nishioka et al. (2018) evaluated the fatigue strength of translucent zirconia, lithium disilicate, and zirconia reinforced lithium silicate using a biaxial piston-on-ball flexural setup. The disc-shaped samples were subjected to 100,000 cycles at an initial load of ~60 % of the mean load-to-failure of the material and a step size of 5 % of the initial load. They reported that translucent zirconia presented higher fatigue strength (370.2 ± 38.7 MPa) than lithium disilicate (175.2 ± 7.5 MPa) and Zirconia reinforced lithium silicate (152.1 ± 7.5 MPa). Baladhandayutham et al. (2015) compared the fracture strength of monolithic ceramic crowns (IPS e.max; Ivoclar Vivadent & LAVA; 3M ESPE) at clinically relevant thicknesses (1.2 & 1.5 mm for LD and 0.6 mm for MZ) after cyclic loading. The crowns were cemented to identical resin dies and subjected to 200,000 load cycles at 25 N at a rate of 40 cycles/min. They found no statistically significant difference between the fracture strength of all crowns at different thicknesses. Furthermore, the mean fracture load of the monolithic zirconia crowns with 0.6 occlusal thickness was comparable to that of lithium disilicate with double the thickness (1669 ± 311 N and 1465 ± 330 N respectively). Garoushi et al. (2021) evaluated the fracture behaviour of monolithic crowns made of partially crystallised lithium disilicate blocks (IPS e.max CAD, Ivoclar Vivadent), full crystallised lithium disilicate blocks (Initial LiSi Block, GC), and zirconia reinforces lithium silicate blocks (Celtra Duo, Dentsply Sirona; and Suprinity, VITA) after cyclic fatigue ageing. The crowns were cemented to metal dies and subjected to 120,000 cycles at a force of 220 N before they were statically loaded to fracture. They found that the load-bearing capacity of all materials was significantly decreased after mechanical ageing. Furthermore, the IPS e.max CAD crowns showed significantly higher load-bearing capacity (1,061 ± 94 N) than both zirconia-reinforced lithium silicate groups. They also reported no significant difference between the load-bearing capacities of both lithium disilicate groups. In an in-vitro study by Lawson et al. (2019), the fracture loads of traditional 3Y-TZP (Lava Plus), translucent 5Y-PSZ (Lava Esthetic), and Lithium disilicate (IPS e.max CAD) crowns were

compared. The crowns were subjected to 100,000 load cycles of 100 N before they were loaded with a steel indenter until fracture. Based on the results of the study, there was no significant difference in the fracture load between translucent 5Y-PSZ and lithium disilicate crowns ($p=1$) whereas 3Y-TZP had a higher fracture load ($p<0.0001$) when the same cement was used.

1.1.11.3 Studies on colour and translucency

Harada et al. (2016) measured the percentage of total light transmittance (T_t%) at a wavelength of 555 nm for five types of translucent zirconias at different thicknesses (0.5 and 1 mm) and compared them with lithium disilicate. Lithium disilicate showed higher translucency than all types of zirconia at all thicknesses. Similarly, Church et al. (2017) compared the translucency parameter (TP) of four high translucency zirconias to lithium disilicate at different thicknesses (0.5, 1, 1.5, and 2 mm). They demonstrated that the translucency was significantly decreased at each thickness increase for each material. Furthermore, Lithium disilicate had significantly higher TP values at each thickness. Furthermore, translucency was significantly decreased at each thickness increase for each material. However, Church and his colleagues found that when the materials were measured at their recommended minimal thicknesses (0.5 mm for zirconia and 1 mm for lithium disilicate), zirconia specimens were more translucent (Church et al., 2017).

Dikicier et al. (2014) demonstrated statistically significant changes in the colour parameters ($p<0.001$) when they investigated the effect of artificial ageing on the colour stability of different all-ceramic systems including zirconia and lithium disilicate. Kurt and Turhan Bal (2019) examined the effect of ageing on the colour stability and translucency of monolithic zirconia and lithium disilicate with different surface treatments. They demonstrated a significant colour change in the zirconia specimens which exceeded the clinically acceptable level, while the lithium disilicate showed high colour stability. Concerning colour replicability, Lehmann et al. (2017) investigated different shade matching techniques and concluded that dental spectrophotometers can produce more accurate shade matching than visual shade matching. Della Bona et al. (2015) found significant differences between the nominal shades of ceramic systems and the corresponding shades of the shade guide systems. They also reported differences between different ceramic systems for the same

shade. Hassel et al. (2009) demonstrated different Easyshade L*a*b* values between teeth and the equivalent 3D master shade tabs.

2. Aim of Study

The purpose of this study was to investigate and compare five aesthetic monolithic dental CAD/CAM ceramic materials in terms of wear abrasiveness and resistance as well as fracture strength and colour stability after thermomechanical ageing. It aimed also to investigate the translucency and colour reproducibility of the tested ceramics.

The null hypotheses stated were:

1. There is no difference in the wear of the materials tested or in their abrasiveness to the opposing enamel.
2. The maximum fracture load will not differ among the tested materials.
3. Thermomechanical ageing will not affect the fracture load.
4. Thermomechanical ageing will not affect the colour of the tested crowns.
5. Different materials will not differ in ΔE values from the selected shade.

3. Materials and Methods

3.1 Materials

The ceramic materials used in the study are listed in Table 1.

Table 1: Shows groups, trade names, compositions, lot numbers, and manufacturers of materials used in the study.

Group Name	Material	Product Name	Composition	Lot. Nr.	Manufacturer
PLD	Partially crystallised lithium disilicate	IPS e.max CAD	57-80 % SiO_2; 11-19 % Li_2O; 0-13 % K_2O; 0-11 % P_2O_5; 0-8 % ZrO_2; 0-8 % ZnO; 0-5 % Al_2O_3; 0-5 % MgO; 0-8 % colouring oxides	X25830	Ivoclar Vivadent, Schaan, Liechtenstein
FLD	Experimental fully crystallised lithium disilicate	GC Initial LiSi Block	No data available	1904251	GC Corporation, Tokyo, Japan
ZLS	Zirconia reinforced lithium silicate	Celtra Duo	58 % SiO_2; 10.1 % ZrO_2; 18.5 % Li_2O; others 13.4 %	16004977	Sirona Dentsply, Milford, DE, USA
SMZ	Super-translucent monolithic zirconia (4Y-TZP)	Katana STML	87-92 % ZrO_2 + HfO_2; 7-9 % Y_2O_3; 0-2 % Other oxides	DZMFB	Kuraray, Tokyo, Japan
UMZ	Ultra-translucent monolithic zirconia (5Y-TZP)	Katana UTML	87-92 % ZrO_2 + HfO_2; 8-11 % Y_2O_3; 0-2 % Other oxides	DYWYA	

3.2 Wear and surface roughness

3.2.1 Ceramic specimens' preparation

Fifty rectangular-shaped specimens (12.0 × 6.5 × 1.5 mm) were cut from the five ceramic materials used in the study (n=10). PLD, FLD and ZLS specimens were cut from prefabricated CAD/CAM blocks of size C14 and shade A3 HT using a low-speed precision

cutting saw (Buehler, Lake Bluff, IL, USA). The cutting was done using a diamond cut-off-wheel saw of thickness 0.6 mm at 2500 rpm and a crosshead speed of 0.080 mm/s under coolant (Fig. 4). SMZ and UMZ monolithic zirconia specimens were fabricated and sintered by the manufacturer and delivered in the same shade and dimensions. A digital micrometre (Mitutoyo, Illinois, USA) was used to confirm the thickness of each specimen (Fig. 5). The surfaces of all specimens were flattened with silicon carbide abrasive papers (#500, #1200, and #4000 grit) using a grinding machine (Exakt 400CS, Norderstedt, Germany) shown in Fig. 6. For the UMZ and SMZ specimens, additional silicon carbide abrasive paper (#350 grit) was used.

Specimens were further processed according to the manufacturers' recommendations. PLD specimens were glazed with IPS e.max CAD Crystall Glaze (Ivoclar Vivadent, Schaan, Liechtenstein) and then subjected to a combined crystallisation/glazing firing cycle. ZLS specimens were only fired without glazing. All the specimens were fired in a sintering furnace (Programat P500 Oven, Ivoclar Vivadent) according to the manufacturers' parameters which are listed in Table 2. The FLD specimens were not subjected to any firing cycles.

Table 2: Firing parameters of PLD and ZLS specimens.

Group	standby temp.	closing time	1st heating rate	intermediate temp.	holding time	2nd heating rate	final temp.	holding time	Vacuum
PLD	403 ˚C	6 min	90 ˚C/min	820 ˚C	10 sec	30 ˚C/min	840 ˚C	7 min	on
ZLS	500 ˚C	1 min	60 ˚C/min	-	-	-	820 ˚C	1 min	off

Fig. 4: Left: LiSi CAD blocks fixed to the holding arm of the precision low speed cutting saw. Right: cutting the rectangular-shaped ceramic specimens from CAD/CAM block size C14 under coolant.

Fig. 5: A digital caliber is used to confirm the thickness of the ceramic specimen at 1.5 mm after sectioning.

Fig. 6: Polishing machine used to flatten and polish the contacting surface of the ceramic specimen before the wear test.

3.2.2 Enamel antagonists

Fifty intact freshly extracted human premolars were collected from a pool of anonymized teeth at the University Dental Hospital, University of Bonn, Germany. The teeth were extracted for medical reasons and entered the pool after written and signed informed consent. The teeth were cleaned with an ultrasonic scaler, then disinfected and stored in 0.9 % NaCl with 0.001 % sodium azide solution at 4 °C. A detailed examination of each tooth under magnification was conducted, and defective teeth were excluded and replaced.

Every tooth was taken out of the storage container the day before the test, rinsed, dried, and embedded in a copper ring filled with cold-curing embedding resin (Technovit 4004, Kulzer GmbH, Werheim, Germany) up to the level of the cementoenamel junction. The

bottom of the ring was drilled, and a screw was fixed in the centre by adding more resin. The role of the screw was to attach the tooth/ring assembly to the wear machine. A flat end cylinder mounted stone was used to flatten the palatal cusp of the tooth. A motor-driven round carbide bur (size 1ø) was inserted halfway in the middle of each tooth surface (buccal, lingual, mesial, and distal). These indentation markings were later used to guide the superimposition of the 3D images. The final assembly is shown in Fig. 7.

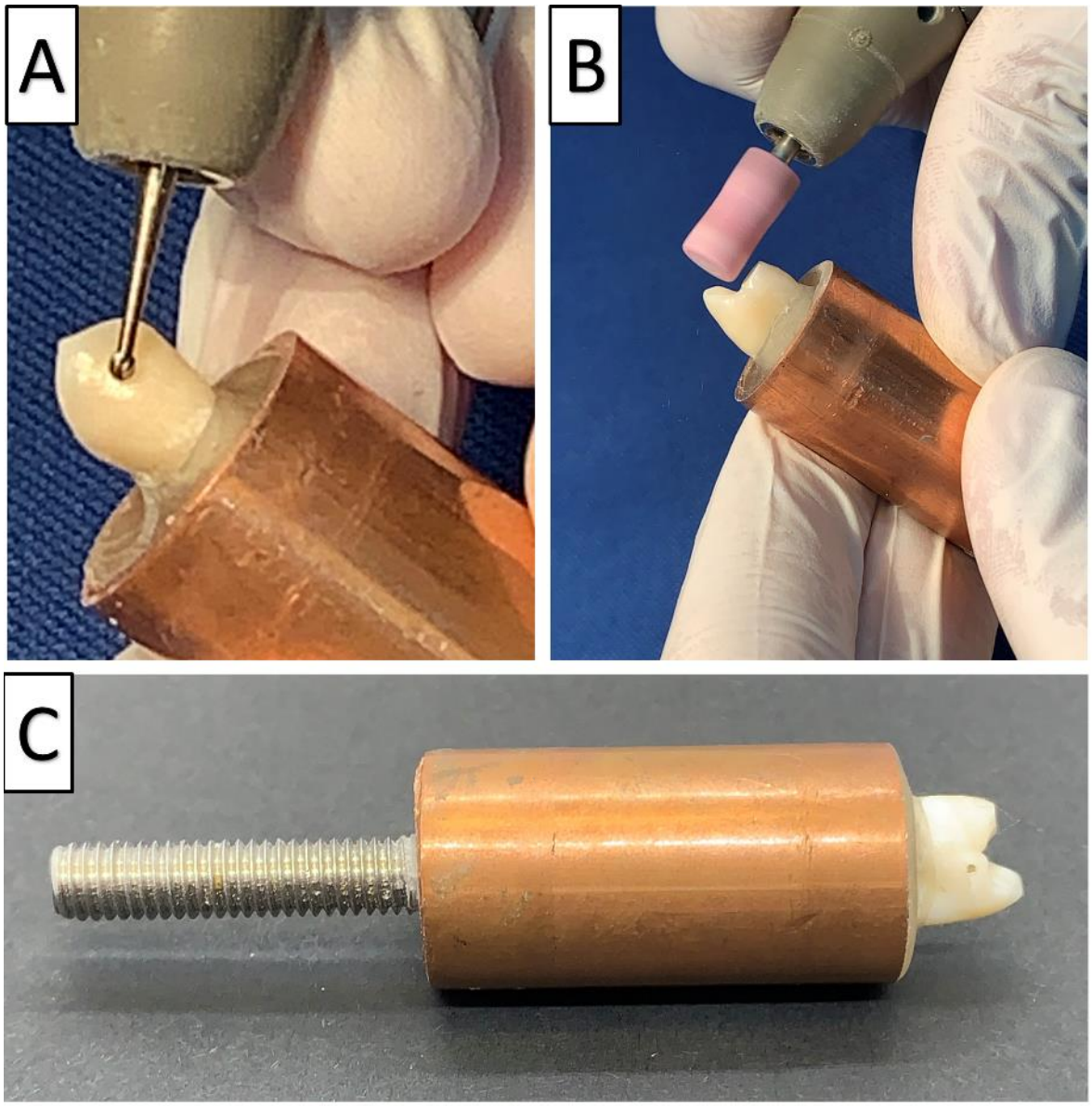

Fig. 7: Preparation of teeth for wear testing. A: creating indentations to act as reference marks during models overlapping, B: flattening of palatal cusp, C: final tooth assembly.

3.2.3 Wear simulation

The ceramic specimens and the enamel antagonists were mounted in a specially designed wear machine at the Department of Oral Technology, University of Bonn, Germany (Fig. 8). The ceramic specimen was glued to a rectangular aluminium plate using Stabilit Express cement (Pattex, Henkel AG & Co. KGaA, Düsseldorf, Germany) and left for one hour to fully set (Fig. 9). The plate was screwed to the moving compartment whereas the tooth was screwed to the pressure arm of the machine. The position of the ceramic specimen was adjusted so that when the pressure arm is activated the buccal cusp of the tooth contacted the centre of the ceramic specimen. When activated, the pressure arm was adjusted to apply a constant force of 20 N on the ceramic specimen. Afterwards, the machine was programmed to perform 200,000 bidirectional wear cycles at a frequency of 1 Hz. For each cycle, the ceramic specimen performed a 2 mm lateral movement back and forth against the buccal cusp of the antagonist premolar to simulate a wear path. In order to simulate the oral environment and keep the enamel antagonist moist, artificial saliva (Glandosane; Stadapharm GmbH, Bad Vilbel, Germany) was used. An automated dispenser was used to deliver the artificial saliva to the tooth/ceramic contact point at a rate of 1 ml/min (Fig. 10).

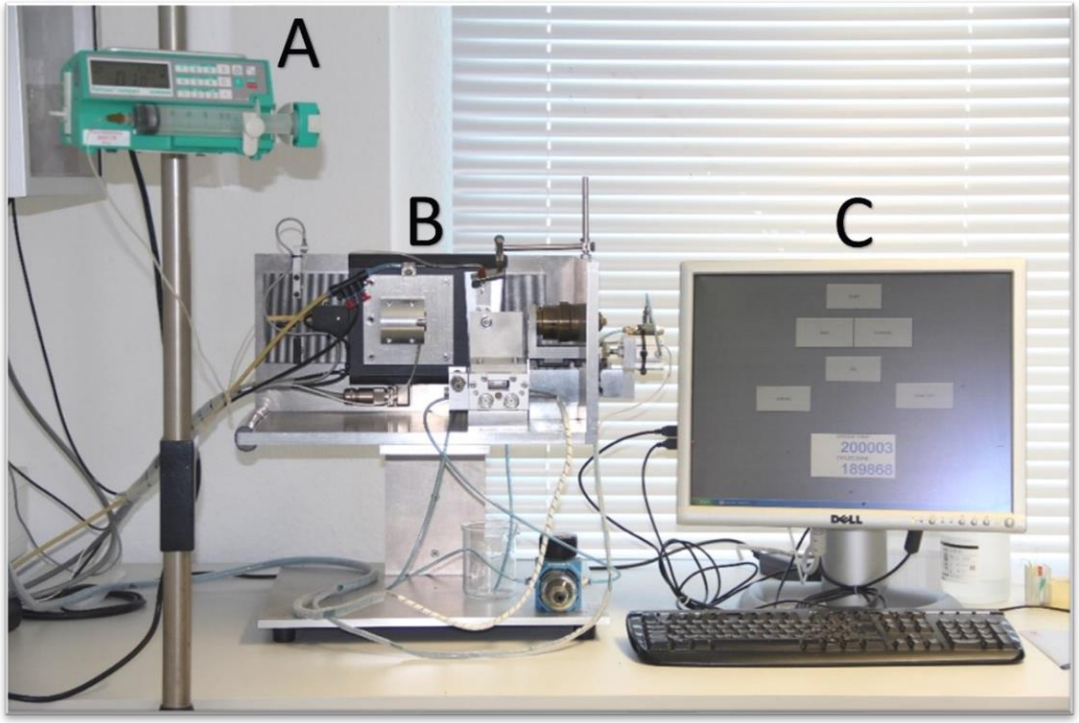

Fig. 8: Wear simulating machine at the Department of Oral Technology at Bonn University. A: automatic lubricant regulator, B: moving compartment, C: digital counter.

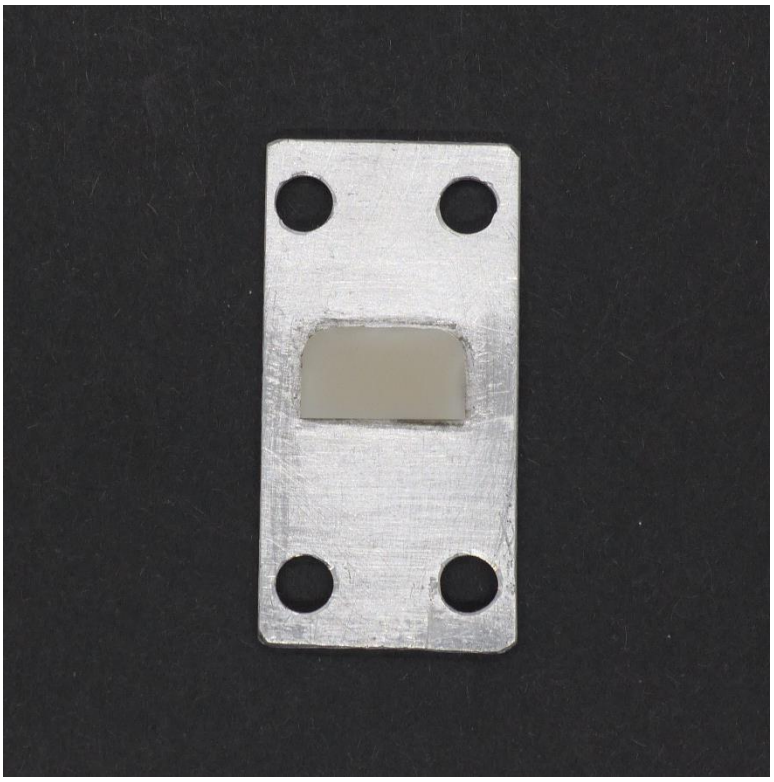

Fig. 9: Ceramic specimen glued to an aluminium plate to facilitate attachment to the wear simulating machine.

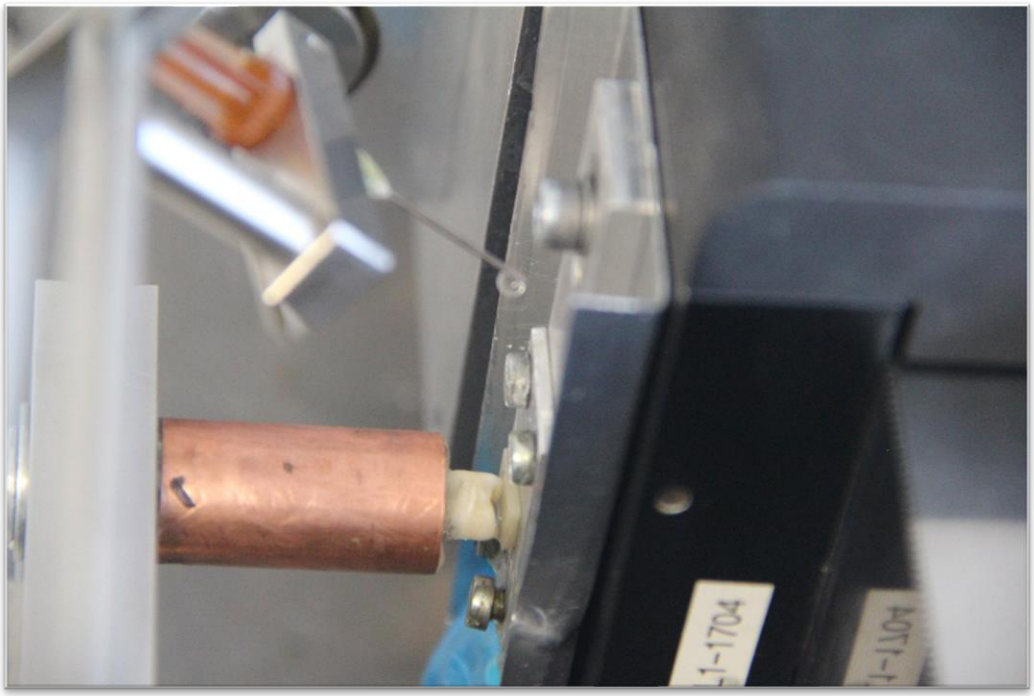

Fig. 10: A needle connected to the automatic regulator delivers the artificial saliva to the contacting surfaces at a rate of 1 ml/min.

3.2.4 Wear quantification

3.2.4.1 Enamel wear

An X-ray microtomograph (Skyscan 1174, Skyscan, Belgium) was utilised to determine the volumetric enamel loss by measuring the difference between two overlapping three-dimensional (3D) virtual models of the tooth taken before and after the wear test. Micro-CT (µCT) imaging was performed at a high resolution (11.5 µm voxel size) using 50 kVp energy, 800 µA intensity,1 mm aluminium filter, 9500 ms integration time, 360° rotation angle, and 0.3° angular step (Fig. 11).

Fig. 11: The tooth is fixed in the X-ray chamber of the Micro-CT and a scan preview is displayed on the screen.

The µCT cuts were converted into DICOM files and transferred to Mimics Research software (Materialise HQ, Leuven, Belgium) to be assembled to form a 3D model of the tooth (Fig. 12).

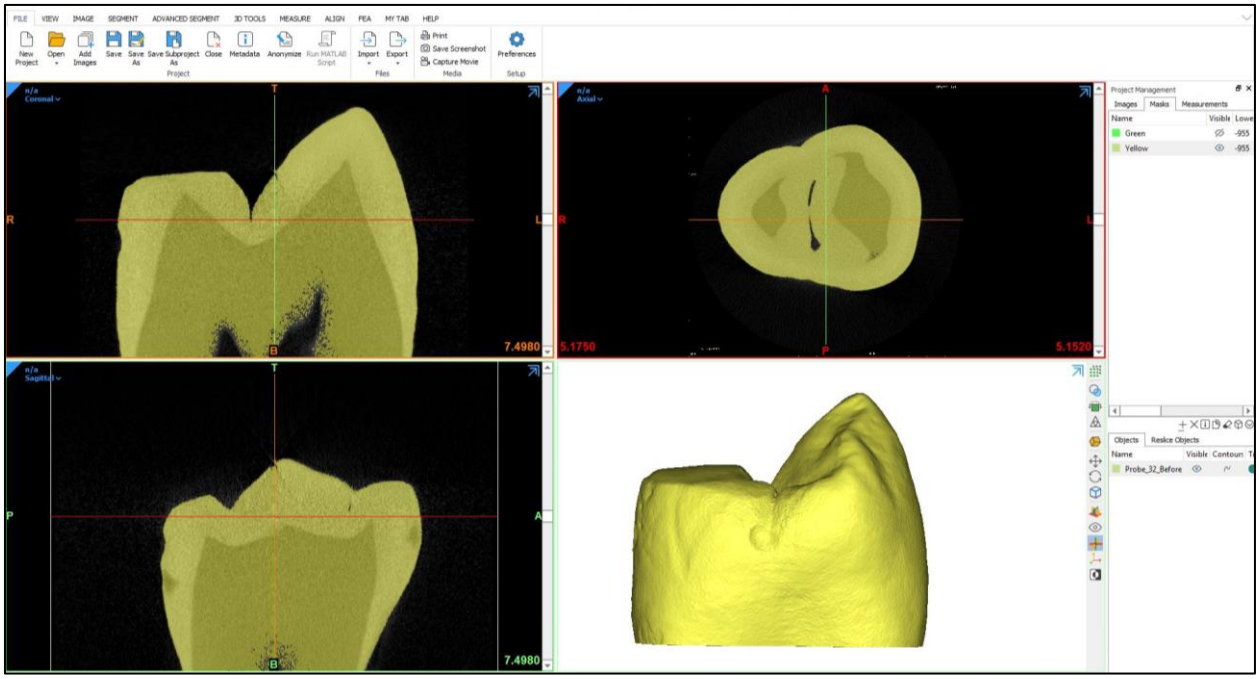

Fig. 12: A 3D model of the tooth before the wear test created from the Micro-CT images using mimics software.

The 3D models generated from both worn and unworn scans of the tooth were then exported as stereolithography files (STL) to 3-Matic software (Materialise HQ, Leuven, Belgium) (Fig. 13). At first, the indentations on every surface of the tooth were marked (Fig. 14). Then each indentation in the non-worn tooth model was assigned to its correspondence in the worn tooth model (Fig. 15a). The overlapping of the two models was then started guided by the marked triangles. It was then possible to overlay the 3D images of the intact and worn tooth models with the help of the preformed indentations and the overlapped mesh elements (Fig. 15b). After complete overlapping, the final combined model was trimmed to remove any extra parts at the base of the model. Then the volume difference between the two models was calculated using Boolean subtraction (Fig. 16).

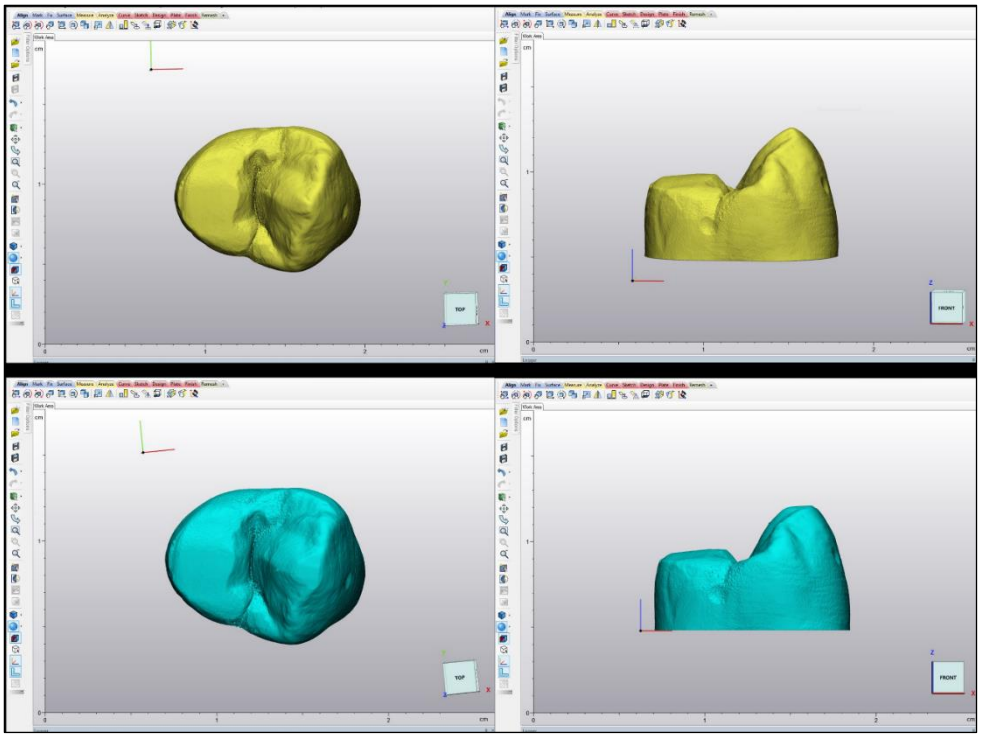

Fig. 13: 3D models of a non-worn (yellow) and worn (Blue) tooth scans after being transferred to 3-Matic software to undergo models overlapping.

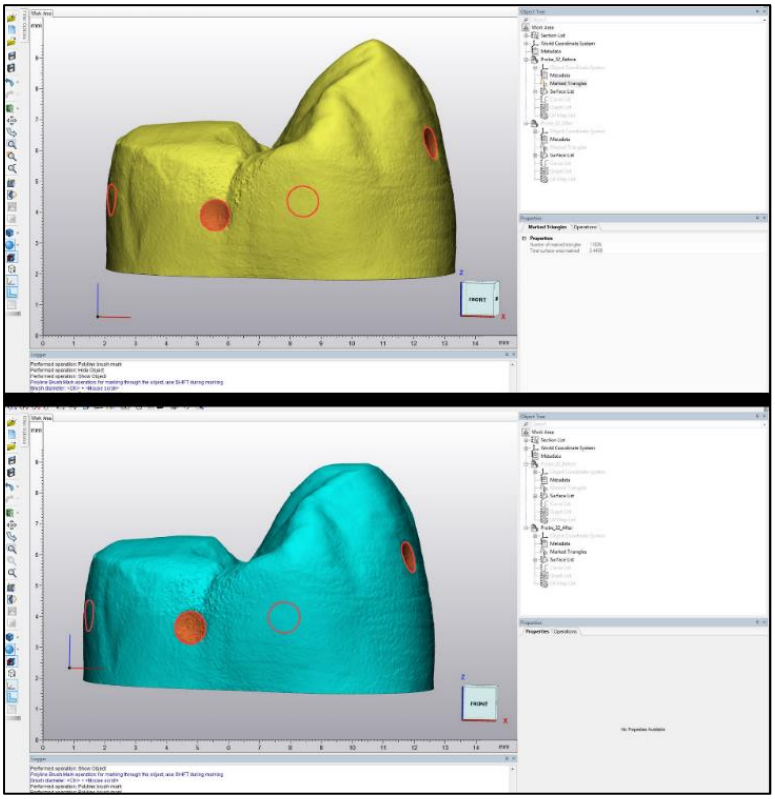

Fig. 14: Indentations are manually marked on each model before overlapping.

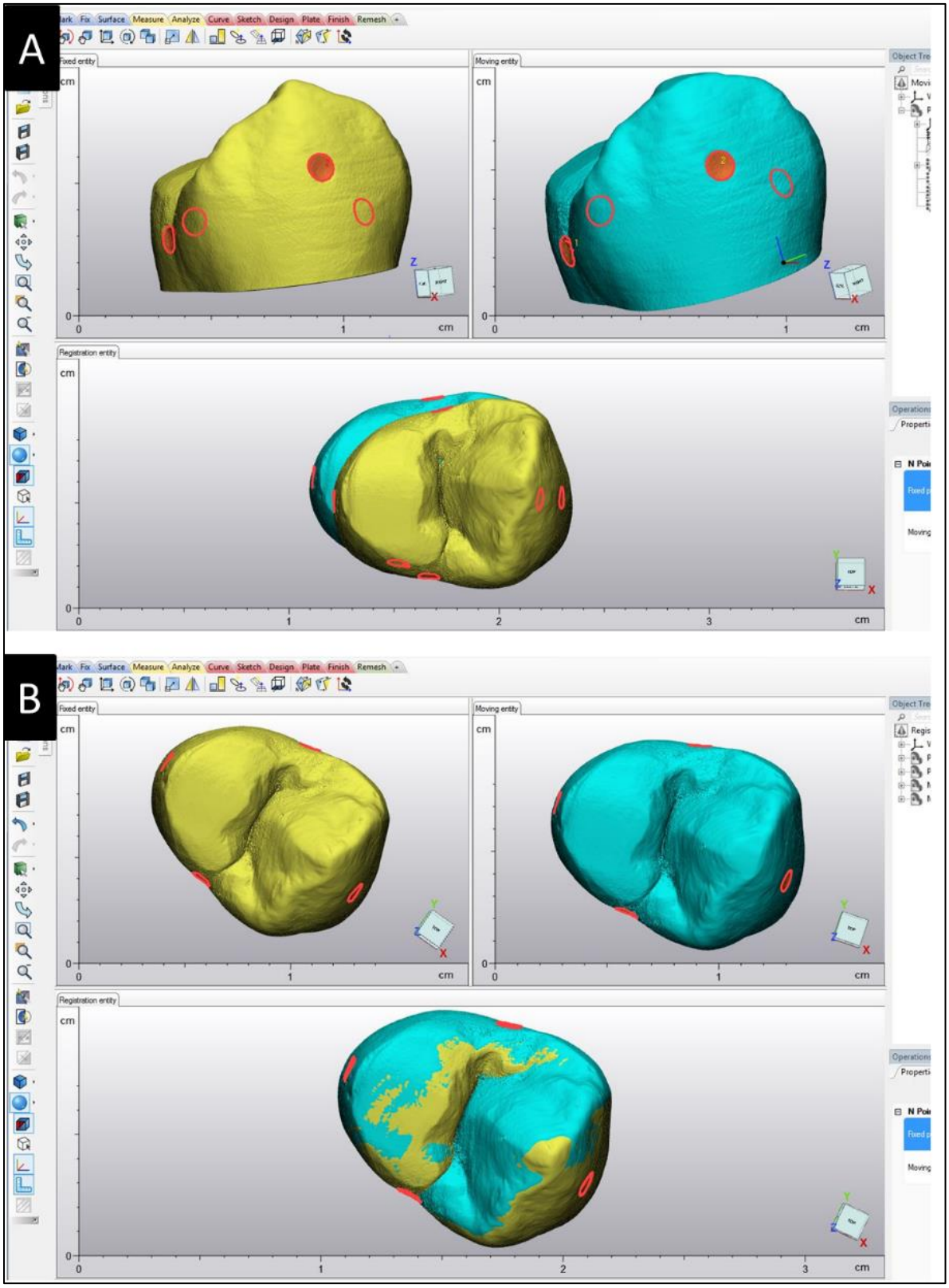

Fig. 15: A: shows the marked indentations of pre- and post-test models assigned to each other to guide the models overlapping process. B: shows the superimposition of the two models.

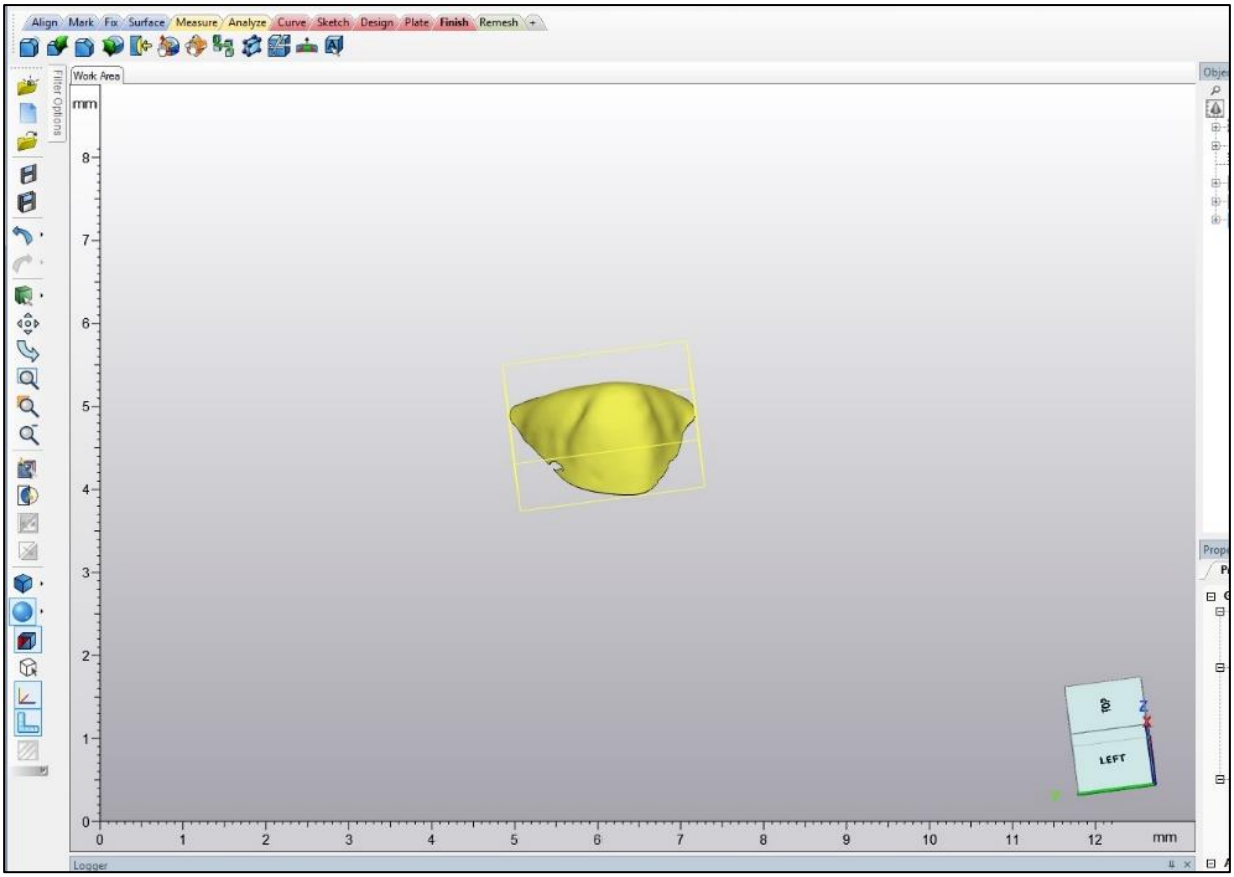

Fig. 16: Boolean subtraction of the worn enamel tip.

3.2.4.2 Ceramic wear

The wear of ceramic samples was determined by measuring weight loss. The ceramic specimen weight was recorded using a precision balance (Mettler Toledo, Switzerland) before being subjected to the wear cycles (Fig. 17). The reading was recorded in grams (g) as R_1. At the end of the 200,000 wear cycles, the ceramic samples were thoroughly cleaned under running water, air dried, re-weighed and the reading was recorded as R_2. The difference in weights was then calculated by subtracting R_2 from R_1 and the reading was converted to milligram (mg).

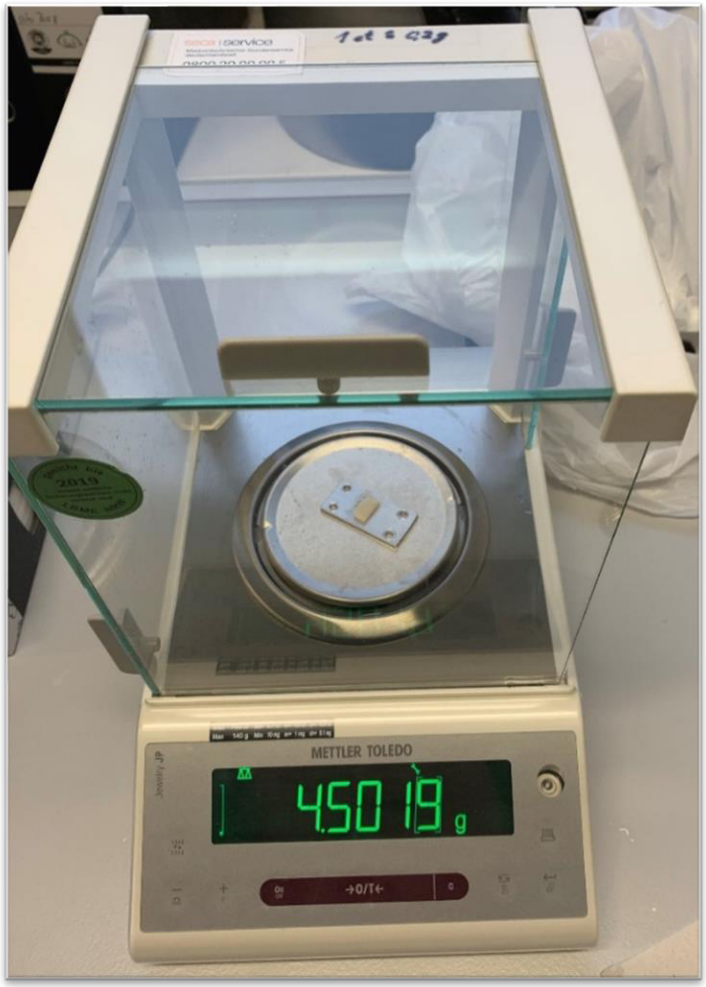

Fig. 17: Sensitive balance for weighing wear specimens. The ceramic specimen is placed on top of the scale table and the display shows the weight in grams.

3.2.5 Surface roughness

A confocal laser scanning microscope CLSM (TCS SP8/AOTF, Leica, Wetzlar, Germany) at the Microscopy Core Facility of the Medical faculty at the University of Bonn was used to measure the surface roughness of the ceramic specimens (Fig. 18). On the stage of the CLSM, each sample was placed with the treated surface facing up and scanned. An Ar/ArKr laser with wavelengths of 488 nm blue, 568 nm green, and 647 nm red was used to generate a reflection image of the surface. The reflection image was generated using Leica's LAS AF v3.x (Wetzlar, Germany). A scan format of 2048 x 2048 pixel was selected, and the scan speed was 400 Hz. Starting from the first detectable light reflex, the stage was moved upward in the z-direction with a measurement step size of 5 µm, starting from

the bottom and ending at the last detectable light reflex. Scan parameters were adjusted based on previously published scanning protocols (Al-Shammery et al., 2007). A gray-scale topographical image was created from the z-stack using the topographic image tool in the software. The average roughness of each specimen (R_a) was calculated using the topographic image for a region of 200 µm x 200 µm within the area of interest.

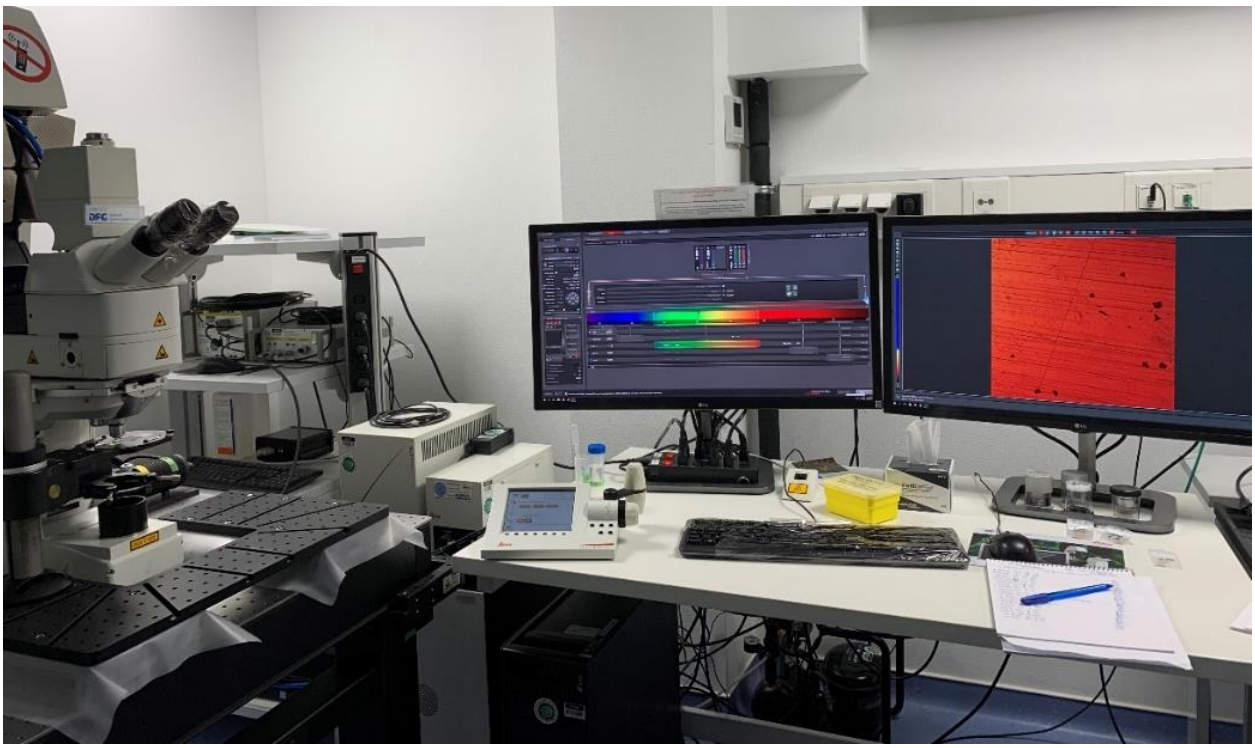

Fig. 18: Confocal laser scanning microscope at the Microscopy Core Facility of the Medical faculty at the University of Bonn.

3.2.6 Scanning electron microscope (SEM)

At the end of the wear test, one specimen from each group was randomly selected and prepared for qualitative analysis of topography and microstructure. Every specimen was attached to the testing table and conductive carbon cement (Leit-C, Plano GmbH, Wetzlar, Germany) was applied to the corners to produce conductive adhesive spots between the sample and the sample plate. Then specimens' surfaces were coated with a thin layer of gold/platinum using a sputter coater (Scancoat six, Edwards High Vacuum, England, UK) (Fig. 19).

The specimen was then placed in the vacuum chamber of the scanning electron microscope (Philips XL 30 CP, Philips, Eindhoven, The Netherlands) (Fig. 20), operated at 10 kV, spot size adjusted to 5, and images were obtained from worn areas at magnifications (25X, 500X and 1000X).

To investigate the crystal morphology of glass ceramics, one specimen from each of the groups FLD, PLD and ZLS was further selected, etched for 30 secs using 4.5 % HF acid (IPS ceramic etching gel; Ivoclar Vivadent), and coat sputtered as previously discussed. Afterwards, specimens were examined under the SEM at magnifications (1200X and 5000X) at spot size 3.

Fig. 19: Sputter Coater. The ceramic specimen is placed inside the vacuum chamber and the gold/platinum coating is applied for 60 sec.

Fig. 20: Scanning electron microscope at the Department of Oral Technology at Bonn University.

3.2.7 Energy Dispersive X-ray Spectroscopy (EDS)

The quantitative analysis of the chemical composition of each glass material was performed using energy dispersive X-ray spectroscopy attached to the SEM. The etched samples were examined under the SEM at a magnification of 2000X operated at 25 kV. Then the images were transferred to the EDS detecting unit (Camscan S4, EDAX Inc., New Jersey, USA) and the element spectrum was collected using EDAX software (Genesis Spectrum, V3.51, EDAX Inc., New Jersey, USA).

3.3 Fracture load testing

3.3.1 Specimen preparation

A prepared premolar die with a heavy chamfer finish line was used in the study (Fig. 21). For duplication, twenty impressions were taken for the die with additional silicon rubber

base (Honigum putty and light, DMG Chemisch-Pharmazeutische Fabrik GmbH, Hamburg, Germany). Every impression was checked with a 2.5x magnification loupe under LED light for the presence of any defects and defective impressions were discarded. The impression was poured with Epoxy resin (Technovit® Epox, Kulzer GmbH, Hanau, Germany) and was left for 24 hours to set. Afterwards, it was examined under magnification for any defects or entrapped air bubbles. Defective dies were discarded and replaced. The base of each die was trimmed on a dry trimmer to remove the excess epoxy and to form a uniform cube-shaped die base (Fig. 22).

3.3.2 Designing and milling of CAD/CAM crowns

The die was inserted in a wax model containing artificial adjacent teeth (Fig. 23) and scanned with Omnicam intraoral scanner (Dentsply Sirona, Bensheim, Germany). A monolithic crown restoration was designed using CEREC software v.4.6.1 (Dentsply Sirona, Bensheim, Germany). The occlusal surface was adjusted to a thickness of 1.5 mm in the central groove, axial walls thickness of 1.5 mm at the buccal and lingual contours. The wall thickness was ensured by using Cerec software tools “cursor details” and “show minimum thickness” (Fig. 24). A total of 100 monolithic crowns were milled using the 5-axis milling unit ceramill® motion 2 (Amann Girrbach AG, Koblach, Austria) at the Department of Prosthetic Dentistry in Ludwig-Maximilians Munich University Hospital in Germany (Fig. 25 & 26) and assorted into five groups according to the ceramic material (n=20) as presented in Table 1.

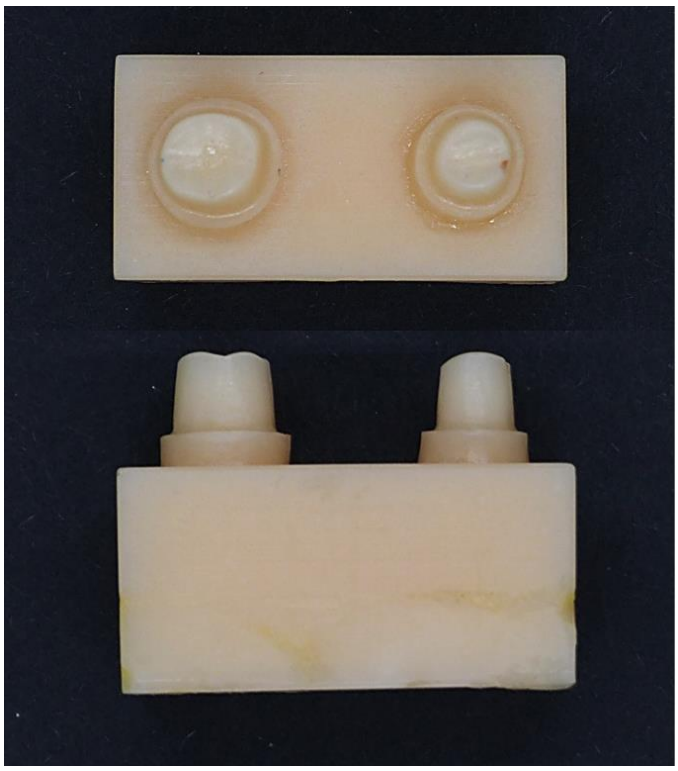

Fig. 21: The master model of prepared premolar that was used in the study. Only the right tooth model was duplicated.

Fig. 22: A die duplicated in transparent epoxy resin.

Fig. 23: shows the die embedded in a wax model and ready for optical scanning.

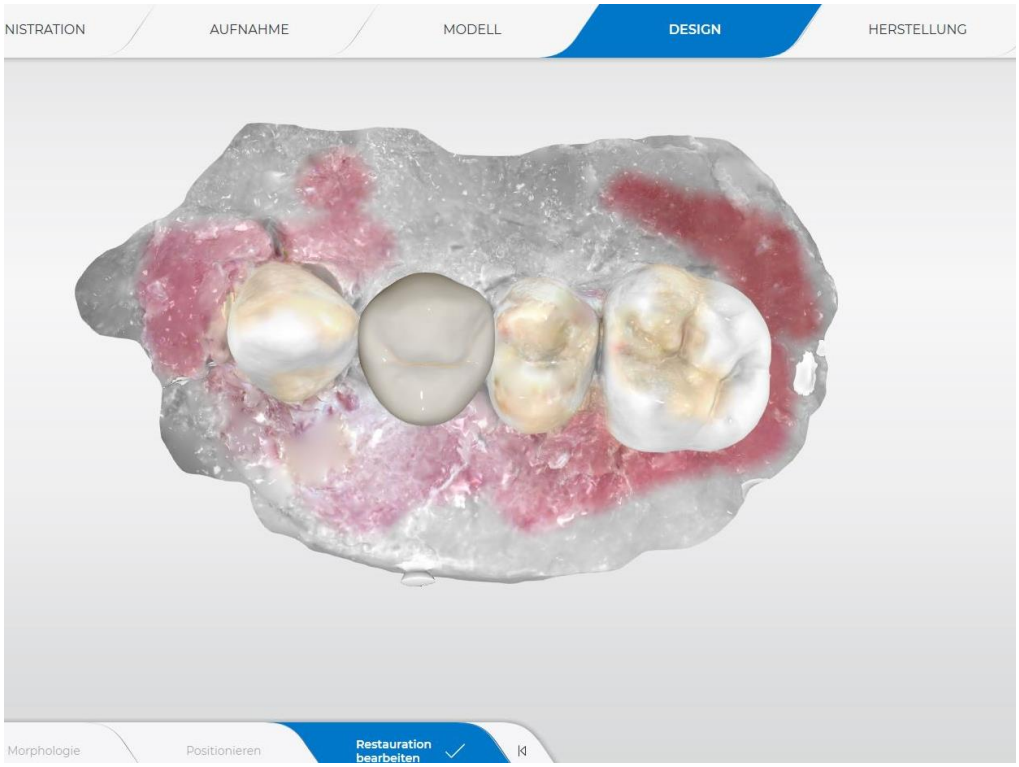

Fig. 24: Shows the final virtual design of a monolithic crown o the CEREC software.

Fig. 25: Shows the Katana UTML Zirconia disc mounted on a 5-axis milling machine ready for milling at the Department of Prosthetic Dentistry in LMU University Hospital.

Fig. 26: Shows the milled zirconia crowns before separation from the disc. All crowns were milled from the same design and have identical dimensions.

3.3.3 Finishing and cementation of crowns

The glass-ceramic crowns were further processed as previously discussed in section 2.2.1. The zirconia crowns were sintered in a sintering furnace (Cercon Heat Plus, DeguDent GmbH, Hanau, Germany) and polished according to the manufacturer's instructions. Thereafter, all crowns were cleaned in an ultrasonic cleaner, air-dried and prepared for adhesive cementation. FLD, ZLS and FLD crowns were etched using 9 % hydrofluoric acid (Porcelain Etch, Ultradent, South Jordan, USA) for 20 seconds (Fig. 27), rinsed with water for 1 min then air-dried. SMZ and UMZ crowns were sandblasted using Alumina particles size 50 µm at 2 bar pressure for 10 seconds. Then the crowns were adhesively cemented to the epoxy dies using the dual-cure Panavia V5 (Kuraray Noritake Dental Inc., Okayama, Japan) with clear shade. Ceramic primer (Clearfil Ceramic Primer Plus, Kuraray Noritake Dental Inc., Okayama, Japan) was applied to the fitting surface of the crown and allowed to dry for one minute. Meanwhile, the tooth primer was applied to the epoxy die, then left for 20 seconds, and then thoroughly dried with mild air. Next, the cement was applied to the crown's fitting surface and the crown was seated on top of the die under 3 kg of static force. The margins were then light-cured for 2-3 seconds, and the excess removed, after which each margin was light-cured for 10 seconds. The final cemented crown is shown in (Fig. 28).

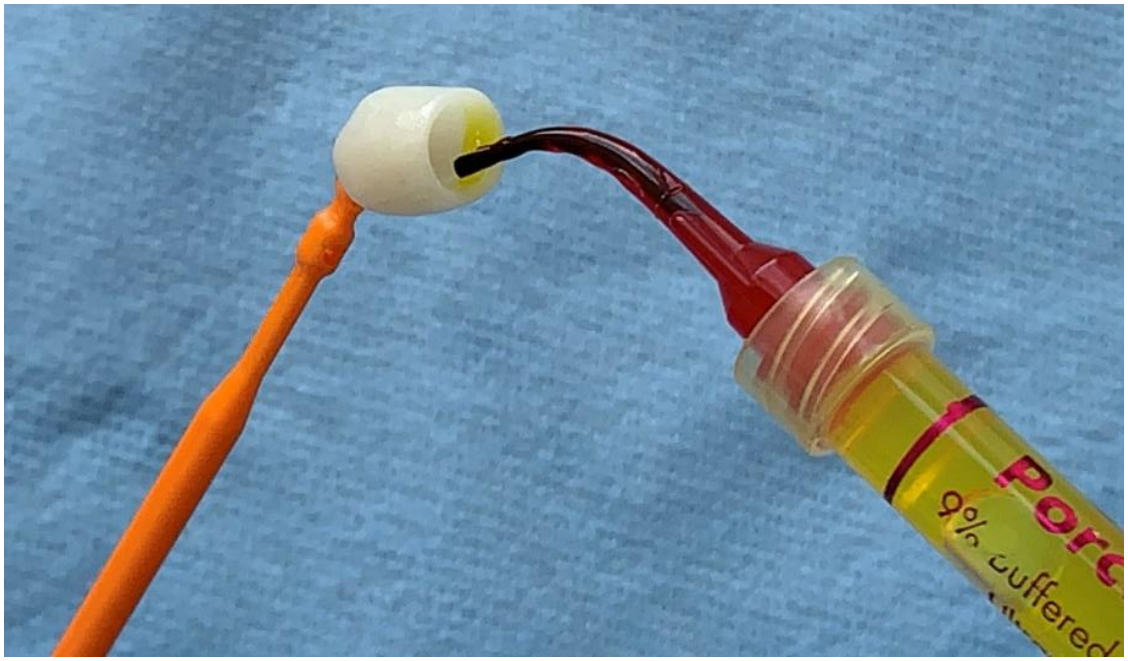

Fig. 27: Hydrofluoric acid gel applied to the fitting surface of a glass-ceramic crown before cementation.

Fig. 28: Shows the final crown cemented to the epoxy die.

3.3.4 Thermomechanical ageing and static loading

Half of the crowns (n=10) were subjected to thermomechanical loading in a specially designed chewing simulator (Fig. 29) at the Department of Dental Biomaterials (Zurich University, Zurich, Switzerland) following a standardised protocol (Zimmermann et al., 2019). The crowns were subjected to 1.2 million load cycles at a force of 49 N applied to the central groove perpendicular to the occlusal table at a frequency of 1.7 Hz. The thermal cycling was 5 °C to 55 °C with 120 s dwell time and 10 s for water change. At the end of the thermomechanical cycles, all the surviving crowns were examined at 10x magnification using a stereomicroscope to exclude any specimens showing signs of fracture from further testing.

Fig. 29: Chewing simulator with thermocycling at University of Zurich, Division of Dental Biomaterials.

The surviving samples from the thermomechanical loading as well as the unfatigued samples were loaded until fracture in a universal testing machine (Zwick, ZwickRoell GmbH, Ulm, Germany). The epoxy dies and the adhesively seated crowns were prepared for the fracture loading test. The base of the die was trimmed to fit centrally in a cylindrical copper tube (ø18 mm & L 5 mm) and fixed with cold-curing resin (Technovit 4004, Kulzer GmbH, Hanau, Germany). After that, the copper cylinder was mounted in a specially designed holder (Fig. 30) of the same diameter and tightly fixed in position with four screws. The holder was securely attached to the Zwick table so that its crown was perpendicular to the floor. A pistol with a tip diameter of 5 mm was applied to the centre of the crown perpendicular to the occlusal surface and driven at a crosshead speed of 1 mm/min (Fig. 31). The software automatically recorded the maximum force to fracture value in Newton (N).

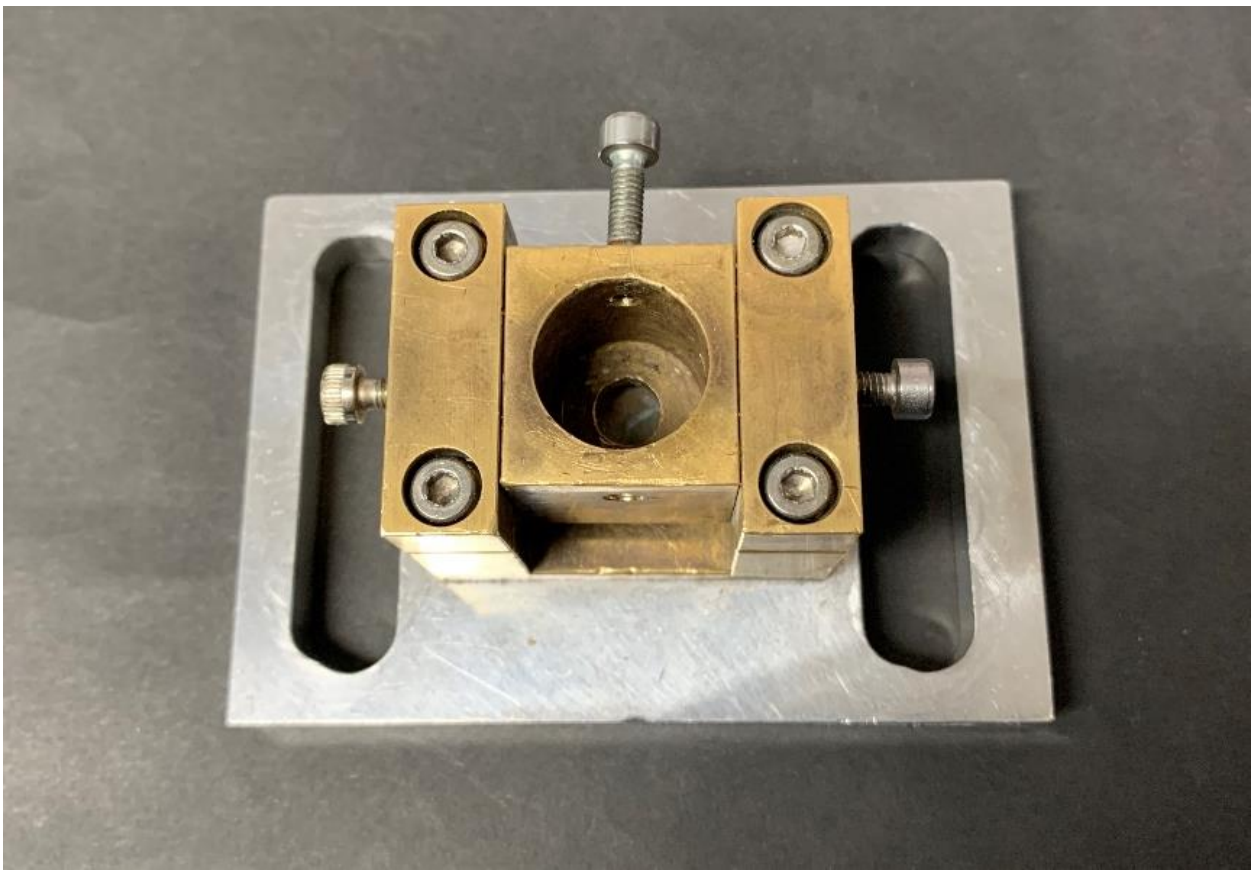

Fig. 30: Shows the attachment unit used to firmly hold the specimen on the table of the universal testing machine.

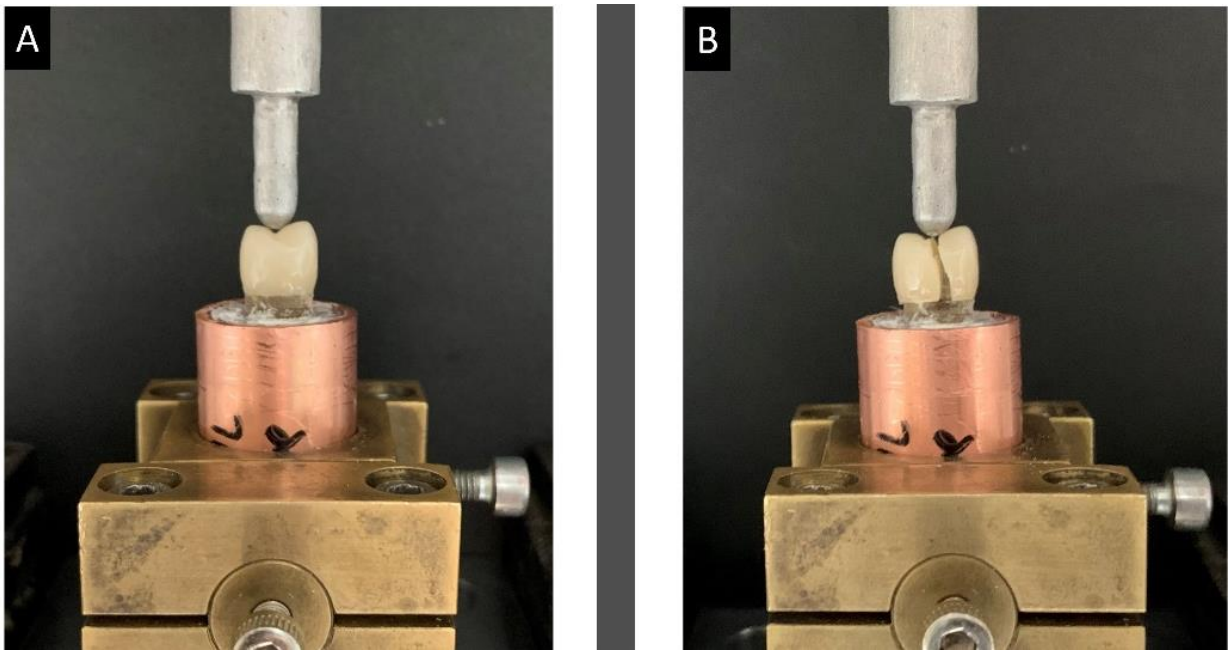

Fig. 31: Fracture load test. A: applying perpendicular load, B: crown fracture.

3.4 Effect of ageing on CIE L*a*b* parameters and change of colour (ΔE)

Prior to subjecting the ceramic crowns to chewing cycles, the Easyshade spectrophotometer (VITA Easyshade V, VITA Zahnfabrik GmbH, Bad Säckingen, Germany) was used to measure the L*, a*, and b* colour parameters of the crowns. Six measurements were taken from the middle third of the buccal surface and the mean value was calculated and recorded as L^*_1, a^*_1, and b^*_1. Under the same testing and lightening conditions, the colour parameters were re-measured at the end of the chewing cycles, and the mean value was calculated and recorded as L^*_2, a^*_2, and b^*_2. Accordingly, the colour difference (ΔE) was calculated based on the following equation:

$$\Delta E = [(\Delta L^*)^2 + (\Delta a^*)^2 + (\Delta b^*)^2]^{1/2} ,$$

where $\Delta L^* = (L_1 - L_2)$, $\Delta a^* = (a_1 - a_2)$ and $\Delta b^* = (b_1 - b_2)$.

3.5 Colour testing

For the measurement of the translucency parameter (TP) and the colour match with shade A3 (ΔE), fifty rectangular-shaped specimens (n=10) were fabricated and finished as previously discussed in section 2.2.1.

3.5.1 Translucency parameter (TP)

For measurement of the translucency, the ceramic specimens were measured with a digital spectrophotometer (VITA Easyshade V, VITA Zahnfabrik GmbH, Bad Säckingen, Germany) and CIE L*a*b* parameters were recorded over black and white backgrounds (Fig. 32). For each measurement, three readings were taken, and the average was calculated. The translucency parameter (TP) was determined by calculating the differences in colour parameters over the black and white backgrounds according to the following equation:

$$TP = \sqrt{(L^*_\omega - L^*_B)^2 + (a^*_\omega - a^*_B)^2 + (b^*_\omega - b^*_B)^2}\ ,$$

where ‘w’ refers to coordinates over the white background and ‘B’ refers to coordinates over the black background.

3.5.2 Colour match to the selected shade

A digital spectrophotometer (VITA Easyshade V, VITA Zahnfabrik GmbH, Bad Säckingen, Germany) was employed in order to verify the shade match of the ceramic specimens to the selected block shade. Delrin rods with natural white colour were cut into 1.5 mm thick discs and served as a background during measurements (Fig. 33). In the spectrophotometer, the "Shade Verification" mode was selected, and A3 was set as the control shade. The spectrophotometer tip was applied vertically to the middle of the specimen in full contact. For each specimen, six readings were recorded, and the average was calculated. Before every reading, the Easyshade device was inserted into the calibration unit.

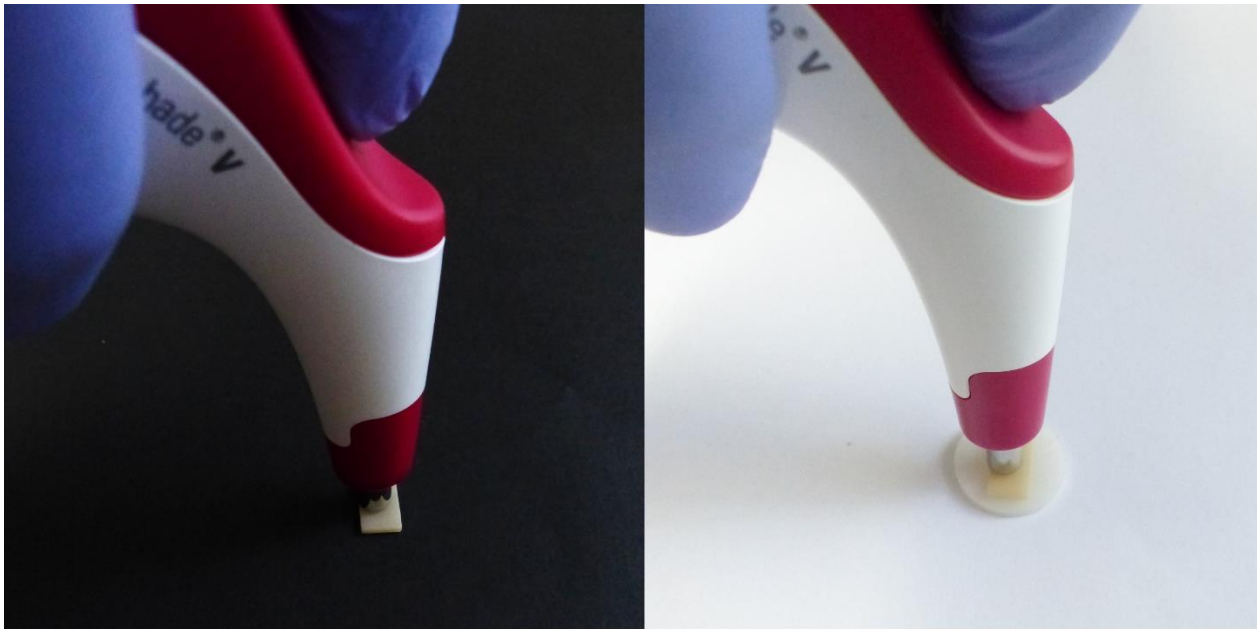

Fig. 32: Measuring the CIEL*a*b* for ceramic samples on black background (left) and white background (right) to calculate the translucency of ceramic specimens.

Fig. 33: Delrin rods are cut into discs and used as a background for the ceramic specimen during colour measurement.

3.6 Statistical analysis

The Shapiro-Wilk test was used to examine if the variables follow a normal distribution. The ceramic wear and surface roughness variables showed parametric distribution; therefore, One-way analysis of variance (ANOVA) was used for comparison between the groups. Tukey's post hoc test was used for pairwise comparison between the groups when the ANOVA test was significant. The enamel wear variables were non-parametric, therefore, Kruskal Wallis test was used for comparison between the groups, followed by Dunn's post hoc test. The maximum loading force data were statistically analysed by Two-way ANOVA followed by multiple comparisons using post hoc Tukey's test ($\alpha = 0.05$). Student t-tests were used to compare the CIE L*a*b* parameters before and after thermomechanical ageing. One-way ANOVA was used to analyse the ΔE and TP data followed by Tukey post hoc test for pairwise comparisons. The significance level was set at $P \leq 0.05$. The statistical analysis was performed using Prism software (PrismV.9, GraphPad Software, San Diego, USA).

4. Results

4.1 Enamel wear

The median and interquartile range of volumetric enamel loss are represented in Fig. 34. According to the Kruskal Wallis test, there were significant differences between the tested materials. The lowest median volumetric enamel loss was reported for SMZ (0.13 ± 0.08 mm^3) followed by UMZ (0.15 ± 0.08 mm^3). On the other hand, the highest median volumetric enamel loss was reported for the ZLS (0.47 ± 0.17 mm^3) group. Both zirconia groups showed a statistically significant difference compared to all the other tested groups except the FLD (0.25 ± 0.10 mm^3) group. Furthermore, there was no statistically significant difference between the two zirconia groups as well as between the PLD (0.29 ± 0.34 mm^3), FLD, and ZLS groups.

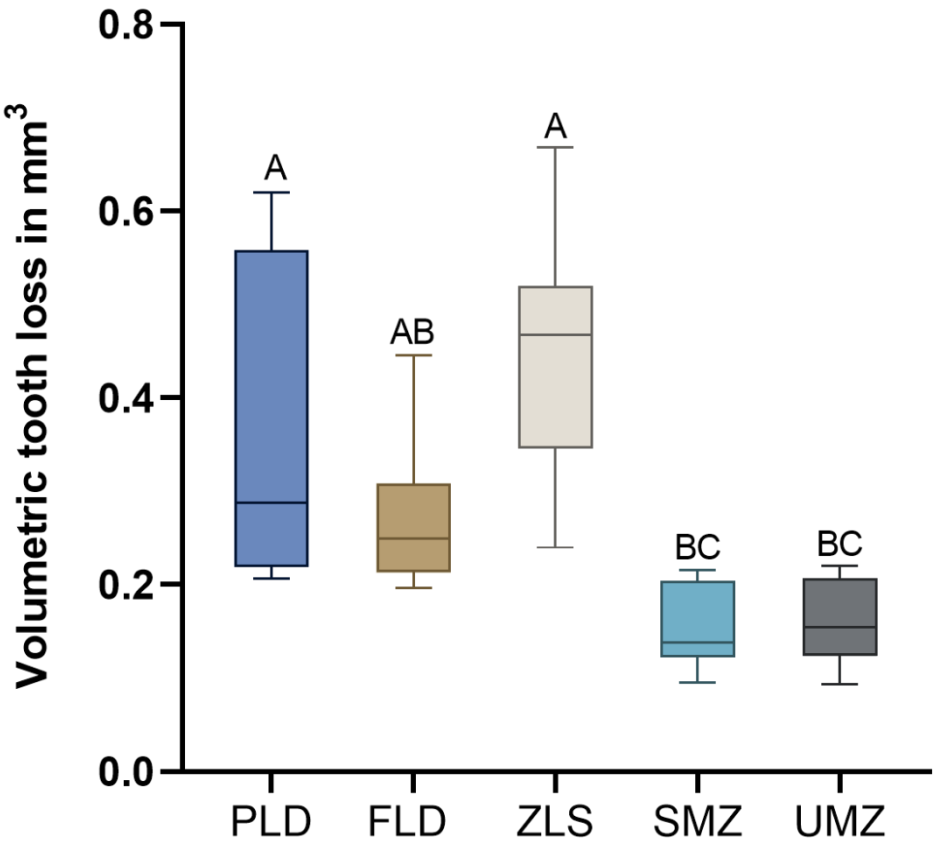

Fig. 34: Median and interquartile range of volumetric enamel loss for the different ceramic groups after 200,000 wear cycles. Groups that do not share the same letter are significantly different.

4.2 Ceramic wear

Results of ceramic wear are presented graphically in Fig. 35. Tukey's post hoc analysis showed no statistically significant difference between the mean ceramic weight loss values of the groups SMZ (0.43 ± 0.10 mg) and UMZ (0.14 ± 0.10 mg), while each of them was statistically significantly different from all other groups. Additionally, there were statistically significant differences between FLD (1.04 ± 0.22 mg) and all other groups. However, no statistically significant difference was found between PLD (2.95 ± 0.35 mg) and ZLS (3.09 ± 0.37 mg).

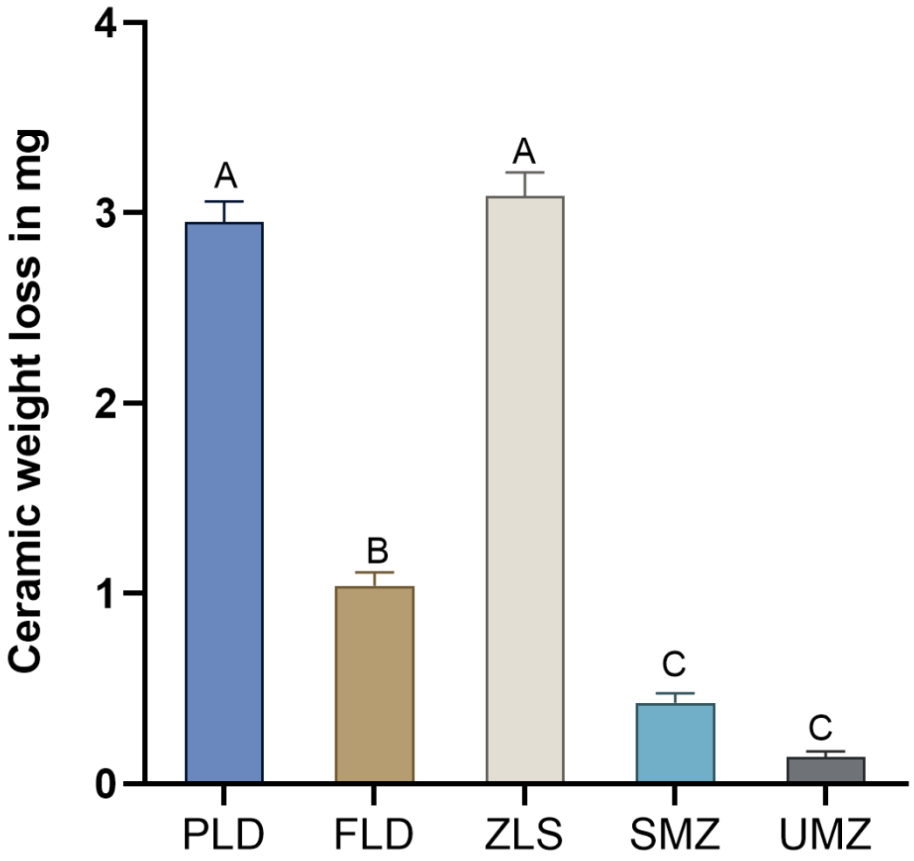

Fig. 35: Mean and standard deviation of ceramic wear for the different ceramic groups after 200,000 wear cycles. Groups that do not share the same letter are significantly different.

4.3 Surface roughness

The mean R_a values and the mean differences are presented in Table 3. The PLD group showed significantly the highest mean difference in R_a values (1.28 ± 0.40 µm) compared to all the other tested groups, followed by ZLS (0.41 ± 0.18 µm), and FLD (0.38 ± 0.16 µm). On the other hand, there were no statistically significant differences between SMZ (-0.06 ± 0.11 µm) and UMZ (-0.04 ± 0.08 µm).

Table 3: Mean, standard deviation, and statistical analysis of Ra values in µm.

Material	R_a (before wear)	R_a (after wear)	P-Value	Difference in R_a	P-Value
PLD	(0.55) ± 0.04	(1.83)*± 0.40	0.002	(1.28) [a] ± 0.40	<0.001
FLD	(0.69) ± 0.02	(1.06)*± 0.16	0.006	(0.38) [b] ± 0.16	
ZLS	(0.45) ± 0.16	(0.85)*± 0.19	0.007	(0.41) [b] ± 0.18	
SMZ	(0.59) ± 0.08	(0.53) ± 0.04	0.31	(-0.06) [c] ± 0.11	
UMZ	(0.54) ± 0.09	(0.51) ± 0.06	0.32	(-0.04) [c] ± 0.08	

Superscript stars represent significance within the row
Superscript letters represent significance within the column

4.4 Microstructural analysis

Fig. 41 shows the SEM images of the worn ceramic samples at magnifications (15X, 500X, and 1000X). The 15X magnification images showed that groups PLD, ZLS, and FLD had wide deep wear facets with distinct wear patterns. On the other hand, the SMZ and UMZ specimens at magnification 25X did not show any noticeable depression on the surface. They only showed a change in the colour of the worn area, however, the surface integrity was preserved intact. At the higher magnifications, the PLD specimens showed the presence of cut debris on the surface and evidence of microcracks represented by the black and white arrows respectively (Fig. 36b & c). ZLS specimens showed irregular multi-leveled surface and microfractures suggesting the complete loss of ceramic particles from these areas. FLD specimens showed less debris and microcracks than the other glass-ceramic groups. No difference was recognized between the surfaces of UMZ and SMZ samples, which showed intact surfaces without any signs of levelling or microcracks.

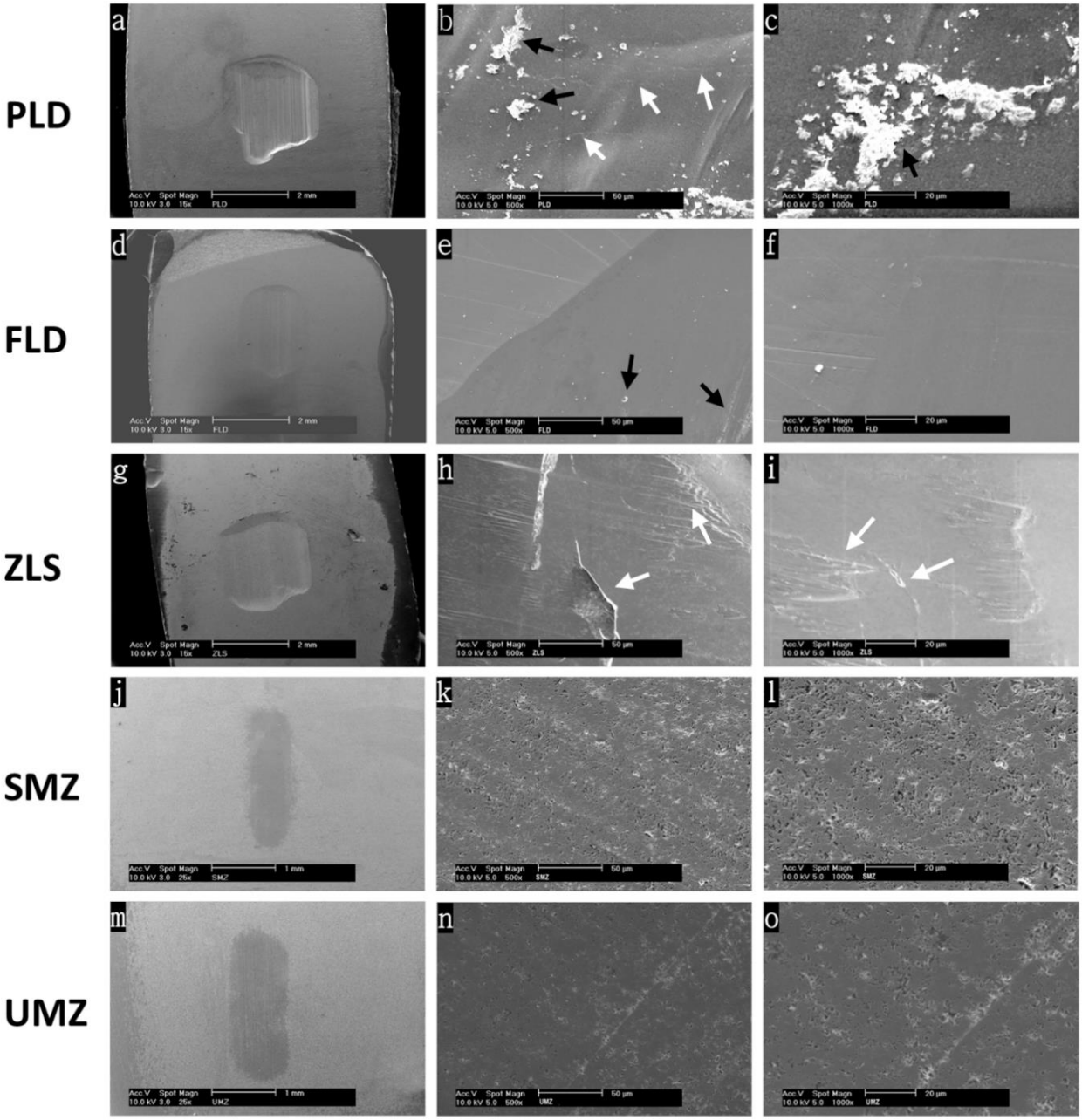

Fig. 36: Scanning electron micrograph images at magnifications 15X,500X,1000X showing the worn surfaces of the ceramic specimens after 200,000 wear cycles against the buccal cusps of natural premolars. PLD shows a lot of wear debris on the cut surface (black arrows). ZLS and PLD show several crack lines (white arrows).

The SEM images of etched glass-ceramic specimens taken at magnifications 1200X, and 5000X for the groups FLD, PLD, and ZLS are presented in Fig. 37. The PLD specimen showed typical interlocking rod-shaped lithium disilicate crystals. Marked areas in Fig. 37a point to deficient areas due to fragments detaching. Fig. 37b shows aggregates of cut debris spreading over the scanned field. The ZLS showed spherical-shaped crystals that are evenly distributed. The crystals are smaller in size and more densely packed compared to the other glass groups (Fig. 37e & f). The morphology of the crystals in the FLD specimen is different from that of PLD. They showed two phases, small rounded densely interlocking crystals and widely scattered less dense platelet-shaped crystals (Fig. 37c & d). The black arrow in (Fig. 37c) points to a crack propagating transversely perpendicular to the direction of wear patterns.

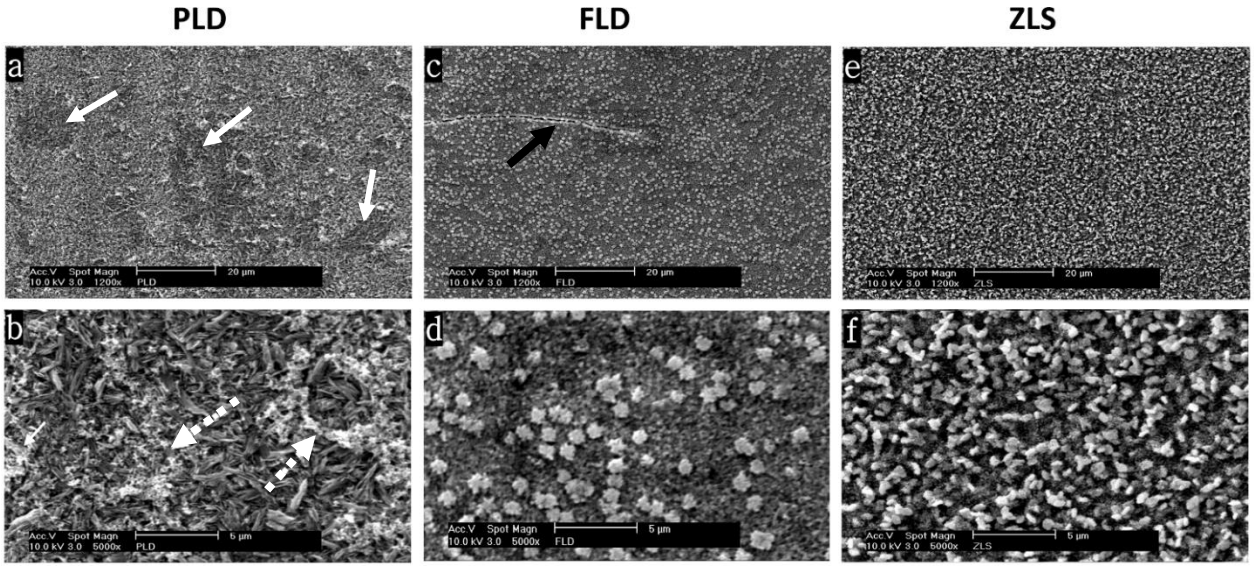

Fig. 37: Scanning electron micrograph images of etched glass-ceramic specimens taken with spot size 3 at magnifications 1200X (a,c,e), and 5000X (b,d,f) showing the crystalline morphology for the worn surfaces. The continuous white arrows point to detached area, the dotted white arrows point to debris and the black arrow points to a transverse crack.

The results of the EDX quantitative element analysis of the tested glass-ceramic specimens are presented as average values (wt.%) in Table 3 and illustrated in Fig. 38, 39 & 40. All glass-ceramic specimens contained oxygen, silicon, aluminium, zirconium, and phosphorus. Potassium and zinc were also detected in all groups except in the ZLS group, however, it was the only group that contained Indium, cerium, and terbium. Lithium was not detected in any of the specimens due to its extremely low energy of characteristic radiation.

Table 4: EDX element quantification for glass-ceramic materials (wt.%).

Element	PLD	FLD	ZLS
O	53.81	50.64	38.35
Al	0.42	2.51	1.21
Si	34.90	36.60	31.75
P	1.02	1.51	5.37
Zr	5.27	6.10	12.67
Zn	0.92	0.46	-
K	3.67	-	-
Ce	-		2.43
Tb	-	-	1.62

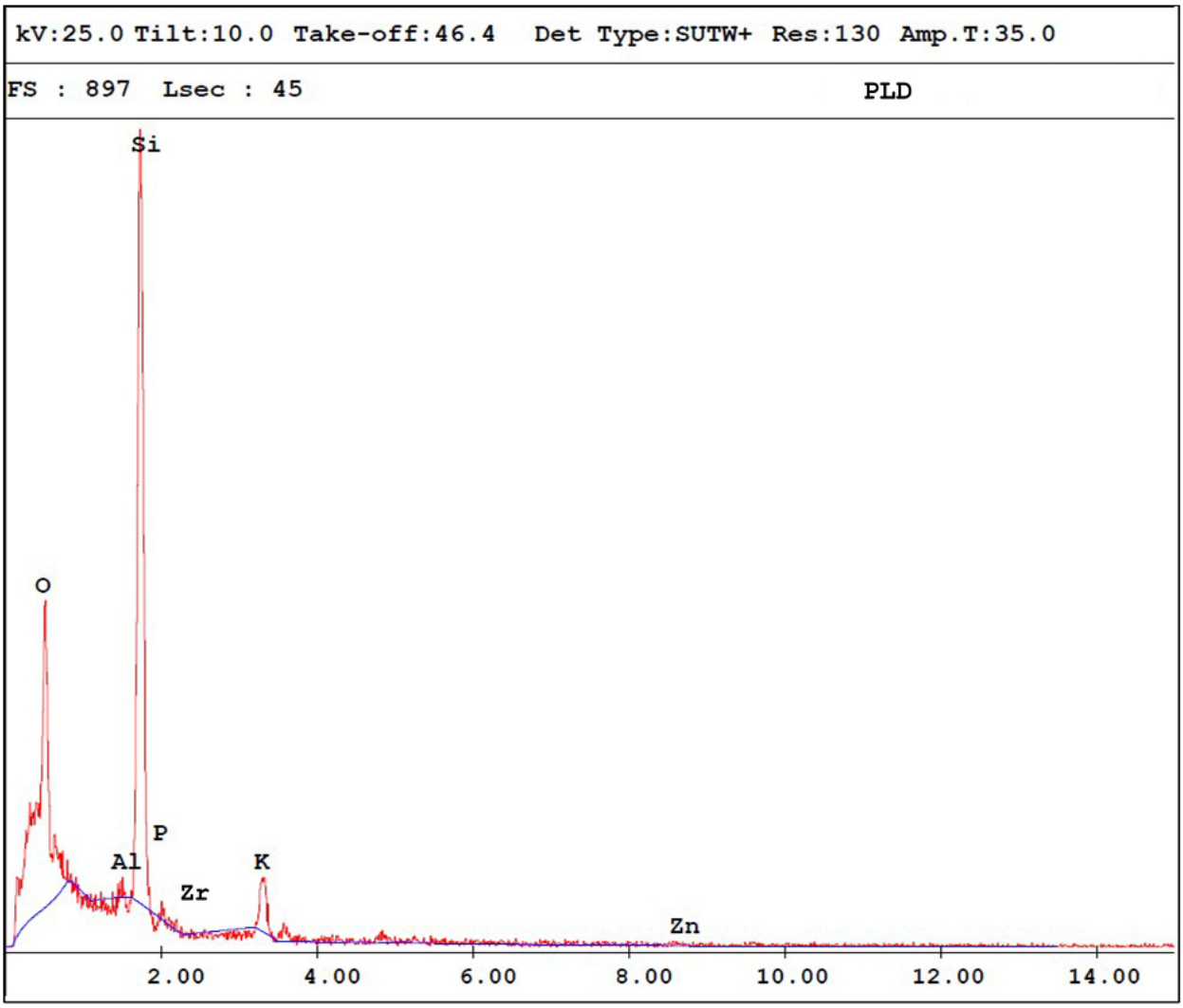

Fig. 38: EDX spectrum of PLD shows the presence of silica, potassium, aluminium, kalium, and zirconia.

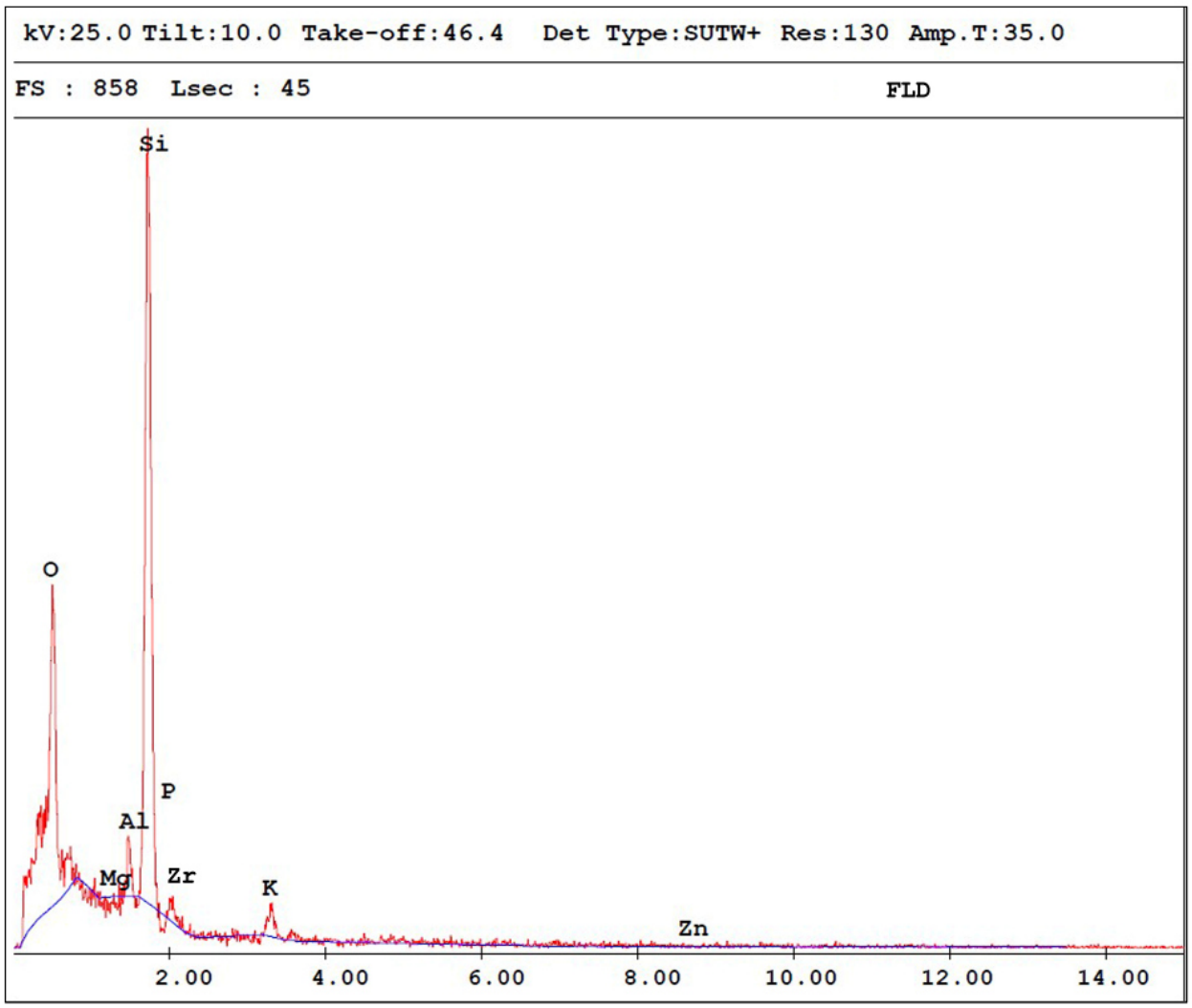

Fig. 39: EDX spectrum of FLD shows the presence of silica, potassium, aluminium, and zirconia.

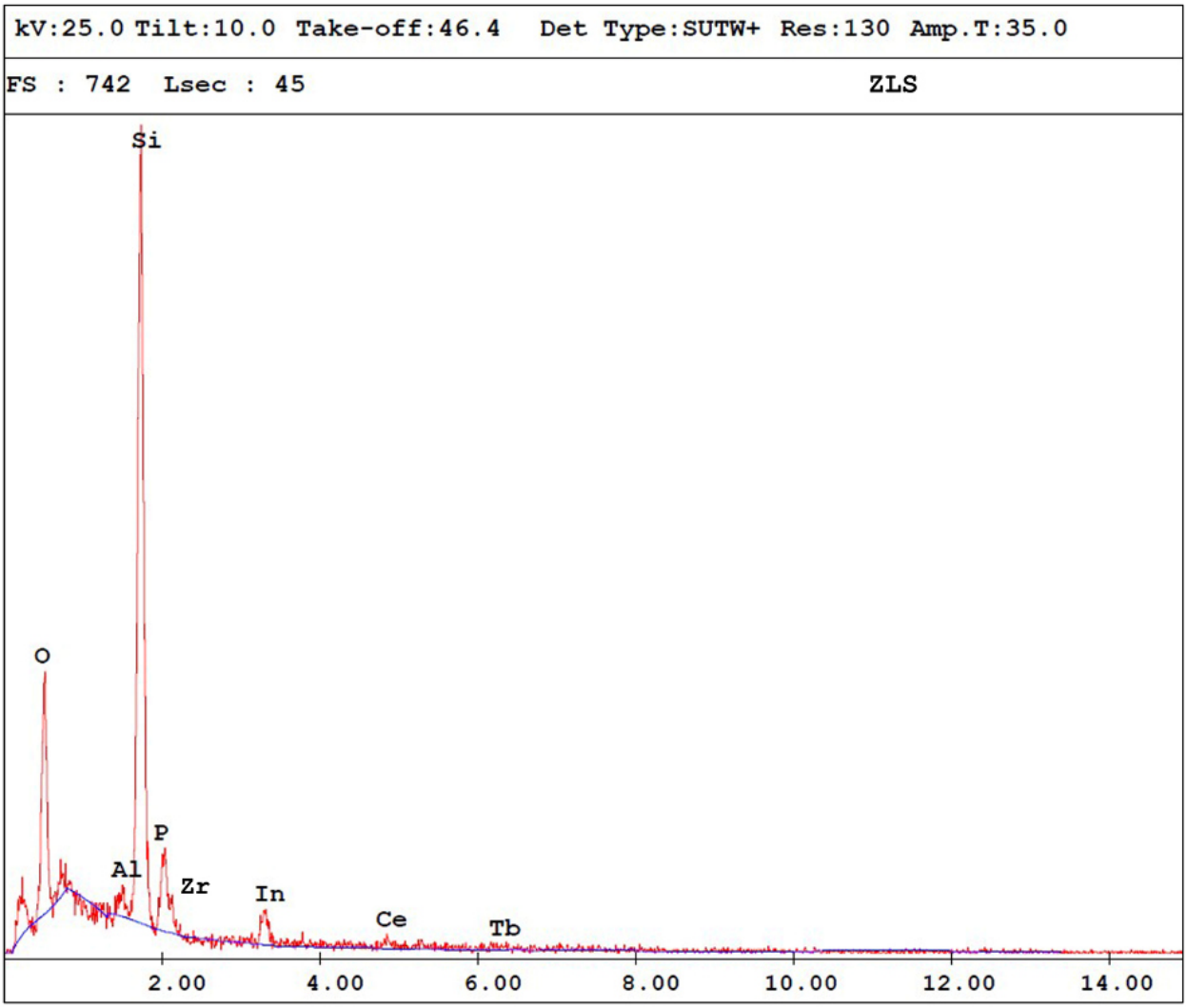

Fig. 40: EDX spectrum of ZLS shows the presence of silica, potassium, aluminium, and zirconia.

4.5 Load to fracture

Only one specimen from the FLD group failed during the thermomechanical cyclic fatigue ageing. Therefore, all the fatigued crowns (except the failed specimen) were subjected to static loading till fracture. According to the Two-way ANOVA analysis, the material type had a significant effect on the load-bearing capacity of the tested crowns ($P<0.001$), while the effect of thermomechanical ageing was statistically non-significant for all groups ($P=0.58$). Means and standard deviations are illustrated in Fig. 41. For the non-fatigued crowns, the two monolithic zirconia groups (SMZ and UMZ) showed the highest mean fracture load of 2390 ± 191 N, and 2379 ± 230 N, respectively, which was statistically significantly higher than all other tested groups. There was no statistically significant difference between ZLS and FLD groups ($P>0.99$) which showed the least mean fracture load of 1176 ± 323 N, and 1237 ± 263 N, respectively. PLD had a mean fracture load value of 1794 ± 288 N, which was lower than zirconia groups and higher than other glass-ceramic groups. After ageing, glass-ceramic groups showed less mean fracture load values, while zirconia groups were fractured at a slightly higher force. The differences between the mean fracture load values of fatigued and non-fatigued crowns were statistically insignificant for all groups.

4.6 Change of Colour (ΔE) after thermomechanical ageing

Means and standard deviations of the L*, a*, and b* values for the ceramic crowns before and after thermomechanical loading are presented in Table 5. T-test for each parameter within each group showed a statistically significant difference after thermomechanical ageing in all colour parameters for all tested groups ($P<0.001$). Analysis of variance test showed statistically significant differences between the mean ΔE values of the tested crowns ($P<0.001$). Means and standard deviations of ΔE are presented in Fig. 42. The highest mean ΔE was recorded for the PLD (7.48 ± 1.12) followed by ZLS (7.21 ± 1.37). The lowest mean ΔE was recorded for the SMZ (5.20 ± 0.91) and UMZ (5.10 ± 0.61). FLD showed a statistically non-significant difference in the mean ΔE (6.09 ± 0.94) compared to all other groups except PLD ($P=0.04$). The difference between SMZ and UMZ groups as well as between PLD and ZLS groups was statistically non-significant.

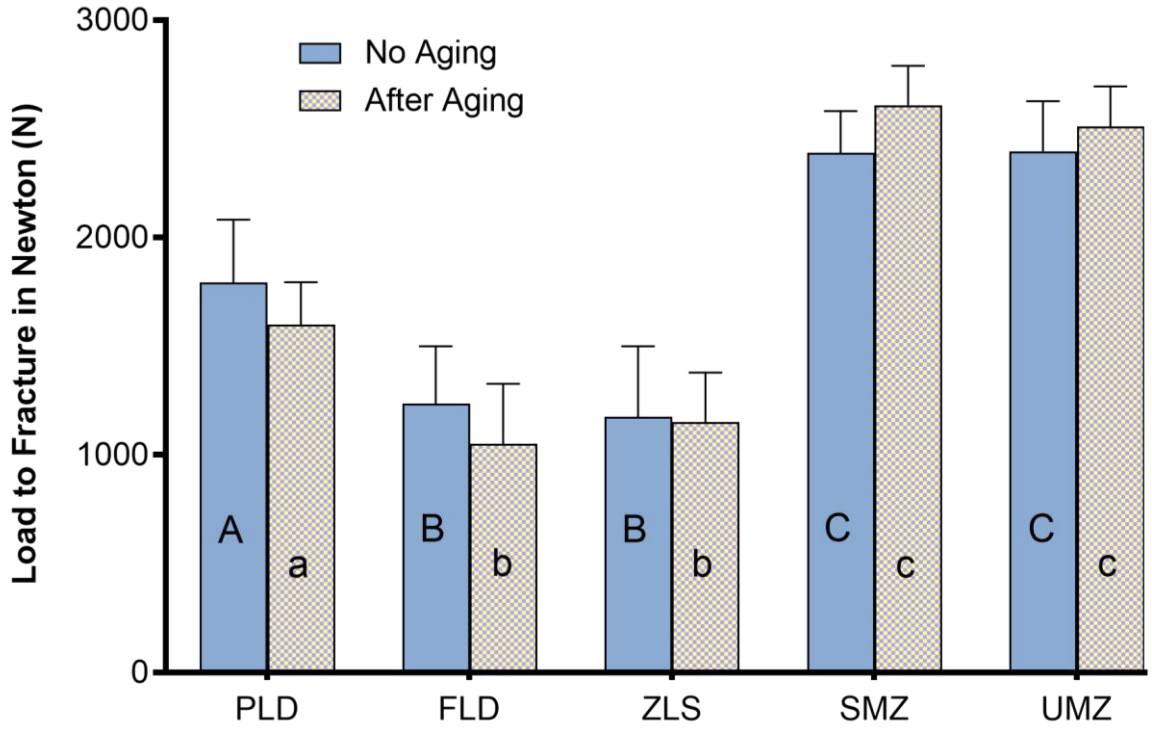

Fig. 41: Mean and standard deviation of Load to fracture test in newton before and after ageing. The capital letters show significant difference among groups without ageing. The small letters show the significant difference among groups after ageing. Means that do not share the same letter are significantly different.

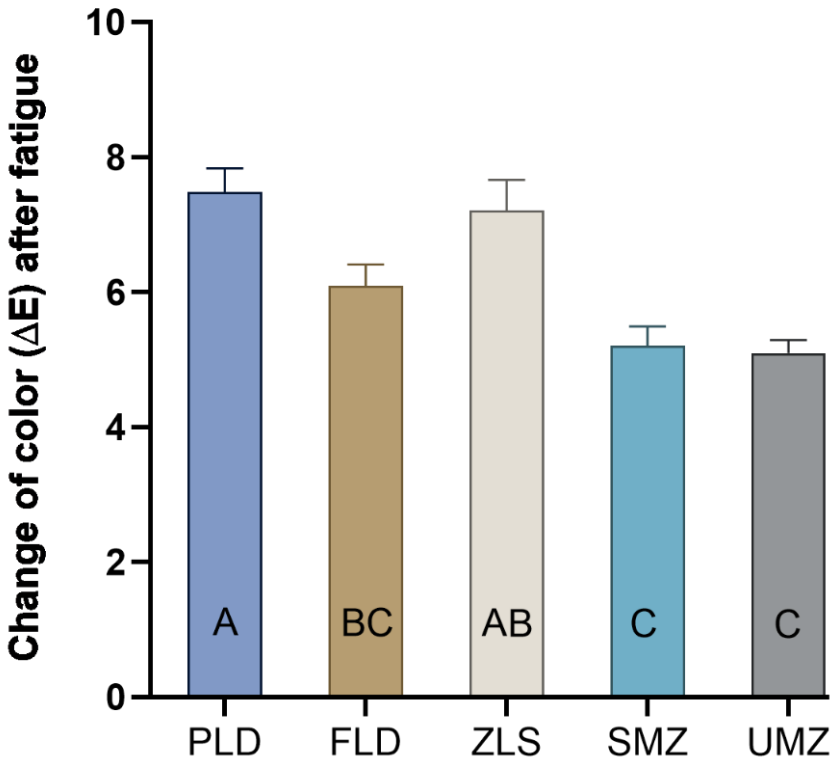

Fig. 42: Mean and standard deviation of the ΔE for ceramic crowns after thermomechanical ageing. The letters show the significant difference among groups. Means that do not share the same letter are significantly different.

Table 5: Mean and Standard deviation of CIElab colour parameters of the crowns before and after thermomechanical ageing

		PLD	FLD	ZLS	SMZ	UMZ
L*	A	70.85 (0.60)	71.47 (1.01)	63.80 (2.10)	75.66 (1.90)	73.37 (0.63)
	B	77.41 (1.19)	75.78 (1.23)	70.08 (1.21)	80.33 (0.77)	77.76 (0.83)
a*	A	-1.76 (0.05)	-3.34 (0.16)	-2.34 (0.13)	-1.33 (0.46)	-2.66 (0.22)
	B	-0.78 (0.11)	-1.62 (0.24)	-1.13 (0.09)	-0.49 (0.46)	-1.81 (0.22)
b*	A	9.42 (0.13)	15.67 (0.88)	7.59 (0.94)	21.50 (1.12)	15.41 (0.92)
	B	12.85 (0.46)	19.69 (1.01)	11.71 (0.62)	22.32 (1.15)	17.80 (0.89)

L* = lightness, a* = colour coordinate that represents the green-red range, and b* = colour coordinate that represents the blue-yellow range. A= before ageing, B= after ageing. T-test for each parameter within each group showed a statistically significant difference after thermomechanical ageing in all colour parameters for all tested groups ($P<0.001$)

4.7 Translucency parameter (TP)

One-way ANOVA showed a statistically significant difference between the mean TP values of the tested groups ($P<0.001$). Descriptive values are presented in Fig. 43. FLD showed the highest mean TP value (18.7 ± 0.7), while both monolithic zirconia groups SMZ and UMZ had the least values of (9.99 ± 0.6 and 9.93 ± 0.6, respectively). PLD and ZLS showed mean TP values of 15.6 ± 0.4, and 16.5 ± 0.6, respectively. The differences between all the groups were statistically significant ($P<0.001$) except for the SMZ and UMZ groups which showed non-significant differences ($P>0.99$). In addition, the difference between the PLD and ZLS groups was only marginally significant ($P=0.03$).

4.8 Change of colour (∆E) from selected shade (A3)

Only the zirconia groups showed ∆E values below the reported clinically perceptible level (>3.7). The ∆E values between the shade of ceramic specimens and the selected shade (A3) showed statistically significant differences between the tested groups ($P<0.001$). Means and standard deviations are presented in Fig. 44. The highest mean ∆E value was reported for the PLD group (7.99 ± 0.24) followed by the FLD group (5.00 ± 0.52) and ZLS group (4.99 ± 0.58). The monolithic zirconia groups SMZ and UMZ showed the least mean ∆E values of 2.2 ± 0.5, and 2.47 ± 0.47, respectively. There was no statistically significant difference, neither between SMZ and UMZ ($P=0.58$) nor between FLD and ZLS ($P>0.99$).

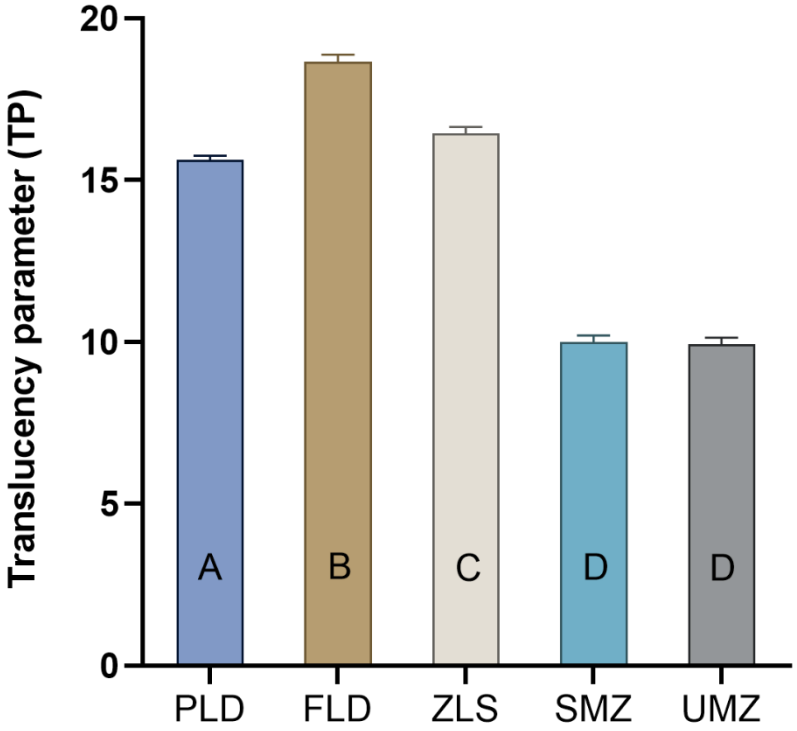

Fig. 43: Mean and standard deviation of translucency parameter for different ceramic groups. The letters show the significant difference among groups. Means that do not share the same letter are significantly different.

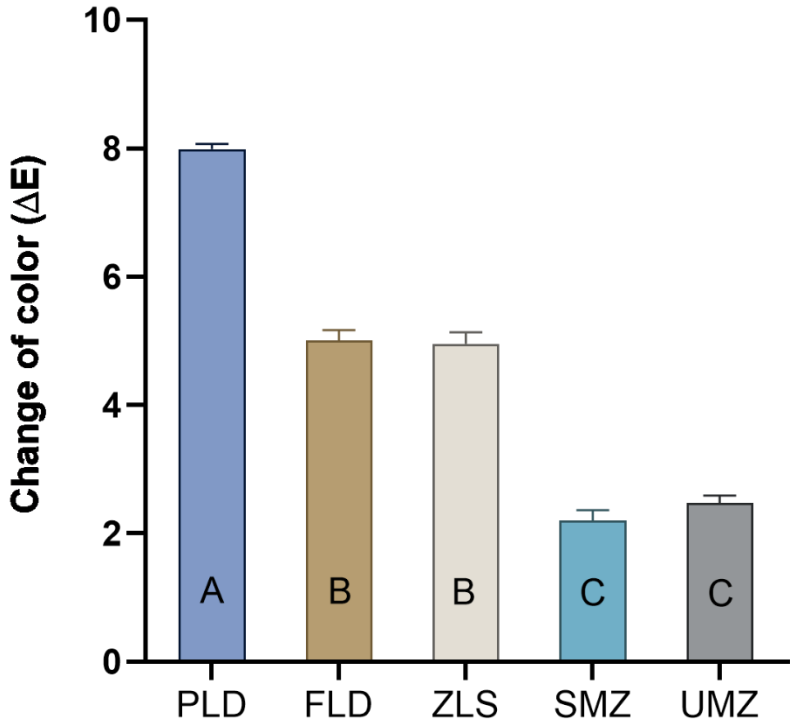

Fig. 44: Mean and standard deviation for the ΔE between ceramic specimen and selected shade (A3). The letters show the significant difference among groups. Means that do not share the same letter are significantly different.

4.9 X-ray diffraction pattern analysis (XRD)

Representative XRD patterns for tested groups are shown in Fig. 45 & 46. The XRD analysis showed no differences in the crystalline morphology for any of the tested materials after thermomechanical ageing. Lithium disilicate ($Li_2Si_2O_5$) and Lithium orthophosphate (Li_3PO_4) crystals were identified in all the glass ceramic groups to varying degrees. Additionally, Lithium silicate (Li_2SiO_3) was identified in the ZLS pattern, whereas FLD reported the presence of silica crystals (SiO_2). In terms of zirconia groups, the experimental lattice patterns of the SMZ and UMZ were quite similar. The SMZ sample showed a lattice pattern that fits very well with the tetragonal zirconia. There was clear splitting in the tetragonal peaks showing additional peaks at 2theta 50.61, 59.82, 74.44, 82.35, and 95.28 which fit with cubic zirconia. The UMZ showed a lattice pattern that matched with the tetragonal phase of yttrium doped zirconia. There was no clear splitting in any of the tetragonal phase peaks, therefore no additional peaks could be identified.

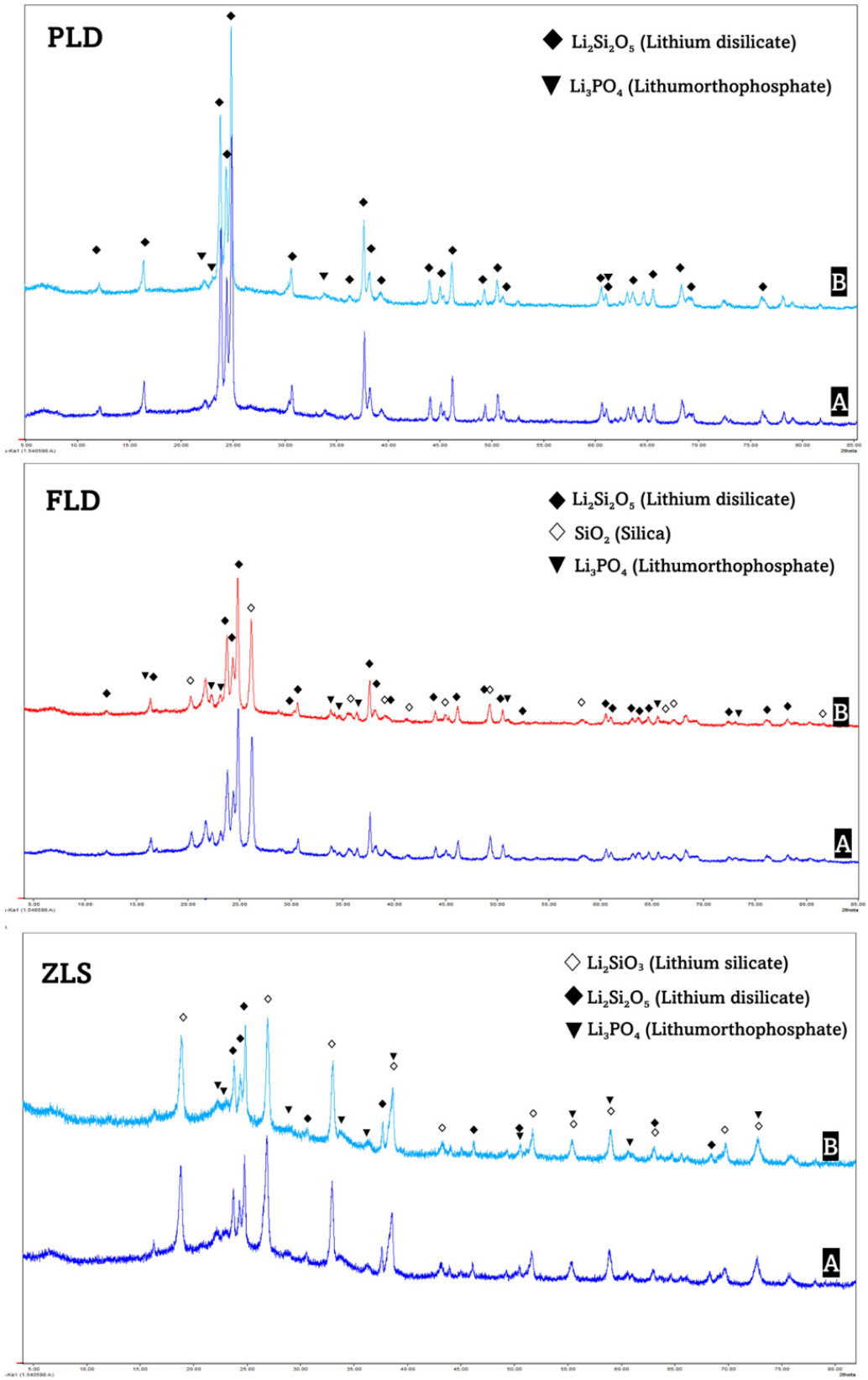

Fig. 45: XRD patterns of glass ceramics. A=before ageing, B=after ageing. The patterns show no difference before and after thermomechanical ageing. FLD pattern shows the presence of silica in addition to the lithium disilicate crystals.

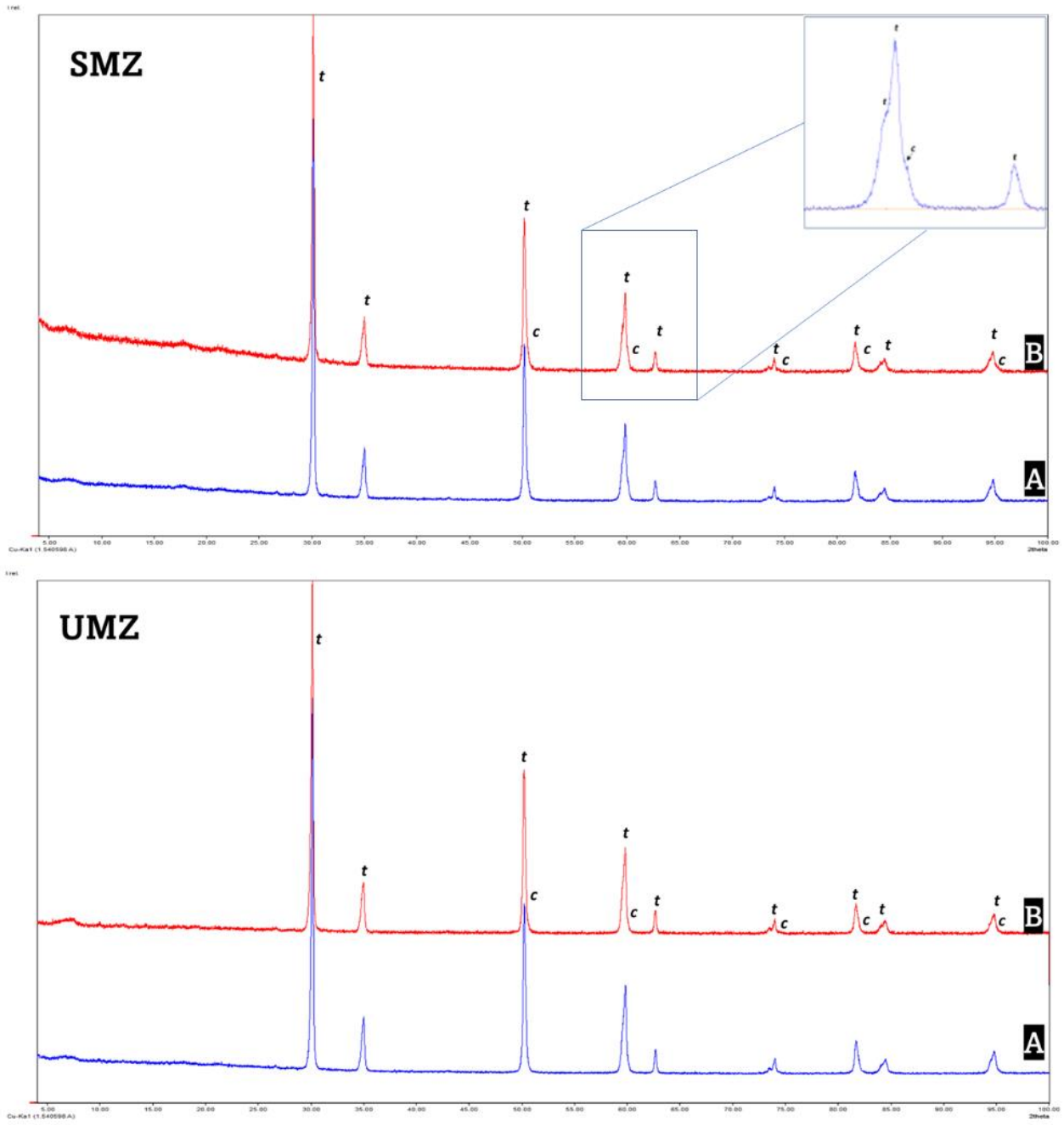

Fig. 46: XRD patterns of Zirconia. A=before ageing, B=after ageing. t=tetragonal zirconium oxide, c=cubic zirconium oxide. No effect for the thermomechanical ageing on the patterns could be recognized. SMZ and UMZ XRD patterns show mainly tetragonal phases. Cubic phases could be identified by splitting in the tetragonal peaks at 2theta 50.61, 59.82, 74.44, 82.35, and 95.28.

5. Discussion

5.1 Discussion of materials selection and methodology

The materials of the study were chosen to include the commonly used ceramic categories indicated for aesthetic CAD/CAM monolithic crowns. IPS e.max CAD is a lithium disilicate based glass-ceramic that is supplied in a partially sintered block. It has been widely investigated in the literature and is considered a gold standard in all-ceramic restorations showing a cumulative survival rate of 96.5 % for complete coverage monolithic restorations after 10 years (Malament et al., 2019). Therefore, comparing the mechanical and physical properties of novel materials to PLD is meaningful. LiSi CAD is a newly introduced lithium disilicate ceramic that is supplied in the form of fully sintered CAD/CAM blocks. At the beginning of this study, this material was still in the experimental testing phase and was not yet delivered to the market. Therefore, there is very limited data in the literature about its composition and clinical performance. The Celtra Duo was added to the current investigation because it is commonly used and falls within the category of modified silicate ceramics. Katana STML and UTML are new high translucent multilayer 4Y-PSZ and 5Y-PSZ that belong to the third and fourth generations of monolithic zirconia. They were claimed to have translucencies similar to glass-ceramics but with higher strength (Zhang and Lawn, 2018). These new zirconia formulations have not yet been adequately studied in the literature therefore they were chosen for the present study.

In the current research, extracted natural teeth were used as antagonists during wear simulation. Even though natural teeth might differ in enamel structure, geometry or surface quality, the use of non-standardised enamel cusps was verified in previous studies as an appropriate choice to simulate the clinical situation during wear investigations (Krejci et al., 1999; Lutz et al., 1992). Moreover, according to Kunzelmann et al. (2001), the standardisation of enamel cusps by means of grinding alters the wear potential and leads to inaccurate results. To minimise the effect of variations, every extracted tooth was carefully examined under magnification for any signs of defect, attrition, or abnormality.

The crowns in the present study were subjected to 1,200,000 chewing cycles at 49 N associated with thermal cycles in a chewing simulator to simulate the intraoral fatigue process and investigate the durability of dental restorations (Özcan and Jonasch, 2018). Furthermore, restorations frequently fail at forces lower than their ultimate fracture

strength after a period of service as previously reported (Baldissara et al., 2010). Several ageing methods are described in the literature, however, the ageing method used in this study was widely accepted and used in previous in-vitro studies (Al-Akhali et al., 2019; Guess et al., 2013; Sasse et al., 2015; Zimmermann et al., 2019). A control group, not subjected to chewing cycles, was added to investigate the effect of thermomechanical ageing on strength and colour.

In the present study, two-body wear was investigated in-vitro. Only in a few studies described in the literature was wear investigated in-vivo, but this was found to be time consuming and complicated (Esquivel-Upshaw et al., 2006; Stober et al., 2014). As a result, wear is typically evaluated in-vitro using wear simulators and under controlled conditions (Heintze, 2006). A novel technique utilizing micro-computed tomography (µ-CT) was used to quantify volumetric enamel wear following the parameters of a recently published study (Kaizer et al., 2019). After demonstrating accuracy and reliability in volumetric wear assessment of prosthetic joint replacements, micro-CT was regarded as a promising technology for wear quantification in different fields including dentistry (Parrilli et al., 2016).

5.2 Discussion of Results

5.2.1 Discussion of wear results

The findings of this study showed that the ceramic material significantly affected the restoration's wear rate and its abrasiveness toward antagonist teeth. Therefore, the first null hypothesis which assumed no difference in wear properties among the evaluated materials has to be rejected.

With the beginning of the use of zirconia as monolithic restorations, questions were raised about the possibility of causing an increased rate of abrasive wear to the opposing natural teeth (Kim et al., 2012). However, the results of the present research came to the contrary, as they showed that SMZ and UMZ resulted in significantly lower volumetric tooth loss in the antagonist teeth than that reported for PLD or ZLS. Equivalent results were reported in previous studies (Amaya-Pajares et al., 2016; Kim et al., 2012; Sripetchdanond and Leevailoj, 2014). Although it has been proposed that abrasiveness is proportional to hardness (Hudson et al., 1995; Jagger and Harrison, 1995), the correlation between ceramic hardness and increased enamel wear is still debatable. According to Oh et al. (2002), the

hardness factor has no significant effect on the rate of enamel wear. Moreover, Ghazal and Kern (2009) concluded that the restoration's surface roughness is more effective. In the present study, the surface analysis revealed that zirconia specimens could keep smooth surfaces throughout the test. On the contrary, after wear cycles, glass-ceramic specimens showed rough surfaces, which might have introduced microcracks and discrepancies on the contacting surface and ramped up the loss of enamel.

The findings of the present study agreed with those of Sripetchdanond and Leevailoj (2014) in which the antagonist enamel showed less wear when occluded against monolithic zirconia versus glass-ceramic. The authors attributed the increased enamel wear caused by glass-ceramic to the formation of an abrasive debris layer on the ceramic surface due to the dislodgment of some glass particles during the wear process, which increased the material's coefficient of friction. Although artificial saliva was used to wash away the cut debris on a regular basis, SEM confirmed the presence of plentiful wear remnants on the worn surfaces of the PLD specimens and small traces on the FLD surfaces. Wear debris formed on the surface of glass-ceramics has been previously reported to accelerate enamel wear (Fischer et al., 2000).

In contrast to our findings, Ludovichetti et al. (2018) found that zirconia caused enamel wear rates comparable to glass-ceramics. The higher elastic modulus and hardness of the 3Y-TZP monolithic zirconia compared to the 4Y-TZP and 5Y-TZP used in our study could explain the mismatch in zirconia abrasiveness between both studies. In addition, the difference in surface treatments (glazing or polishing) could affect the wear behaviour of zirconia. In a clinical study conducted by Selvaraj et al. (2021), polished zirconia caused significantly less enamel wear in antagonists than glazed zirconia after one year. Furthermore, in an in-vitro study by Kaizer et al. (2019) it was shown that polished zirconia caused significantly less antagonist wear than non-polished and glazed zirconia after 1.25 million chewing cycles.

Occlusal surfaces of posterior teeth are subjected to approximately 20 – 38 µm physiological enamel loss per year in normal situations, which corresponds to 0.07 – 0.14 mm^3 (Gkantidis et al., 2020). Provided that our test parameters correspond to nearly a year of clinical service (Mormann et al., 2013), the enamel wear produced by the zirconia

specimens appear to fall within the normal wear rate range. The glass-ceramic specimens, on the other hand, resulted in nearly double the reported normal wear rate.

Ceramic wear is a dynamic process that involves many wear mechanisms and is dependent on many factors such as operating parameters, material intrinsic properties and microstructure or defects (Wang and Hsu, 1996). Under tribological stress, when the plastic deformation surpasses the material's critical limit of plasticity, microfractures are induced and wear debris is produced (Mecholsky, 1995). The wear mechanism of brittle materials such as ceramics is predominantly due to the development of microfractures on the surface rather than due to plastic deformation (Anusavice, 2013). The ability of the brittle material to resist the propagation of induced cracks and flaws is described by a mechanical property called "fracture toughness" (Ilie et al., 2012). The higher fracture toughness of zirconia could explain the findings of the present study, in which SMZ and UMZ specimens had significantly lower wear values than ZLS, PLD, and FLD specimens. Furthermore, the zirconia specimens were less susceptible to developing microcracks along the surface during the wear test. Moreover, zirconia is characterised by the presence of the "transformation toughening" phenomenon which helps to stop the propagation of induced surface microcracks and increase the resistance of the material to fracture (Sripetchdanond and Leevailoj, 2014). This was reflected on the higher ability of zirconia specimens to retain a smooth surface based on the surface roughness (R_a) measurements and as shown in the SEM scans.

Unlike zirconia, which is polycrystalline, silicate-based glass-ceramics are composed of crystalline phases distributed throughout a glass matrix. Since the glassy phase is weak, it could be easily worn out under continuous friction from the antagonist resulting in irregularities on the surface. This assumption is in line with the surface analysis results which showed a significant increase in the Ra values for the glass-ceramic groups PLD and ZLS after wear cycles, while the surface roughness values of both zirconia groups showed nearly no change.

The ceramic wear measurements were consistent with the SEM micrographs. The lower magnification images matched those obtained by Lawson et al. (2016) for PLD and ZLS ceramics. The pattern of abrasive wear differed between materials in terms of shape and size. A large wide wear scar with distinguished wear tracks was seen in the three glass-

ceramic materials at the area where the tooth contacted the specimen's surface, indicating extensive wear action. In contrast, zirconia showed no surface indentation, but only thin scratch lines along the length of the wear track, which were limited to the size of the antagonists' cusp tip. This could be explained by zirconia's higher hardness (Miyazaki et al., 2013), which has been shown to play a role in determining ceramic wear resistance (Preis et al., 2012).

Despite differences in microstructure and composition, no statistically significant difference in wear properties was found between the PLD and ZLS groups. Lawson et al., (2016) reported similar enamel wear results for PLD (0.420 mm^3) and ZLS (0.276 mm^3). This similarity in wear behaviour could be attributed to the similarity of Young's modulus (Belli et al., 2017). The wear resistance of the experimental FLD was statistically significantly higher than other glass-ceramic groups. This could be due to variations in chemical composition, microstructure, surface treatment, and milling state between materials. The EDX analysis showed similar compositions for the two lithium disilicate ceramics except that FLD had a higher aluminium content (2.51 wt.%) than PLD (0.42 wt.%). In general, fillers are introduced into glass ceramic matrices to improve strength, microhardness, resistance to crack propagation and other mechanical properties (Orlova et al., 2013). The addition of fine alumina fillers in the range of 0 – 20 wt.% has been shown to significantly improve the wear resistance of dental composites by up to the three fold (Patnaik et al., 2008; Sawyer et al., 2003).

The wear properties of ceramic materials are affected by milling and post milling treatments (Mota et al., 2017; Yara et al., 2005). The milling process induces the formation of intrinsic flaws that negatively affect the strength and raise the abrasiveness of dental ceramics (May et al., 2021). Glazing of ceramic restorations was once thought to seal the surface defects caused by milling and reduce the wear of antagonist teeth (Baharav et al., 1999). However, some researchers believe that polishing can achieve comparable, if not better, results (Alao et al., 2017). It has been proposed that residual compressive stresses are created beneath the surface during polishing, which could deflect crack forces and prevent further crack growth (Giordano et al., 1995). Furthermore, the polishing step can be performed chairside without the need for special equipment, thus reducing the treatment’s duration and cost.

Soft milling is suitable for hard materials such as zirconia and lithium disilicate, not only to simplify the milling process and preserve the milling burs but also to overcome the milling-induced flaws in the final restoration (Tinschert et al., 2004). Despite being milled in a fully crystallised state, FLD specimens demonstrated greater wear resistance than other glass-ceramic groups in the present study. This could be explained by the ability of hard materials to confine newly formed surface flaws to the superficial surface layer, limiting their propagation. Milling the ceramic in a soft state, on the other hand, enables the generated flaws to extend into deeper layers. According to Mota et al. (2017), ceramic restorations milled out of fully crystallised blocks showed smoother surfaces than those milled in an intermediate state and then fired.

Ceramics' wear behaviour can also be influenced by microstructural differences (Seghi et al., 1991). SEM images at high magnification revealed differences in size, shape, and distribution of crystals between glass-ceramics. The images of PLD showed holes that represented the areas from which soluble lithium phosphate crystals were stripped away during the intermediate phase milling (Denry and Holloway, 2010; Lien et al., 2015). The presence of defective areas in the PLD image (Fig. 37a) could be a sign of the removal of the glaze layer due to friction with enamel. Furthermore, the images showed a dense layer of wear debris covering the worn areas. The SEM examination of FLD displayed two crystalline phases: densely interlocking rod-shaped lithium disilicate crystals and uniformly scattered spherically shaped crystals. It has been reported that adding less than 10 % ZrO_2 to the glass matrix of lithium disilicate material acts as a nucleating agent and changes the crystalline structure from a rod-like shape to a spherical (Fu et al., 2020). The second crystalline phase might have aided in the prevention of crack propagation by acting as micro-fillers or via the bridging mechanism that was suggested by Huang et al. (2014).

5.2.2 Discussion of fracture strength results

The results of the present study demonstrated that the ceramic material had a significant effect on fracture resistance. However, within each material, the thermomechanical ageing did not significantly alter the maximum fracture load of the crowns. Therefore, the second null hypothesis is rejected, while the third null hypothesis is accepted.

In a normal patient, the intra-oral posterior biting force ranges from 490 N to 520 N (Apostolov et al., 2014), while in abnormal conditions such as bruxism, it can reach 790 N (Nishigawa et al., 2001). If a material can withstand biting loads of 500 N for the premolar area and 900N for the molar area, it could be considered for posterior indications (Özcan and Jonasch, 2018). The average fracture loads reported for the crowns in this study range from 1176 N to 2397 N for non-aged crowns and 1051 N to 2609 N for the aged ones, both of which are greater than the maximum clinical mastication loads. As a result, all the tested materials demonstrated enough strength to withstand the clinical biting forces.

The mean fracture loads of the glass-ceramic crowns did not significantly decrease after ageing, indicating that glass-ceramic materials could retain their mechanical strength when subjected to load cycles. Meanwhile, the mean fracture load values of zirconia crowns slightly increased after ageing; however, the increase was also insignificant. One reason could be increasing the yttrium oxide content to more than 3 mol% which increased the material's resistance to low-temperature degradation (LTD) (Flinn et al., 2017; Zhang and Lawn, 2018). No difference was observed between the XRD patterns of aged and non-aged specimens. XRD patterns of zirconia specimens were similar to those reported by Pereira et al. (2018) who found no change in the SMZ and UMZ patterns after ageing.

The 4Y-TZP and 5Y-TZP zirconia specimens, which were investigated in the present study, demonstrated higher fracture resistance than all glass-ceramic groups. This finding is consistent with previous studies (Johansson et al., 2014; Lawson et al., 2019; Nakamura et al., 2015; Sun et al., 2014). The 3Y-TZP is the toughest among all zirconia generations (flexural strength >1000 MPa and fracture toughness ~5 MPa$\sqrt{m}$) owing to the transformation toughening mechanism (Kern et al., 2016). Increasing the stabilizer percentage above 3 mol% aimed to enhance the translucency; however, it was associated with a decline in mechanical strength due to the interruption of the t-m transformation phenomenon (Stawarczyk et al., 2017). Nevertheless, still these translucent zirconia generations are more fracture-resistant than other ceramics.

The claim that the new zirconia products with increased yttrium content are mainly cubic was not confirmed in the present study. The XRD analysis demonstrated that the dominant phase in SMZ and UMZ is tetragonal. Cubic phases with rather small lattice parameters were identified in the SMZ pattern. No splitting in the tetragonal peaks or additional

peaks could be identified in the UMZ pattern. However, it is not necessarily due to the absence of cubic phases. If the lattice parameters of both phases are quite close, the cubic phase might be totally superimposed by the tetragonal.

In contrast to our findings, Garoushi et al. (2021) observed a significant change in the fracture load values of monolithic crowns after thermomechanical fatigue. They reported a reduction in the mean fracture load of PLD from 1280 N to 1050 N, FLD from 1400 N to 900 N, and ZLS from 1300 N to 900 N. In the mentioned study, a different crown design and cyclic fatigue protocol were used which could explain the difference in results. The authors utilised anterior crowns and applied the loading forces in an inclined direction. Furthermore, they subjected the crowns to 220 N force for 120,000 cycles, which is much higher than the force applied in the present study (F = 49 N).

Our findings are in accordance with several previous studies (Baladhandayutham et al., 2015; Church et al., 2017; Johansson et al., 2014; Nakamura et al., 2015; Nishioka et al., 2018; Sun et al., 2014; Zhang et al., 2016b). Zhang et al. (2016b) reported that zirconia required a significantly higher load (5780 ± 1050 N) to cause a full split in the crown than lithium disilicate (3640 ± 330 N). Baladhandayutham et al. (2015) reported similar fracture load values for lithium disilicate (1465 ± 330 N). Compared to our findings, they reported lower fracture load values for translucent monolithic zirconia crowns (1669 ± 311 N). An explanation is that the authors of that study performed the test on zirconia crowns milled at the minimal clinical occlusal thickness (0.6 mm); whereas all the crowns in the present study were milled at the recommended occlusal thickness for all-ceramic restorations (1.5 mm). Similarly, Nakamura et al. (2015) and Sun et al. (2014) documented the fracture of monolithic translucent zirconia crowns at significantly higher loads than lithium disilicate. The authors however reported higher fracture loads for zirconia crowns than our reported values (4110 N and 5558 N, respectively), which could be attributed to differences in zirconia, die material, cement type, and crown design. Furthermore, the findings of the present study are similar to those of Johansson et al. (2014), who demonstrated mean fracture load values for monolithic zirconia 3038 ± 264 N (Z-CAD, Metoxit) higher than lithium disilicate 1856 ± 161 N (Emax press, Ivoclar Vivadent) after subjecting the crowns to thermomechanical load cycles.

The fracture strength of ceramic materials is highly influenced by their microstructure (Kelly, 1995). Adding crystalline phases to glass matrices in dental ceramics was intended to improve their mechanical properties (Seghi et al., 1995). The composition, size, and distribution of the crystalline phases determine the characteristics of the final product (Huang et al., 2014). The dense distribution and high interlocking of lithium disilicate crystals in PLD limit the spread of cracks (Furtado de Mendonca et al., 2019; Ohashi et al., 2017). In ZLS, tetragonal zirconia fillers were added to increase the strength and improve the optical property (Zarone et al., 2021). However, still this assumption a controversial issue in the literature (Elsaka and Elnaghy, 2016; Gomes et al., 2017; Hamza and Sherif, 2019; Zarone et al., 2019). The current findings revealed higher fracture resistance for PLD than ZLS. Similar findings were previously reported by Choi et al. (2017). The declined strength could be attributed to the change in the shape of lithium disilicate crystals from small needle-shaped in PLD to larger crystals with more round and elongated morphology in ZLS (Furtado de Mendonca et al., 2019), which might reduce the crystals interlocking effect. Moreover, the XRD pattern of ZLS demonstrated a higher percentage of the weaker lithium metasilicate phase in the final product. In a previous study that investigated the mechanical properties of monolithic CAD/CAM restorations, PLD had significantly higher flexural strength than ZLS, while the fracture loads did not significantly differ (Furtado de Mendonca et al., 2019). However, the investigated ZLS product in the present study has a different milling state and microstructure (Zarone et al., 2021).

FLD crowns were milled from fully crystallised lithium disilicate CAD/CAM blocks that were still in the experimental phase. According to the manufacturer, the crowns can be polished after milling and directly cemented without the need for further glazing or firing. There is not enough data about the microstructure of the set material available in the literature. FLD crowns demonstrated lower fracture strength than PLD. This could be attributed to the ability of the firing cycle to redistribute the crystals inside the material to repair the internal cracks and surface flaws that are induced during the machining of the brittle ceramics (Thompson and Rekow, 2004). Moreover, both materials differ in the fabrication method, which could influence the physical and mechanical properties of the final product (Choi et al., 2017). Further laboratory studies are recommended on the mechanical, physical, and microstructural characteristics of FLD.

5.2.3 Discussion of colour and translucency results

Aesthetic restorations are expensive and should be able to function for several years without the need to be replaced because of colour changes. Therefore, investigating the ageing effect on the colour stability of aesthetic dental ceramics in-vitro is crucial for predicting their long-term success (Heydecke et al., 2001; Turgut and Bagis, 2011). According to the findings of the present study, thermomechanical ageing significantly affected the colour in all groups. Therefore, the fourth null hypothesis is rejected. After ageing, all crowns became more reddish and more yellowish. Similar findings were reported in previous studies (Bagis and Turgut, 2013; Luo and Zhang, 2010). The change of colour was greater than the clinical perception threshold (>3.5) (Bagis and Turgut, 2013). The colour of SMZ and UMZ was the least affected by ageing among the tested groups. In contrast, PLD and ZLS demonstrated the highest ΔE values after ageing. In contrast, a study by Kurt and Turhan Bal (2019) demonstrated a minimal change of colour in lithium disilicate after ageing (ΔE = 0.41), while in zirconia the colour change was significantly higher (ΔE = 5.03). The authors of the study used white zirconia specimens that were dipped in colouring liquids after sintering. To assess the ageing effect, they subjected the specimens to ultraviolet light which differs from the ageing protocol used in the present study. The ultraviolet radiation was reported to dissolve the metal oxides in the colouring agents (Dikicier et al., 2014; Ertan and Sahin, 2005; Pires-de-Souza et al., 2009) which could explain the significant colour change in zirconia specimens in their findings. In our study, the colour was measured for crowns that were cemented to translucent epoxy resin dies. Any change in the die colour might influence the final colour of the translucent restoration.

Regarding the colour reproducibility, none of the tested materials was able to precisely match the selected shade; therefore, the fifth null hypothesis is rejected. All the tested crowns were milled from pre-shaded CAD\CAM blocks of shade A3; however, they demonstrated different CIELab colour values. Glass-ceramics demonstrated remarkably high ΔE values above the clinically acceptable level. SMZ and UMZ had better matching to the selected shade without additional characterization (ΔE = ~2.5). It has been previously reported that different dental ceramic brands that share the same shade can result in a perceivably different colour in the final restoration (Seghi et al., 1986). Bagis and Turgut (2013) found that none of the full ceramic systems tested in their study could match

the corresponding colour tab in the Chromascop shade guide from Ivoclar Vivadent. Similar findings were published by Della Bona et al. (2015) who reported very high colour differences (ΔEs 6.32 – 13.42) when compared four different full ceramic systems to their corresponding nominal shades in the Vita-Classic shade guide. The authors also reported that Emax CAD HT with A3 shade demonstrated the worst match to the corresponding shade (ΔE = 13.42) which is in agreement with our results.

According to our findings, standardisation of colour conceptions among manufacturers is missing. Therefore, the achievement of a perfect shade match depending on the block shade only might be tricky. The individual characterization of the final restoration before cementation might be a necessary step to improve colour matching to adjacent teeth. Until the manufacturers adhere to a standard shade parameter during the fabrication of ceramic products and shade guides, it is recommended that dentists and technicians use the appropriate shade guide for every product.

The translucency of the material is a key aesthetic factor and an important consideration during the selection of the restoration material (Bagis and Turgut, 2013; Kelly et al., 1996). For restoration to appear natural, it must have the same colour and translucency as natural teeth (Jurisic et al., 2015). Compared to zirconia specimens, glass-ceramic specimens showed higher TP values, which is in line with findings from several previous studies (Harada et al., 2016; Harianawala et al., 2014; Kim and Kim, 2014; Kurt and Turhan Bal, 2019). Glass ceramics have superior translucency owing to their higher glass content (Zhang and Lawn, 2018). Although the translucency of the new monolithic zirconia generations is significantly improved compared to conventional ones, it remains lower than that of lithium disilicate at the same thickness (Kurt and Turhan Bal, 2019; Vichi et al., 2016). Kurt and Turhan Bal (2019) reported similar TP values to our findings for lithium disilicate (15.63 ± 1.29) and polished monolithic zirconia (8.54 ± 0.49) at 1.5 mm thickness. Likewise, Harada et al. (2016) found that lithium disilicate (Emax CAD LT) had higher light transmittance (Tt%) than all tested monolithic zirconias, including SMZ and UMZ, at thicknesses of 0.5 mm and 1.0 mm. There is a significant correlation between restoration thickness and translucency. Church et al., (2017) found that zirconia had significantly higher TP values at 0.5 mm than lithium disilicates at larger thicknesses. Similarly, the (Tt%) of SMZ and UMZ at the thickness of 0.5 mm was reported to be greater

than lithium disilicate at the thickness of 1 mm (Harada et al., 2016). Consequently, it is reasonable to conclude that when used at their clinically recommended thickness, the monolithic zirconia ceramics may have similar or even better translucency than lithium disilicate ceramics.

Among the glass-ceramic groups, the difference in TP values shown in the present study could be attributed to the variations in the type and percentage of crystalline phases between the tested products. FLD had higher TP values than PLD and ZLS. The XRD analysis detected silica (SiO_2) crystals in the FLD pattern. Moreover, the percentage of the lithium disilicate ($Li_2Si_2O_5$) phase was lower in the FLD pattern than in the PLD. In general, decreasing the crystalline content can increase transparency (Bagis and Turgut, 2013). Furthermore, FLD specimens were not subjected to a firing stage, which is reported to influence the opacity of the material (Campanelli de Morais et al., 2021).

5.3 Conclusions

In conclusion, the null hypotheses that materials will show no differences in wear resistance, abrasiveness, fracture resistance and shade reproducibility were rejected. The null hypothesis that ageing will not affect fracture load of tested materials was accepted, while the hypothesis that ageing will not affect the colour was rejected.

Highly translucent monolithic zirconia had high fracture resistance, excellent wear resistance and minimal abrasiveness to antagonist teeth; therefore, could be recommended in cases where high wear rates are anticipated e.g., bruxism. The experimental fully crystalized lithium disilicate was the most translucent and showed minimal abrasiveness to antagonist. It could be a good aesthetic alternative for treatments in the anterior part of the jaw. All materials can withstand intra-oral masticatory forces. None of the materials was able to accurately reproduce the selected shade or retain the colour after thermomechanical ageing. Post-milling characterization and finishing are recommended to achieve better shade matching.

6. Summary

The success of a restoration is determined by its ability to restore function and aesthetics, as well as to withstand the harsh oral environment for many years without fracture or change in colour and without causing excessive wear to the opposing teeth. The ability of restorative materials to resist fatigue is another critical aspect that affects long-term success and should be investigated. Examining the long-term durability of ceramic restorations should also include the stability of colour over time.

The purpose of this study was to investigate and compare five aesthetic monolithic dental CAD/CAM ceramic materials in terms of wear abrasiveness and resistance as well as fracture strength and colour stability after thermomechanical ageing. It aimed also to investigate the translucency and colour reproducibility of the tested ceramics.

Rectangular-shaped specimens were sectioned from CAD/CAM ceramic blocks and sorted according to the block material into five groups (n=10): PLD; partially-crystallised lithium disilicate, FLD; experimental fully-crystallised lithium disilicate, ZLS; zirconia-reinforced lithium silicate, SMZ; 4Y-TZP super translucent monolithic zirconia, and UMZ; 5Y-TZP ultra translucent monolithic zirconia. The specimens were subjected to 200.000 wear cycles against human premolars. Micro-CT scans for the teeth were taken before and after the test and the volumetric enamel loss was calculated through the overlapping of the generated 3D models. Weights and surface roughness (R_a) values of specimens were measured before and after the test and the differences were calculated. Representative specimens were randomly selected for SEM and EDX microstructural analysis. Digital spectrophotometer was used to measure CIEL*a*b* values over black and white backgrounds to calculate the translucency parameter (TP). The shade verification mode was used to calculate (ΔE) to shade A3.

Additionally, one hundred crowns of uniform thickness were milled from the tested blocks (n=20). Half of the crowns (n=10) were subjected to thermomechanical ageing in a chewing simulator. Thereafter, both aged and non-aged specimens were loaded until fracture in a universal testing machine and the fracture load was recorded. CIEL*a*b* values were measured Using a digital spectrophotometer before and after ageing, and (ΔE) was calculated. Data were statistical analysed using One-way and Two-way ANOVAs and equivalent test for non-parametric results. The significance level was set at $P \leq 0.05$.

Tested materials showed significantly different ceramic and antagonist wear rates ($p<0.001$). PLD and ZLS had the highest ceramic loss (2.95 ± 0.35 and 3.09 ± 0.37 mg), and they were the most abrasive to antagonist teeth (0.29 ± 0.34 and 0.47 ± 0.17 mm^3). On the other hand, SMZ and UMZ had the lowest ceramic and antagonist wear values. FLD produced wear rates in antagonist teeth similar to PLD and ZLS, but they had significantly lower ceramic wear (1.04 ± 0.22 mg). Ageing did not affect the fracture resistance in any of the tested groups. SMZ and UMZ had the highest fracture load values (2390 ± 191 and 2379 ± 230 N). A significant colour change was observed after ageing in all groups ($P<0.001$). FLD had the highest TP followed by ZLS and PLD. The lowest TP was reported for SMZ & UMZ. Zirconia groups had the best match to selected colour; meanwhile, PLD had the worst colour matching (ΔE 7.99 ± 0.24).

In conclusion, the new generations of monolithic zirconia demonstrated high fracture and wear resistance, minimal abrasiveness to the antagonist teeth and clinically acceptable colour matching to selected shade. Glass ceramics had high ceramic wear and were highly abrasive to antagonist teeth. Although glass ceramics were more translucent than zirconia, they had inferior colour matching to the selected shade. The new experimental fully crystallised lithium disilicate demonstrated high translucency and favourable wear behaviour; however, fracture resistance is lower than conventional lithium disilicate.

7. Figures

Fig. 1: Shows the three crystallographic forms of zirconia: monoclinic, tetragonal, and cubic. Transformation between phases is accompanied by volume change……. **19**

Fig. 2: Shows the mechanism of the “transformation toughening phenomenon”. The volume increase accompanied with t-m phase transformation at the propagating crack’s tip creates compressive stresses that limits further crack propagation……..... **20**

Fig. 3: The CIELAB colour space defined by the International Commission on Illumination. It consists of three axes that represent the colour: L axis indicates the lightness and ranges from 0 (black) to 100 (white), a* axis indicates the green-red colour range, and b* axis indicates the blue-yellow colour range……..... **31**

Fig. 4: Left: LiSi CAD blocks fixed to the holding arm of the precision low speed cutting saw. Right: cutting the rectangular-shaped ceramic specimens from CAD/CAM block size C14 under coolant…….. **43**

Fig. 5: A digital caliber is used to confirm the thickness of the ceramic specimen at 1.5 mm after sectioning…… **44**

Fig. 6: Polishing machine used to flatten and polish the contacting surface of the ceramic specimen before the wear test…….. **45**

Fig. 7: Preparation of teeth for wear testing. A: creating indentations to act as reference marks during models overlapping, B: flattening of palatal cusp, C: final tooth assembly. **46**

Fig. 8: Wear simulating machine at the Department of Oral Technology at Bonn University. A: automatic lubricant regulator, B: moving compartment, C: digital counter…… **47**

Fig. 9: Ceramic specimen glued to an aluminium plate to facilitate attachment to the wear simulating machine…… **48**

Fig. 10: A needle connected to the automatic regulator delivers the artificial saliva to the contacting surfaces at a rate of 1 ml/min…… **48**

Fig. 11: The tooth is fixed in the X-ray chamber of the Micro-CT and a scan preview is displayed on the screen…… **49**

Fig. 12: A 3D model of the tooth before the wear test created from the Micro-CT images using mimics software…… **50**

Fig. 13: 3D models of a non-worn (yellow) and worn (Blue) tooth scans after being transferred to 3-Matic software to undergo models overlapping…… **51**

Fig. 14: Indentations are manually marked on each model before overlapping…… **51**

Fig. 15: A: shows the marked indentations of pre- and post-test models assigned to each other to guide the models overlapping process. B: shows the superimposition of the two models…….. **52**

Fig. 16: Boolean subtraction of the worn enamel tip…… **53**

Fig. 17: Sensitive balance for weighing wear specimens. The ceramic specimen is placed on top of the scale table and the display shows the weight in grams…… **54**

Fig. 18: Confocal laser scanning microscope at the Microscopy Core Facility of the Medical faculty at the University of Bonn…… **55**

Fig. 19: Sputter Coater. The ceramic specimen is placed inside the vacuum chamber and the gold/platinum coating is applied for 60 sec…… **56**

Fig. 20: Scanning electron microscope at the Department of Oral Technology at Bonn University…… **57**

Fig. 21: The master model of prepared premolar that was used in the study. Only the right tooth model was duplicated…….. **59**

Fig. 22: A die duplicated in transparent epoxy resin…… **59**

Fig. 24: Shows the final virtual design of a monolithic crown o the CEREC software… **60**

Fig. 23: shows the die embedded in a wax model and ready for optical scanning……. **60**

Fig. 25: Shows the Katana UTML Zirconia disc mounted on a 5-axis milling machine ready for milling at the Department of Prosthetic Dentistry in LMU University Hospital……. **61**

Fig. 26: Shows the milled zirconia crowns before separation from the disc. All crowns were milled from the same design and have identical dimensions..... **61**

Fig. 27: Hydrofluoric acid gel applied to the fitting surface of a glass-ceramic crown before cementation..... **63**

Fig. 28: Shows the final crown cemented to the epoxy die..... **63**

Fig. 29: Chewing simulator with thermocycling at University of Zurich, Division of Dental Biomaterials..... **64**

Fig. 30: Shows the attachment unit used to firmly hold the specimen on the table of the universal testing machine..... **65**

Fig. 31: Fracture load test. A: applying perpendicular load, B: crown fracture..... **66**

Fig. 32: Measuring the CIEL*a*b* for ceramic samples on black background (left) and white background (right) to calculate the translucency of ceramic specimens..... **68**

Fig. 33: Delrin rods are cut into discs and used as a background for the ceramic specimen during colour measurement..... **68**

Fig. 34: Median and interquartile range of volumetric enamel loss for the different ceramic groups after 200,000 wear cycles. Groups that do not share the same letter are significantly different..... **70**

Fig. 35: Mean and standard deviation of ceramic wear for the different ceramic groups after 200,000 wear cycles. Groups that do not share the same letter are significantly different..... **71**

Fig. 36: Scanning electron micrograph images at magnifications 15X,500X,1000X showing the worn surfaces of the ceramic specimens after 200,000 wear cycles against the buccal cusps of natural premolars. PLD shows a lot of wear debris on the cut surface (black arrows). ZLS and PLD show several crack lines (white arrows)..... **73**

Fig. 37: Scanning electron micrograph images of etched glass-ceramic specimens taken with spot size 3 at magnifications 1200X (a,c,e), and 5000X (b,d,f) showing the crystalline morphology for the worn surfaces. The continuous white arrows point to detached area,

the dotted white arrows point to debris and the black arrow points to a transverse crack.....**74**

Fig. 38: EDX spectrum of PLD shows the presence of silica, potassium, aluminium, kalium, and zirconia..... **76**

Fig. 39: EDX spectrum of FLD shows the presence of silica, potassium, aluminium, and zirconia..... **77**

Fig. 40: EDX spectrum of ZLS shows the presence of silica, potassium, aluminium, and zirconia..... **78**

Fig. 41: Mean and standard deviation of Load to fracture test in newton before and after ageing. The capital letters show significant difference among groups without ageing. The small letters show the significant difference among groups after ageing. Means that do not share the same letter are significantly different..... **80**

Fig. 42: Mean and standard deviation of the ΔE for ceramic crowns after thermomechanical ageing. The letters show the significant difference among groups. Means that do not share the same letter are significantly different..... **81**

Fig. 43: Mean and standard deviation of translucency parameter for different ceramic groups. The letters show the significant difference among groups. Means that do not share the same letter are significantly different..... **83**

Fig. 44: Mean and standard deviation for the ΔE between ceramic specimen and selected shade (A3). The letters show the significant difference among groups. Means that do not share the same letter are significantly different..... **83**

Fig. 45: XRD patterns of glass ceramics. A=before ageing, B=after ageing. The patterns show no difference before and after thermomechanical ageing. FLD pattern shows the presence of silica in addition to the lithium disilicate crystals..... **85**

Fig. 46: XRD patterns of Zirconia. A=before ageing, B=after ageing. t=tetragonal zirconium oxide, c=cubic zirconium oxide. No effect for the thermomechanical ageing on the patterns could be recognized. SMZ and UMZ XRD patterns show mainly tetragonal phases. Cubic phases could be identified by splitting in the tetragonal peaks at 2theta 50.61, 59.82, 74.44, 82.35, and 95.28..... **86**

8. Tables

Table 1: Shows groups, trade names, compositions, lot numbers, and manufacturers of materials used in the study…… **41**

Table 2: Firing parameters of PLD and ZLS specimens…….. **42**

Table 3: Mean, standard deviation, and statistical analysis of Ra values in µm…….. **72**

Table 4: EDX element quantification for glass-ceramic materials (wt.%)…….. **75**

Table 5: Mean and Standard deviation of CIElab colour parameters of the crowns before and after thermomechanical ageing…… **82**

9. References

Abd El-Ghany OS, Sherief AH. Zirconia based ceramics, some clinical and biological aspects: Review. Futur Dent 2016; 2: 55-64

Abdul-Hamid NG, Anita OR, Yahya R. An Overview of the Development and Strengthening of All-Ceramic Dental Materials. Biomed Pharmacol 2018; 11: 1553-1563

Abduo J, Lyons K, Bennamoun M. Trends in computer-aided manufacturing in prosthodontics: a review of the available streams. Int J Dent 2014; 2014: 783948

Aboushelib MN, Wang H, Kleverlaan CJ, Feilzer AJ. Fatigue behavior of zirconia under different loading conditions. Dent Mater 2016; 32: 915-920

Akar GC, Pekkan G, Cal E, Eskitascioglu G, Özcan M. Effects of surface-finishing protocols on the roughness, color change, and translucency of different ceramic systems. J Prosthet Dent 2014; 112: 314-321

Al-Akhali M, Kern M, Elsayed A, Samran A, Chaar MS. Influence of thermomechanical fatigue on the fracture strength of CAD-CAM-fabricated occlusal veneers. J Prosthet Dent 2019; 121: 644-650

Al-Shammery HA, Bubb NL, Youngson CC, Fasbinder DJ, Wood DJ. The use of confocal microscopy to assess surface roughness of two milled CAD-CAM ceramics following two polishing techniques. Dent Mater 2007; 23: 736-741

Alao AR, Stoll R, Song XF, Abbott JR, Zhang Y, Abduo J, Yin L. Fracture, roughness and phase transformation in CAD/CAM milling and subsequent surface treatments of lithium metasilicate/disilicate glass-ceramics. J Mech Behav Biomed Mater 2017; 74: 251-260

Albakry M, Guazzato M, Swain MV. Biaxial flexural strength, elastic moduli, and x-ray diffraction characterization of three pressable all-ceramic materials. J Prosthet Dent 2003; 89: 374-380

Alghazzawi TF. Advancements in CAD/CAM technology: Options for practical implementation. J Prosthodont Res 2016; 60: 72-84

Amaya-Pajares SP, Ritter AV, Vera Resendiz C, Henson BR, Culp L, Donovan TE. Effect of Finishing and Polishing on the Surface Roughness of Four Ceramic Materials after Occlusal Adjustment. J Esthet Restor Dent 2016; 28: 382-396

Amer R, Kurklu D, Kateeb E, Seghi RR. Three-body wear potential of dental yttrium-stabilized zirconia ceramic after grinding, polishing, and glazing treatments. J Prosthet Dent 2014; 112: 1151-1155

Anusavice KJ, Shen C, Rawls HR. Phillips' science of dental materials. Philadelphia – United states: St. Louis, Mo.: Elsevier/Saunders, 2013: 48-67

Apostolov N, Chakalov I, Drajev T. Measurement of the Maximum Bite Force in the Natural Dentition with a Gnathodynamometer. J Med Dent Pract 2014; 1: 70-75

Attaallah AM, Zayed EM, Dabees SM, Ashour YY, Fahmy AE-E. Comparison between Biaxial Flexural Strength and Microstructure of Polished and Glaze-Fired Specimens of Zirconia Lithium Silicate Glass Ceramic. J Dent Mater Tech 2019; 8: 114-120

Badr Z, Culp L, Duqum I, Lim CH, Zhang Y, T AS. Survivability and fracture resistance of monolithic and multi-yttria-layered zirconia crowns as a function of yttria content: A mastication simulation study. J Esthet Restor Dent 2022; 34: 633-640

Bagis B, Turgut S. Optical properties of current ceramics systems for laminate veneers. J Dent 2013; 41 Suppl 3: e24-e30

Baharav H, Laufer BZ, Pilo R, Cardash HS. Effect of glaze thickness on the fracture toughness and hardness of alumina-reinforced porcelain. J Prosthet Dent 1999; 81: 515-519

Bajraktarova-Valjakova E, Korunoska-Stevkovska V, Kapusevska B, Gigovski N, Bajraktarova-Misevska C, Grozdanov A. Contemporary Dental Ceramic Materials, A Review: Chemical Composition, Physical and Mechanical Properties, Indications for Use. Open Access Maced J Med Sci 2018; 6: 1742-1755

Baladhandayutham B, Lawson NC, Burgess JO. Fracture load of ceramic restorations after fatigue loading. J Prosthet Dent 2015; 114: 266-271

Baldissara P, Özcan M, Melilli D, Valandro LF. Effect of cyclic loading on fracture strength and microleakage of a quartz fiber dowel with different adhesive, cement and resin core material combinations. Minerva Stomatol 2010; 59: 407-414

Baldwin DC. Appearance and aesthetics in oral health. Community Dent Oral Epidemiol 1980; 8: 244-256

Barizon KT, Bergeron C, Vargas MA, Qian F, Cobb DS, Gratton DG, Geraldeli S. Ceramic materials for porcelain veneers. Part I: Correlation between translucency parameters and contrast ratio. J Prosthet Dent 2013; 110: 397-401

Belli R, Wendler M, de Ligny D, Cicconi MR, Petschelt A, Peterlik H, Lohbauer U. Chair-side CAD/CAM materials. Part 1: Measurement of elastic constants and microstructural characterization. Dent Mater 2017; 33: 84-98

Bindl A, Mormann WH. An up to 5-year clinical evaluation of posterior in-ceram CAD/CAM core crowns. Int J Prosthodont 2002; 15: 451-456

Blatz MB, Conejo J. The Current State of Chairside Digital Dentistry and Materials. Dent Clin North Am 2019; 63: 175-197

Blatz MB, Sadan A, Kern M. Resin-ceramic bonding: a review of the literature. J Prosthet Dent 2003; 89: 268-274

Borrero-Lopez O, Guiberteau F, Zhang Y, Lawn BR. Wear of ceramic-based dental materials. J Mech Behav Biomed Mater 2019; 92: 144-151

Borrero-Lopez O, Pajares A, Constantino PJ, Lawn BR. A model for predicting wear rates in tooth enamel. J Mech Behav Biomed Mater 2014; 37: 226-234

Brodbelt RH, O'Brien WJ, Fan PL. Translucency of dental porcelains. J Dent Res 1980; 59: 70-75

Bumgardner JD, Lucas LC. Cellular response to metallic ions released from nickel-chromium dental alloys. J Dent Res 1995; 74: 1521-1527

Byeon S-M, Song J-J. Mechanical Properties and Microstructure of the Leucite-Reinforced Glass-Ceramics for Dental CAD/CAM. J Dent Hyg Sci 2018; 18: 42-49

Cales B. Zirconia as a sliding material - Histologic, laboratory, and clinical data. Clin Orthop Relat R 2000; 94-112

Campanelli de Morais D, de Oliveira Abu-Izze F, Rivoli Rossi N, Gallo Oliani M, de Assuncao ESRO, de Siqueira Anzolini Saavedra G, Bottino MA, Marques de Melo Marinho R. Effect of Consecutive Firings on the Optical and Mechanical Properties of Silicate and Lithium Disilicate Based Glass-Ceramics. J Prosthodont 2021; 30: 776-782

Camposilvan E, Leone R, Gremillard L, Sorrentino R, Zarone F, Ferrari M, Chevalier J. Aging resistance, mechanical properties and translucency of different yttria-stabilized zirconia ceramics for monolithic dental crown applications. Dent Mater 2018; 34: 879-890

Chen XP, Xiang ZX, Song XF, Yin L. Machinability: Zirconia-reinforced lithium silicate glass ceramic versus lithium disilicate glass ceramic. J Mech Behav Biomed Mater 2020; 101: 103435

Chen YM, Smales RJ, Yip KH, Sung WJ. Translucency and biaxial flexural strength of four ceramic core materials. Dent Mater 2008; 24: 1506-1511

Cheng SC. New Interpretation of X-ray Diffraction Pattern of Vitreous Silica. Ceramics-Basel 2021; 4: 83-96

Chiu A, Chen YW, Hayashi J, Sadr A. Accuracy of CAD/CAM Digital Impressions with Different Intraoral Scanner Parameters. Sensors 2020; 20: 1157

Choi S, Yoon HI, Park EJ. Load-bearing capacity of various CAD/CAM monolithic molar crowns under recommended occlusal thickness and reduced occlusal thickness conditions. J Adv Prosthodont 2017; 9: 423-431

Christensen GJ. Is the rush to all-ceramic crowns justified?. J Am Dent Assoc 2014; 145: 192-194

Church TD, Jessup JP, Guillory VL, Vandewalle KS. Translucency and strength of high-translucency monolithic zirconium oxide materials. Gen Dent 2017; 65: 48-52

Ciancaglini R, Gherlone EF, Redaelli S, Radaelli G. The distribution of occlusal contacts in the intercuspal position and temporomandibular disorder. J Oral Rehabil 2002; 29: 1082-1090

Clarke DR, Schwartz B. Transformation toughening of glass ceramics. J Mater Res 2011; 2: 801-804

Conejo J, Nueesch R, Vonderheide M, Blatz MB. Clinical Performance of All-Ceramic Dental Restorations. Curr Oral Health Rep 2017; 4: 112-123

Conrad HJ, Seong WJ, Pesun IJ. Current ceramic materials and systems with clinical recommendations: a systematic review. J Prosthet Dent 2007; 98: 389-404

Corciolani G, Vichi A, Goracci C, Ferrari M. Colour correspondence of a ceramic system in two different shade guides. J Dent 2009; 37: 98-101

Corciolani G, Vichi A, Louca C, Ferrari M. Color match of two different ceramic systems to selected shades of one shade guide. J Prosthet Dent 2011; 105: 171-176

Curd FM, Jasinevicius TR, Graves A, Cox V, Sadan A. Comparison of the shade matching ability of dental students using two light sources. J Prosthet Dent 2006; 96: 391-396

Da Silva GR, Roscoe MG, Ribeiro CP, da Mota AS, Martins LR, Soares CJ. Impact of rehabilitation with metal-ceramic restorations on oral health-related quality of life. Braz Dent J 2012; 23: 403-408

Dahl BE, Dahl JE, Ronold HJ. Internal fit of three-unit fixed dental prostheses produced by computer-aided design/computer-aided manufacturing and the lost-wax metal casting technique assessed using the triple-scan protocol. Eur J Oral Sci 2018; 126: 66-73

Datla S, Alla RK, Alluri V, P J, Konakanchi A. Dental Ceramics: Part II – Recent Advances in Dental Ceramics. Am J Mater Eng Technol. 2015; 3: 19-26

Davidowitz G, Kotick PG. The use of CAD/CAM in dentistry. Dent Clin North Am 2011; 55: 559-570

Davies SJ, Gray RJ, Qualtrough AJ. Management of tooth surface loss. Br Dent J 2002; 192: 11-23

Davis LG, Ashworth PD, Spriggs LS. Psychological effects of aesthetic dental treatment. J Dent 1998; 26: 547-554

Della Bona A, Kelly JR. The clinical success of all-ceramic restorations. J Am Dent Assoc 2008; 139 Suppl 1: S8-S13

Della Bona A, Nogueira AD, Pecho OE. Optical properties of CAD-CAM ceramic systems. J Dent 2014; 42: 1202-1209

Della Bona A, Pecho OE, Ghinea R, Cardona JC, Perez MM. Colour parameters and shade correspondence of CAD-CAM ceramic systems. J Dent 2015; 43: 726-734

Delong R, Pintado MR, Douglas WH. The wear of enamel opposing shaded ceramic restorative materials: an in vitro study. J Prosthet Dent 1992; 68: 42-48

DeLong R, Sasik C, Pintado MR, Douglas WH. The wear of enamel when opposed by ceramic systems. Dent Mater 1989; 5: 266-271

Denry I, Holloway JA. Ceramics for Dental Applications: A Review. Materials 2010; 3: 351-368

Dikicier S, Ayyildiz S, Ozen J, Sipahi C. Effect of varying core thicknesses and artificial aging on the color difference of different all-ceramic materials. Acta Odontol Scand 2014; 72: 623-629

Dolev E, Bitterman Y, Meirowitz A. Comparison of marginal fit between CAD-CAM and hot-press lithium disilicate crowns. J Prosthet Dent 2019; 121: 124-128

Dupree R, Holland D, Mortuza MG. A MAS-NMR investigation of lithium silicate glasses and glass ceramics. J Non Cryst Solids 1990; 116: 148-160

Eccles JD. Tooth surface loss from abrasion, attrition and erosion. Dent Update 1982; 9: 373-381

Elsaka SE, Elnaghy AM. Mechanical properties of zirconia reinforced lithium silicate glass-ceramic. Dent Mater 2016; 32: 908-914

Ertan AA, Sahin E. Colour stability of low fusing porcelains: an in vitro study. J Oral Rehabil 2005; 32: 358-361

Esquivel-Upshaw JF, Anusavice KJ, Young H, Jones J, Gibbs C. Clinical performance of a lithia disilicate-based core ceramic for three-unit posterior FPDs. Int J Prosthodont 2004; 17: 469-475

Esquivel-Upshaw JF, Young H, Jones J, Yang M, Anusavice KJ. In vivo wear of enamel by a lithia disilicate-based core ceramic used for posterior fixed partial dentures: first-year results. Int J Prosthodont 2006; 19: 391-396

Fernandez-Segura E, Warley A. Electron probe X-ray microanalysis for the study of cell physiology. Methods Cell Biol 2008; 88:19-43

Fischer TE, Anderson MP, Jahanmir S. Influence of Fracture Toughness on the Wear Resistance of Yttria-Doped Zirconium Oxide. J Am Ceram Soc 1989; 72: 252-257

Fischer TE, Zhu Z, Kim H, Shin DS. Genesis and role of wear debris in sliding wear of ceramics. Wear 2000; 245: 53-60

Flinn BD, Raigrodski AJ, Mancl LA, Toivola R, Kuykendall T. Influence of aging on flexural strength of translucent zirconia for monolithic restorations. J Prosthet Dent 2017; 117: 303-309

Freddo RA, Kapczinski MP, Kinast EJ, de Souza Junior OB, Rivaldo EG, da Fontoura Frasca LC. Wear Potential of Dental Ceramics and its Relationship with Microhardness and Coefficient of Friction. J Prosthodont 2016; 25: 557-562

Fu L, Engqvist H, Xia W. Glass-Ceramics in Dentistry: A Review. Materials 2020; 13: 1049

Furtado de Mendonca A, Shahmoradi M, Gouvea CVD, De Souza GM, Ellakwa A. Microstructural and Mechanical Characterization of CAD/CAM Materials for Monolithic Dental Restorations. J Prosthodont 2019; 28: e587-e594

Garoushi S, Säilynoja E, Vallittu PK, Lassila L. Fracture-behavior of CAD/CAM ceramic crowns before and after cyclic fatigue aging. Int J Prosthodont 2021; 10: 11607

Garvie R, Hannink R, Pascoe R. Ceramic steel?. Nature 1975; 258: 703-704

Ghazal M, Kern M. The influence of antagonistic surface roughness on the wear of human enamel and nanofilled composite resin artificial teeth. J Prosthet Dent 2009; 101: 342-349

Ghuman T, 2016: Wear Performance of Monolithic Dental Ceramics against Enamel. https://cdr.lib.unc.edu 21.10.2021

Gigilashvili D, Thomas JB, Hardeberg JY, Pedersen M. Translucency perception: A review. J Vis 2021; 21: 1-41

Giordano R. Materials for chairside CAD/CAM-produced restorations. J Am Dent Assoc 2006; 137 Suppl 1: S14-S21

Giordano R, Cima M, Pober R. Effect of surface finish on the flexural strength of feldspathic and aluminous dental ceramics. Int J Prosthodont 1995; 8: 311-319

Gkantidis N, Dritsas K, Ren Y, Halazonetis D, Katsaros C. An accurate and efficient method for occlusal tooth wear assessment using 3D digital dental models. Sci Rep 2020; 10: 10103

Gomes RS, Souza CMC, Bergamo ETP, Bordin D, Del Bel Cury AA. Misfit and fracture load of implant-supported monolithic crowns in zirconia-reinforced lithium silicate. J Appl Oral Sci 2017; 25: 282-289

Gonon M. Case Studies in the X-ray Diffraction of Ceramics. In Pomeroy M ed. Encyclopedia of Materials: Technical Ceramics and Glasses. Elsevier. 2021: 560-577

Gracis S, Thompson VP, Ferencz JL, Silva NR, Bonfante EA. A new classification system for all-ceramic and ceramic-like restorative materials. Int J Prosthodont 2015; 28: 227-235

Griggs JA. Recent advances in materials for all-ceramic restorations. Dent Clin North Am 2007; 51: 713-727

Guess PC, Schultheis S, Wolkewitz M, Zhang Y, Strub JR. Influence of preparation design and ceramic thicknesses on fracture resistance and failure modes of premolar partial coverage restorations. J Prosthet Dent 2013; 110: 264-273

Hamza TA, Sherif RM. Fracture Resistance of Monolithic Glass-Ceramics Versus Bilayered Zirconia-Based Restorations. J Prosthodont 2019; 28: e259-e264

Hannink RHJ, Kelly PM, Muddle BC. Transformation toughening in zirconia-containing ceramics. J Am Ceram Soc 2000; 83: 461-487

Harada K, Raigrodski AJ, Chung KH, Flinn BD, Dogan S, Mancl LA. A comparative evaluation of the translucency of zirconias and lithium disilicate for monolithic restorations. J Prosthet Dent 2016; 116: 257-263

Harianawala HH, Kheur MG, Apte SK, Kale BB, Sethi TS, Kheur SM. Comparative analysis of transmittance for different types of commercially available zirconia and lithium disilicate materials. J Adv Prosthodont 2014; 6: 456-461

Hassel AJ, Doz P, Nitschke I, Rammelsberg P. Comparing L*a*b* color coordinates for natural teeth shades and corresponding shade tabs using a spectrophotometer. Int J Prosthodont 2009; 22: 72-74

Heintze SD. How to qualify and validate wear simulation devices and methods. Dent Mater 2006; 22: 712-734

Heintze SD, Cavalleri A, Forjanic M, Zellweger G, Rousson V. Wear of ceramic and antagonist—A systematic evaluation of influencing factors in vitro. Dent Mater 2008; 24: 433-449

Heintze SD, Zellweger G, Grunert I, Munoz-Viveros CA, Hagenbuch K. Laboratory methods for evaluating the wear of denture teeth and their correlation with clinical results. Dent Mater 2012; 28: 261-272

Heydecke G, Zhang F, Razzoog ME. In vitro color stability of double-layer veneers after accelerated aging. J Prosthet Dent 2001; 85: 551-557

Holand W, Schweiger M, Frank M, Rheinberger V. A comparison of the microstructure and properties of the IPS Empress (R) 2 and the IFS Empress (R) glass-ceramics. J Biomed Mater Res 2000; 53: 297-303

Huang X, Zheng X, Zhao G, Zhong B, Zhang X, Wen G. Microstructure and mechanical properties of zirconia-toughened lithium disilicate glass–ceramic composites. Mater Chem Phys 2014; 143: 845-852

Hudson JD, Goldstein GR, Georgescu M. Enamel wear caused by three different restorative materials. J Prosthet Dent 1995; 74: 647-654

Ilie N, Hickel R, Valceanu AS, Huth KC. Fracture toughness of dental restorative materials. Clin Oral Investig 2012; 16: 489-498

Jacobi R, Shillingburg HT, Jr., Duncanson MG, Jr. A comparison of the abrasiveness of six ceramic surfaces and gold. J Prosthet Dent 1991; 66: 303-309

Jagger DC, Harrison A. An in vitro investigation into the wear effects of unglazed, glazed, and polished porcelain on human enamel. J Prosthet Dent 1994; 72: 320-323

Jagger DC, Harrison A. An in vitro investigation into the wear effects of selected restorative materials on enamel. J Oral Rehabil 1995; 22: 275-281

Janyavula S, Lawson N, Cakir D, Beck P, Ramp LC, Burgess JO. The wear of polished and glazed zirconia against enamel. J Prosthet Dent 2013; 109: 22-29

Jian YT, Tang TY, Swain MV, Wang XD, Zhao K. Effect of core ceramic grinding on fracture behaviour of bilayered zirconia veneering ceramic systems under two loading schemes. Dent Mater 2016; 32: 1453-1463

Johansson A, Kiliaridis S, Haraldson T, Omar R, Carlsson GE. Covariation of Some Factors Associated with Occlusal Tooth Wear in a Selected High-Wear Sample. Scand J Dent Res 1993; 101: 398-406

Johansson C, Kmet G, Rivera J, Larsson C, Vult Von Steyern P. Fracture strength of monolithic all-ceramic crowns made of high translucent yttrium oxide-stabilized zirconium dioxide compared to porcelain-veneered crowns and lithium disilicate crowns. Acta Odontol Scand 2014; 72: 145-153

Joiner A. Tooth colour: a review of the literature. J Dent 2004; 32: 3-12

Jurisic S, Jurisic G, Zlataric DK. In Vitro Evaluation and Comparison of the Translucency of Two Different All-Ceramic Systems. Acta Stomatol Croat 2015; 49: 195-203

Kaidonis JA. Tooth wear: the view of the anthropologist. Clin Oral Investig 2008; 12 Suppl 1: S21-S26

Kaizer MR, Bano S, Borba M, Garg V, Dos Santos MBF, Zhang Y. Wear Behavior of Graded Glass/Zirconia Crowns and Their Antagonists. J Dent Res 2019; 98: 437-442

Kaizer MR, Kolakarnprasert N, Rodrigues C, Chai H, Zhang Y. Probing the interfacial strength of novel multi-layer zirconias. Dent Mater 2020; 36: 60-67

Kelly JR. Perspectives on strength. Dent Mater 1995; 11: 103-110

Kelly JR. Ceramics in restorative and prosthetic dentistry. Annu Rev Mater Sci 1997; 27: 443-468

Kelly JR. Dental ceramics: current thinking and trends. Dent Clin North Am 2004; 48: 513-530

Kelly JR, Nishimura I, Campbell SD. Ceramics in dentistry: historical roots and current perspectives. J Prosthet Dent 1996; 75: 18-32

Kern F, Lindner V, Gadow R. Low-Temperature Degradation Behaviour and Mechanical Properties of a 3Y-TZP Manufactured from Detonation-Synthesized Powder. J Ceram Sci Technol 2016; 7: 313-321

Kim-Pusateri S, Brewer JD, Davis EL, Wee AG. Reliability and accuracy of four dental shade-matching devices. J Prosthet Dent 2009; 101: 193-199

Kim HK, Kim SH. Effect of the number of coloring liquid applications on the optical properties of monolithic zirconia. Dent Mater 2014; 30: e229-237

Kim MJ, Oh SH, Kim JH, Ju SW, Seo DG, Jun SH, Ahn JS, Ryu JJ. Wear evaluation of the human enamel opposing different Y-TZP dental ceramics and other porcelains. J Dent 2012; 40: 979-988

Kim SK, Kim KN, Chang IT, Heo SJ. A study of the effects of chewing patterns on occlusal wear. J Oral Rehabil 2001; 28: 1048-1055

Kirsch C, Ender A, Attin T, Mehl A. Trueness of four different milling procedures used in dental CAD/CAM systems. Clin Oral Investig 2017; 21: 551-558

Kolakarnprasert N, Kaizer MR, Kim DK, Zhang Y. New multi-layered zirconias: Composition, microstructure and translucency. Dent Mater 2019; 35: 797-806

Koottathape N, Takahashi H, Iwasaki N, Kanehira M, Finger WJ. Two- and three-body wear of composite resins. Dent Mater 2012; 28: 1261-1270

Krejci I, Albert P, Lutz F. The influence of antagonist standardization on wear. J Dent Res 1999; 78: 713-719

Kunzelmann KH, Jelen B, Mehl A, Hickel R. Wear evaluation of MZ100 compared to ceramic CAD/CAM materials. Int J Comput Dent 2001; 4: 171-184

Kurt M, Turhan Bal B. Effects of accelerated artificial aging on the translucency and color stability of monolithic ceramics with different surface treatments. J Prosthet Dent 2019; 121: 712.e1-712.e8

Lagouvardos PE, Fougia AG, Diamantopoulou SA, Polyzois GL. Repeatability and interdevice reliability of two portable color selection devices in matching and measuring tooth color. J Prosthet Dent 2009; 101: 40-45

Lambrechts P, Braem M, Vuylsteke-Wauters M, Vanherle G. Quantitative in vivo wear of human enamel. J Dent Res 1989; 68: 1752-1754

Lawson NC, Bansal R, Burgess JO. Wear, strength, modulus and hardness of CAD/CAM restorative materials. Dent Mater 2016; 32: e275-e283

Lawson NC, Jurado CA, Huang CT, Morris GP, Burgess JO, Liu PR, Kinderknecht KE, Lin CP, Givan DA. Effect of Surface Treatment and Cement on Fracture Load of Traditional Zirconia (3Y), Translucent Zirconia (5Y), and Lithium Disilicate Crowns. J Prosthodont 2019; 28: 659-665

Lee YK. Translucency of human teeth and dental restorative materials and its clinical relevance. J Biomed Opt 2015; 20: 045002

Lehmann K, Devigus A, Wentaschek S, Igiel C, Scheller H, Paravina R. Comparison of visual shade matching and electronic color measurement device. Int J Esthet Dent 2017; 12: 396-404

Lewis R, Dwyer-Joyce RS. Wear of human teeth: A tribological perspective. P I MECH ENG J-J ENG 2005; 219: 1-18

Li RW, Chow TW, Matinlinna JP. Ceramic dental biomaterials and CAD/CAM technology: state of the art. J Prosthodont Res 2014; 58: 208-216

Liebermann A, Mandl A, Eichberger M, Stawarczyk B. Impact of resin composite cement on color of computer-aided design/computer-aided manufacturing ceramics. J Esthet Restor Dent 2021; 33: 786-794

Lien W, Roberts HW, Platt JA, Vandewalle KS, Hill TJ, Chu TM. Microstructural evolution and physical behavior of a lithium disilicate glass-ceramic. Dent Mater 2015; 31: 928-940

Llena C, Lozano E, Amengual J, Forner L. Reliability of two color selection devices in matching and measuring tooth color. J Contemp Dent Pract 2011; 12: 19-23

Ludovichetti FS, Trindade FZ, Werner A, Kleverlaan CJ, Fonseca RG. Wear resistance and abrasiveness of CAD-CAM monolithic materials. J Prosthet Dent 2018; 120: 318.e1-318.e8

Luo XP, Zhang L. Effect of veneering techniques on color and translucency of Y-TZP. J Prosthodont 2010; 19: 465-470

Lutz F, Krejci I, Barbakow F. Chewing pressure vs. wear of composites and opposing enamel cusps. J Dent Res 1992; 71: 1525-1529

Magne P, Oh WS, Pintado MR, DeLong R. Wear of enamel and veneering ceramics after laboratory and chairside finishing procedures. J Prosthet Dent 1999; 82: 669-679

Mair LH, Stolarski TA, Vowles RW, Lloyd CH. Wear: mechanisms, manifestations and measurement. Report of a workshop. J Dent 1996; 24: 141-148

Makhija SK, Lawson NC, Gilbert GH, Litaker MS, McClelland JA, Louis DR, Gordan VV, Pihlstrom DJ, Meyerowitz C, Mungia R, McCracken MS, National Dental PCG. Dentist material selection for single-unit crowns: Findings from the National Dental Practice-Based Research Network. J Dent 2016; 55: 40-47

Malament KA, Natto ZS, Thompson V, Rekow D, Eckert S, Weber HP. Ten-year survival of pressed, acid-etched e.max lithium disilicate monolithic and bilayered complete-coverage restorations: Performance and outcomes as a function of tooth position and age. J Prosthet Dent 2019; 121: 782-790

Marchesi G, Camurri Piloni A, Nicolin V, Turco G, Di Lenarda R. Chairside CAD/CAM Materials: Current Trends of Clinical Uses. Biology 2021; 10: 1170

Marquardt P, Strub JR. Survival rates of IPS empress 2 all-ceramic crowns and fixed partial dentures: results of a 5-year prospective clinical study. Quintessence Int 2006; 37: 253-259

May MM, Fraga S, May LG. Effect of milling, fitting adjustments, and hydrofluoric acid etching on the strength and roughness of CAD-CAM glass-ceramics: A systematic review and meta-analysis. J Prosthet Dent 2021

Mecholsky JJ. Fracture mechanics principles. Dent Mater 1995; 11: 111-112

Metzler KT, Woody RD, Miller AW, 3rd, Miller BH. In vitro investigation of the wear of human enamel by dental porcelain. J Prosthet Dent 1999; 81: 356-364

Mitov G, Heintze SD, Walz S, Woll K, Muecklich F, Pospiech P. Wear behavior of dental Y-TZP ceramic against natural enamel after different finishing procedures. Dent Mater 2012; 28: 909-918

Miyazaki T, Nakamura T, Matsumura H, Ban S, Kobayashi T. Current status of zirconia restoration. J Prosthodont Res 2013; 57: 236-261

Montazerian M, Zanotto ED. Bioactive and inert dental glass-ceramics. J Biomed Mater Res A 2017; 105: 619-639

Mormann WH. The evolution of the CEREC system. J Am Dent Assoc 2006; 137 Suppl 1: S7-S13

Mormann WH, Stawarczyk B, Ender A, Sener B, Attin T, Mehl A. Wear characteristics of current aesthetic dental restorative CAD/CAM materials: two-body wear, gloss retention, roughness and Martens hardness. J Mech Behav Biomed Mater 2013; 20: 113-125

Mota EG, Smidt LN, Fracasso LM, Burnett LH, Jr., Spohr AM. The effect of milling and postmilling procedures on the surface roughness of CAD/CAM materials. J Esthet Restor Dent 2017; 29: 450-458

Najafi-Abrandabadi S, Vahidi F, Janal MN. Effects of a shade-matching light and background color on reliability in tooth shade selection. Int J Esthet Dent 2018; 13: 198-206

Nakamura K, Harada A, Inagaki R, Kanno T, Niwano Y, Milleding P, Örtengren U. Fracture resistance of monolithic zirconia molar crowns with reduced thickness. Acta Odontol Scand 2015; 73: 602-608

Nakashima J, Taira Y, Sawase T. In vitro wear of four ceramic materials and human enamel on enamel antagonist. Eur J Oral Sci 2016; 124: 295-300

Nedelcu R, Olsson P, Nystrom I, Ryden J, Thor A. Accuracy and precision of 3 intraoral scanners and accuracy of conventional impressions: A novel in vivo analysis method. J Dent 2018; 69: 110-118

Nishigawa K, Bando E, Nakano M. Quantitative study of bite force during sleep associated bruxism. J Oral Rehabil 2001; 28: 485-491

Nishioka G, Prochnow C, Firmino A, Amaral M, Bottino MA, Valandro LF, Renata Marques de M. Fatigue strength of several dental ceramics indicated for CAD-CAM monolithic restorations. Braz Oral Res 2018; 32: e53-e61

Oh WS, Delong R, Anusavice KJ. Factors affecting enamel and ceramic wear: a literature review. J Prosthet Dent 2002; 87: 451-459

Ohashi K, Kameyama Y, Wada Y, Midono T, Miyake K, Kunzelmann K-H, Nihei T. Evaluation and comparison of the characteristics of three pressable lithium disilicate glass ceramic materials. Int J Dev Res 2017; 07: 10731

Orasugh JT, Ghosh SK, Chattopadhyay D. Nanofiber-reinforced biocomposites. in: Han B, Sharma S, Nguyen TA, Longbiao L, Bhat KS, eds. Fiber-Reinforced Nanocomposites: Fundamentals and Applications. Chennai: Elsevier, 2020: 199-233

Orlova LA, Chainikova AS, Popovich NV, Lebedeva YE. Composites based on aluminum-silicate glass ceramic with discrete fillers. GLASS CERAM+ 2013; 70: 149-154

Özcan M, Jonasch M. Effect of Cyclic Fatigue Tests on Aging and Their Translational Implications for Survival of All-Ceramic Tooth-Borne Single Crowns and Fixed Dental Prostheses. J Prosthodont 2018; 27: 364-375

Ozturk O, Uludag B, Usumez A, Sahin V, Celik G. The effect of ceramic thickness and number of firings on the color of two all-ceramic systems. J Prosthet Dent 2008; 100: 99-106

Paradella TC, Bottino MA. Scanning Electron Microscopy in modern dentistry research. Brazilian Dental Science 2012; 15: 43-48

Paravina RD, Ghinea R, Herrera LJ, Bona AD, Igiel C, Linninger M, Sakai M, Takahashi H, Tashkandi E, Mar Perez MD. Color difference thresholds in dentistry. J Esthet Restor Dent 2015; 27: S1-S9

Parrilli A, Falcioni S, Fini M, Affatato S. Is micro-computed tomography useful for wear assessment of ceramic femoral heads? A preliminary evaluation of volume measurements. J Appl Biomater Funct Mater 2016; 14: e483-e489

Patnaik A, Satapathy A, Mahapatra SS, Dash RR. A Comparative Study on Different Ceramic Fillers Affecting Mechanical Properties of Glass—Polyester Composites. J Reinf Plast Compos 2008; 28: 1305-1318

Pecho OE, Ghinea R, Ionescu AM, Cardona JC, Paravina RD, Pérez MM. Color and translucency of zirconia ceramics, human dentine and bovine dentine. J Dent 2012; 40 Suppl 2: e34-e40

Pereira GKR, Guilardi LF, Dapieve KS, Kleverlaan CJ, Rippe MP, Valandro LF. Mechanical reliability, fatigue strength and survival analysis of new polycrystalline translucent zirconia ceramics for monolithic restorations. J Mech Behav Biomed Mater 2018; 85: 57-65

Perez MM, Ghinea R, Ugarte-Alvan LI, Pulgar R, Paravina RD. Color and translucency in silorane-based resin composite compared to universal and nanofilled composites. J Dent 2010; 38 Suppl 2: e110-e116

Piconi C, Maccauro G. Zirconia as a ceramic biomaterial. Biomaterials 1999; 20: 1-25

Pires-de-Souza Fde C, Casemiro LA, Garcia Lda F, Cruvinel DR. Color stability of dental ceramics submitted to artificial accelerated aging after repeated firings. J Prosthet Dent 2009; 101: 13-18

Pjetursson BE, Sailer I, Zwahlen M, Hammerle CHF. A systematic review of the survival and complication rates of all-ceramic and metal-ceramic reconstructions after an observation period of at least 3 years. Part I: single crowns. Clin Oral Implan Res 2007; 18: 73-85

Poggio CE, Ercoli C, Rispoli L, Maiorana C, Esposito M. Metal-free materials for fixed prosthodontic restorations. Cochrane Database Syst Rev 2017; 12: CD009606

Posavec I, Prpic V, Zlataric DK. Influence of Light Conditions and Light Sources on Clinical Measurement of Natural Teeth Color using VITA Easyshade Advance 4,0((R)) Spectrophotometer. Pilot Study. Acta Stomatol Croat 2016; 50: 337-347

Preis V, Behr M, Handel G, Schneider-Feyrer S, Hahnel S, Rosentritt M. Wear performance of dental ceramics after grinding and polishing treatments. J Mech Behav Biomed Mater 2012; 10: 13-22

Raimondo RL, Jr., Richardson JT, Wiedner B. Polished versus autoglazed dental porcelain. J Prosthet Dent 1990; 64: 553-557

Raju DS, Krishna AR, Ramaraju AV, Babu PJ, Konakanchi A. Dental Ceramics: Part II – Recent Advances in Dental Ceramics. Am J Mater Eng Technol 2015; 3: 19-26

Ramos NC, Campos TM, Paz IS, Machado JP, Bottino MA, Cesar PF, Melo RM. Microstructure characterization and SCG of newly engineered dental ceramics. Dent Mater 2016; 32: 870-878

Raptis NV, Michalakis KX, Hirayama H. Optical behavior of current ceramic systems. Int J Periodontics Restorative Dent 2006; 26: 31-41

Rauch A, Schrock A, Schierz O, Hahnel S. Material selection for tooth-supported single crowns-a survey among dentists in Germany. Clin Oral Investig 2021; 25: 283-293

Reich S, Endres L, Weber C, Wiedhahn K, Neumann P, Schneider O, Rafai N, Wolfart S. Three-unit CAD/CAM-generated lithium disilicate FDPs after a mean observation time of 46 months. Clin Oral Investig 2014; 18: 2171-2178

Rekow ED, Silva NR, Coelho PG, Zhang Y, Guess P, Thompson VP. Performance of dental ceramics: challenges for improvements. J Dent Res 2011; 90: 937-952

Ritzberger C, Apel E, Holand W, Peschke A, Rheinberger VM. Properties and Clinical Application of Three Types of Dental Glass-Ceramics and Ceramics for CAD-CAM Technologies. Materials 2010; 3: 3700-3713

Rosenblum MA, Schulman A. A review of all-ceramic restorations. J Am Dent Assoc 1997; 128: 297-307

Ruiz L, Readey MJ. Effect of Heat Treatment on Grain Size, Phase Assemblage, and Mechanical Properties of 3 mol% Y-TZP. J Am Ceram Soc 1996; 79: 2331-2340

Sadan A, Blatz MB, Lang B. Clinical considerations for densely sintered alumina and zirconia restorations: Part 1. Int J Periodont Rest 2005; 25: 213-219

Saghiri MA, Asgar K, Lotfi M, Karamifar K, Saghiri AM, Neelakantan P, Gutmann JL, Sheibaninia A. Back-scattered and secondary electron images of scanning electron microscopy in dentistry: a new method for surface analysis. Acta Odontol Scand 2012; 70: 603-609

Sailer I, Makarov NA, Thoma DS, Zwahlen M, Pjetursson BE. All-ceramic or metal-ceramic tooth-supported fixed dental prostheses (FDPs)? A systematic review of the survival and complication rates. Part I: Single crowns (SCs). Dent Mater 2015; 31: 603-623

Sasse M, Krummel A, Klosa K, Kern M. Influence of restoration thickness and dental bonding surface on the fracture resistance of full-coverage occlusal veneers made from lithium disilicate ceramic. Dent Mater 2015; 31: 907-915

Sawyer WG, Freudenberg KD, Bhimaraj P, Schadler LS. A study on the friction and wear behavior of PTFE filled with alumina nanoparticles. Wear 2003; 254: 573-580

Schultheis S, Strub JR, Gerds TA, Guess PC. Monolithic and bi-layer CAD/CAM lithium-disilicate versus metal-ceramic fixed dental prostheses: comparison of fracture loads and failure modes after fatigue. Clin Oral Investig 2013; 17: 1407-1413

Schweitzer F, Spintzyk S, Geis-Gerstorfer J, Huettig F. Influence of minimal extended firing on dimensional, optical, and mechanical properties of crystalized zirconia-reinforced lithium silicate glass ceramic. J Mech Behav Biomed Mater 2020; 104: 103644

Seghi RR, Denry IL, Rosenstiel SF. Relative fracture toughness and hardness of new dental ceramics. J Prosthet Dent 1995; 74: 145-150

Seghi RR, Johnston WM, O'Brien WJ. Spectrophotometric analysis of color differences between porcelain systems. J Prosthet Dent 1986; 56: 35-40

Seghi RR, Rosenstiel SF, Bauer P. Abrasion of human enamel by different dental ceramics in vitro. J Dent Res 1991; 70: 221-225

Selvaraj U, Koli DK, Jain V, Nanda A. Evaluation of the wear of glazed and polished zirconia crowns and the opposing natural teeth: A clinical pilot study. J Prosthet Dent 2021; 126: 52-57

Shenoy A, Shenoy N. Dental ceramics: An update. J Conserv Dent 2010; 13: 195-203

Shono NN, Al Nahedh HN. Contrast ratio and masking ability of three ceramic veneering materials. Oper Dent 2012; 37: 406-416

Silva LH, Lima E, Miranda RBP, Favero SS, Lohbauer U, Cesar PF. Dental ceramics: a review of new materials and processing methods. Braz Oral Res 2017; 31: e58-e72

Spink LS, Rungruanganut P, Megremis S, Kelly JR. Comparison of an absolute and surrogate measure of relative translucency in dental ceramics. Dent Mater 2013; 29: 702-707

Sripetchdanond J, Leevailoj C. Wear of human enamel opposing monolithic zirconia, glass ceramic, and composite resin: an in vitro study. J Prosthet Dent 2014; 112: 1141-1150

Stawarczyk B, Keul C, Eichberger M, Figge D, Edelhoff D, Lumkemann N. Three generations of zirconia: From veneered to monolithic. Part I. Quintessence Int 2017; 48: 369-380

Stejskal VD, Danersund A, Lindvall A, Hudecek R, Nordman V, Yaqob A, Mayer W, Bieger W, Lindh U. Metal-specific lymphocytes: biomarkers of sensitivity in man. Neuro Endocrinol Lett 1999; 20: 289-298

Stober T, Bermejo JL, Rammelsberg P, Schmitter M. Enamel wear caused by monolithic zirconia crowns after 6 months of clinical use. J Oral Rehabil 2014; 41: 314-322

Subasi MG, Alp G, Johnston WM, Yilmaz B. Effect of thickness on optical properties of monolithic CAD-CAM ceramics. J Dent 2018; 71: 38-42

Sulaiman F, Chai J, Jameson LM, Wozniak WT. A comparison of the marginal fit of In-Ceram, IPS Empress, and Procera crowns. Int J Prosthodont 1997; 10: 478-484

Sun T, Zhou S, Lai R, Liu R, Ma S, Zhou Z, Longquan S. Load-bearing capacity and the recommended thickness of dental monolithic zirconia single crowns. J Mech Behav Biomed Mater 2014; 35: 93-101

Tabatabaian F. Color in Zirconia-Based Restorations and Related Factors: A Literature Review. J Prosthodont 2018; 27: 201-211

Tabatabaian F, Beyabanaki E, Alirezaei P, Epakchi S. Visual and digital tooth shade selection methods, related effective factors and conditions, and their accuracy and precision: A literature review. J Esthet Restor Dent 2021; 33: 1084-1104

Thompson VP, Rekow DE. Dental ceramics and the molar crown testing ground. J Appl Oral Sci 2004; 12: 26-36

Tinschert J, Natt G, Hassenpflug S, Spiekermann H. Status of current CAD/CAM technology in dental medicine. Int J Comput Dent 2004; 7: 25-45

Turgut S, Bagis B. Colour stability of laminate veneers: an in vitro study. J Dent 2011; 39 Suppl 3: e57-e64

Turon-Vinas M, Anglada M. Strength and fracture toughness of zirconia dental ceramics. Dent Mater 2018; 34: 365-375

Tysowsky GW. The science behind lithium disilicate: a metal-free alternative. Dent Today 2009; 28: 112-113

Vanderburgt TP, Tenbosch JJ, Borsboom PCF, Kortsmit WJPM. A Comparison of New and Conventional Methods for Quantification of Tooth Color. J Prosthet Dent 1990; 63: 155-162

Vardhaman S, Borba M, Kaizer MR, Kim D, Zhang Y. Wear behavior and microstructural characterization of translucent multilayer zirconia. Dent Mater 2020; 36: 1407-1417

Venclikova Z, Benada O, Bartova J, Joska L, Mrklas L. Metallic pigmentation of human teeth and gingiva: morphological and immunological aspects. Dent Mater J 2007; 26: 96-104

Vernon-Parry KD. Scanning electron microscopy: an introduction. III-Vs Rev. 2000; 13: 40-44

Vichi A, Ferrari M, Davidson CL. Influence of ceramic and cement thickness on the masking of various types of opaque posts. J Prosthet Dent 2000; 83: 412-417

Vichi A, Louca C, Corciolani G, Ferrari M. Color related to ceramic and zirconia restorations: a review. Dent Mater 2011; 27: 97-108

Vichi A, Sedda M, Fabian Fonzar R, Carrabba M, Ferrari M. Comparison of Contrast Ratio, Translucency Parameter, and Flexural Strength of Traditional and "Augmented Translucency" Zirconia for CEREC CAD/CAM System. J Esthet Restor Dent 2016; 28 Suppl 1: S32-S39

Wang G, Li Y, Wang S, Yang X, Sun Y. Two-Body and Three-Body Wear Behavior of a Dental Fluorapatite Glass-Ceramic. Coatings 2019; 9: 580-590

Wang YS, Hsu SM. Wear and wear transition mechanisms of ceramics. Wear 1996; 195: 112-122

Warreth A, Abuhijleh E, Almaghribi MA, Mahwal G, Ashawish A. Tooth surface loss: A review of literature. Saudi Dent J 2020; 32: 53-60

Wee AG, Monaghan P, Johnston WM. Variation in color between intended matched shade and fabricated shade of dental porcelain. J Prosthet Dent 2002; 87: 657-666

Weyhrauch M, Igiel C, Pabst AM, Wentaschek S, Scheller H, Lehmann KM. Interdevice agreement of eight equivalent dental color measurement devices. Clin Oral Investig 2015; 19: 2309-2318

Wiedenmann F, Bohm D, Eichberger M, Edelhoff D, Stawarczyk B. Influence of different surface treatments on two-body wear and fracture load of monolithic CAD/CAM ceramics. Clin Oral Investig 2020; 24: 3049-3060

Wiedhahn K. From blue to white: new high-strength material for Cerec--IPS e.max CAD LT. Int J Comput Dent 2007;10: 79-91

Winter R. Visualizing the natural dentition. J Esthet Dent 1993; 5: 102-117

Wolfart S, Eschbach S, Scherrer S, Kern M. Clinical outcome of three-unit lithium-disilicate glass-ceramic fixed dental prostheses: up to 8 years results. Dent Mater 2009; 25: e63-e71

Xiao B, Walter B, Gkioulekas I, Zickler T, Adelson E, Bala K. Looking against the light: how perception of translucency depends on lighting direction. J Vis 2014; 14: 1-22

Yamaguchi Y. Chapter 2: Wear. in: Yamaguchi Y, Briscoe BJ, Lancaster JK, eds. Tribology of Plastic Materials-Tribology Series. Elsevier, 1990: 93-142

Yara A, Ogura H, Shinya A, Tomita S, Miyazaki T, Sugai Y, Sakamoto Y. Durability of diamond burs for the fabrication of ceramic crowns using dental CAD/CAM. Dent Mater J 2005; 24: 134-139

Yeo IS, Yang JH, Lee JB. In vitro marginal fit of three all-ceramic crown systems. J Prosthet Dent 2003; 90: 459-464

Yilmaz B, Karaagaclioglu L. In Vitro Evaluation of Color Replication of Metal Ceramic Specimens Using Visual and Instrumental Color Determinations. J Prosthet Dent 2011; 105: 21-27

Yu B, Ahn JS, Lee YK. Measurement of translucency of tooth enamel and dentin. Acta Odontol Scand 2009; 67: 57-64

Yuzbasioglu E, Kurt H, Turunc R, Bilir H. Comparison of digital and conventional impression techniques: evaluation of patients' perception, treatment comfort, effectiveness and clinical outcomes. BMC Oral Health 2014; 14: 10

Zandparsa R, El Huni RM, Hirayama H, Johnson MI. Effect of different dental ceramic systems on the wear of human enamel: An in vitro study. J Prosthet Dent 2016; 115: 230-237

Zarone F, Di Mauro MI, Ausiello P, Ruggiero G, Sorrentino R. Current status on lithium disilicate and zirconia: a narrative review. BMC Oral Health 2019; 19: 134

Zarone F, Ruggiero G, Leone R, Breschi L, Leuci S, Sorrentino R. Zirconia-reinforced lithium silicate (ZLS) mechanical and biological properties: A literature review. J Dent 2021; 109: 103661

Zarone F, Russo S, Sorrentino R. From porcelain-fused-to-metal to zirconia: clinical and experimental considerations. Dent Mater 2011; 27: 83-96

Zhang F, Inokoshi M, Batuk M, Hadermann J, Naert I, Van Meerbeek B, Vleugels J. Strength, toughness and aging stability of highly-translucent Y-TZP ceramics for dental restorations. Dent Mater 2016a; 32: e327-e337

Zhang F, Reveron H, Spies BC, Van Meerbeek B, Chevalier J. Trade-off between fracture resistance and translucency of zirconia and lithium-disilicate glass ceramics for monolithic restorations. Acta Biomater 2019; 91: 24-34

Zhang Y. Making yttria-stabilized tetragonal zirconia translucent. Dent Mater 2014; 30: 1195-1203

Zhang Y, Kelly JR. Dental Ceramics for Restoration and Metal Veneering. Dent Clin North Am 2017; 61: 797-819

Zhang Y, Lawn BR. Novel Zirconia Materials in Dentistry. J Dent Res 2018; 97: 140-147

Zhang Y, Mai Z, Barani A, Bush M, Lawn B. Fracture-resistant monolithic dental crowns. Dent Mater 2016b; 32: 442-449

Zhang Y, Sailer I, Lawn BR. Fatigue of dental ceramics. J Dent 2013; 41: 1135-1147

Zierden K, Acar J, Rehmann P, Wostmann B. Wear and Fracture Strength of New Ceramic Resins for Chairside Milling. Int J Prosthodont 2018; 31: 74-76

Zimmermann M, Ender A, Egli G, Özcan M, Mehl A. Fracture load of CAD/CAM-fabricated and 3D-printed composite crowns as a function of material thickness. Clin Oral Investig 2019; 23: 2777-2784

Zmak I, Coric D, Mandic V, Curkovic L. Hardness and Indentation Fracture Toughness of Slip Cast Alumina and Alumina-Zirconia Ceramics. Materials 2019; 13: 122-139

Zurek AD, Alfaro MF, Wee AG, Yuan JC, Barao VA, Mathew MT, Sukotjo C. Wear Characteristics and Volume Loss of CAD/CAM Ceramic Materials. J Prosthodont 2019; 28: e510-e518

10. Acknowledgments

I'm extremely grateful to Prof. Dr. Christoph Bourauel for his patience, guidance, and endless support throughout my study. Prof. Bourauel has been for me the ideal "Doktorvater" I would ever dream to have. Without his assistance and dedicated involvement in every step throughout the research, this thesis would have never been accomplished. I place on record, my sincere thank you to Prof. Dr. Helmut Stark, Director of the University Dental Hospital and Head of the Prosthetic Department for facilitating access to the department clinic and lectures.

I especially want to thank Prof. Dr. Bogna Stawarczyk the Director of Material Science Research at the Department of Prosthetic Dentistry, LMU Munich, Germany for the cooperation and facilitating the use of the milling machine. I also thank Prof. Dr. Mutlu Özcan Head of the Department of Dental Materials Science, University of Zurich, Switzerland for cooperation and offering the chewing simulator. I would like to extend my sincere thanks to Prof. Dr. Robert Glaum from the Institute of Inorganic Chemistry at Bonn University for facilitating the use of X-ray diffractometer and for giving me a large part of his time to teach me how to analyse the results.

I would like to thank Prof. Dr. Osama Atta, all members of the Fixed Prosthodontics Department, and all faculty members at Faculty of Dentistry, Suez Canal University in Ismailia, Egypt for the guidance and support during the proposal preparation and the application for the Egyptian Government Scholarship.

Special thanks to my colleague and friend Anna Weber for her continuous support and for teaching me how to work on several machines in the Laboratory. Thanks should also go to Mr. Manfred Grüner for helping me with the wear machine. I also had the pleasure of working with Dr. Keilig and all my colleagues at the Department of Oral Technology at Bonn University. I am also very grateful to my dear friend Dr. Mohamed Taqi who made my days easier in Germany and guided me a lot during my papers' submissions and thesis writing.

I'd like to acknowledge the Missions Department at the Ministry of Higher Education in Egypt for the financial support at the beginning of my study.

Last, but definitely not least, words cannot express my deep gratitude to my family for the tremendous support, encouragement, and love they gave to me during my journey abroad. Their love and support were the fuel that kept me moving, and without them I would not have been able to achieve any success in my life.